



الجمهورية الجزائرية الديمقراطية الشعبية

Democratic and Popular Republic of Algeria

وزارة التعليم العالي والبحث العلمي

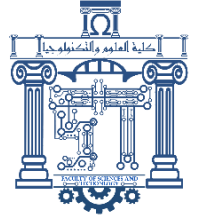
Ministry of Higher Education and Scientific Research

جامعة الشهيد الشيخ العربي التبسي - تبسة

Chahid Cheikh Larbi Tébessi University – Tébessa –

Faculty of Science and Technology

Civil Engineering Department



A thesis submitted in partial fulfilment of the requirements for the degree of Master Research in  
Structural Engineering

By: Boumendjel Saif eddine

Topic

# Parametric study of the Inelastic buckling of perforated steel plates under combined stresses

Thesis defended on June 7<sup>th</sup> 2023

## Thesis committee

Harketi. El Hadi	Grade P.R	President
LABED Abderrahim	Grade MCB	Supervisor
HMIDAN H'mida	Grade MAA	Examiner

Promotion: 2022/2023

بِسْمِ اللَّهِ الرَّحْمَنِ الرَّحِيمِ

## **ACKNOWLEDGEMENTS**

First, I would like to thank my parents for allowing me to realize my own Potential, All the support they have provided me over the years was the greatest gift anyone has ever given me. Also, I must express my very profound gratitude to my brothers for providing me with unfailing support and continuous encouragement throughout my years of study and through the process of researching and writing this thesis, I would also like to thank my sisters, they were always supporting me and encouraging me with their best wishes. This accomplishment would not have been possible without them. Thank you.

Next, I would like to express my deepest gratitude to my advisor, Dr. Abderrahim LABED, for his excellent guidance, caring, patience, and providing me with an excellent atmosphere for doing research.

## CONTENTS

<b>Acknowledgements</b>	/
<b>Contents</b>	I
<b>Abstract</b>	I
<b>List of Figures</b>	I
<b>List of Tables</b>	I
<b>List of Symbols</b>	I
<b>Introduction</b>	a
<b>CHAPTER 1: GENERAL INTRODUCTION TO BUCKLING OF STEEL PLATES</b>	
<b>1.1. General</b>	<b>3</b>
<b>1.2. Plate Elements in Steel Members</b>	<b>3</b>
<b>1.3. Buckling of steel members</b>	<b>5</b>
<b>1.4. Buckling of steel thin plates</b>	<b>5</b>
<b>1.5. Local Buckling</b>	<b>6</b>
<b>1.6. Non-linear buckling capacity</b>	<b>7</b>
<b>1.7. Perforated Steel Plates</b>	<b>8</b>
<b>1.7.1. General</b>	<b>8</b>
<b>1.7.2. Buckling of perforated steel plates</b>	<b>8</b>
<b>1.8. Succinct literature review of the buckling of thin plates</b>	<b>9</b>
<b>1.9. Conclusion</b>	<b>10</b>
<b>CHAPTER 2: ELASTIC AND INELASTIC ANALYTICAL BUCKLINGS OF STEEL THIN PLATES</b>	
<b>2.1 Plate Theory Development And Buckling</b>	<b>12</b>
<b>2.1.1 Introduction</b>	<b>12</b>
<b>2.1.2 Definition and terminology</b>	<b>12</b>
<b>2.1.3 General behaviour of plates</b>	<b>13</b>
<b>2.1.4. Brief history of theory of plates</b>	<b>13</b>
<b>2.2 Analytical Elastic Local Buckling Of Flat Plates</b>	<b>15</b>
<b>2.2.1 General</b>	<b>15</b>
<b>2.2.2 Loadings</b>	<b>16</b>
<b>2.3 Inelastic Buckling, Post-Buckling, And Strength Of Flat Plates</b>	<b>23</b>
<b>2.4 Interaction Between Plate Elements</b>	<b>26</b>
<b>CHAPTER 3: ANALYSIS OF STEEL STRUCTURES BUCKLING USING FINITE ELEMENT</b>	
<b>3.1. Introduction</b>	<b>29</b>
<b>3.2. General Concept Of FEA</b>	<b>29</b>
<b>3.3. Experimental Investigations And Its Role For Finite Element Modelling</b>	<b>30</b>
<b>3.4. Review Of The General Steps Of Finite Element Analysis</b>	<b>30</b>
<b>3.4.1. General</b>	<b>30</b>
<b>3.4.2. Approaches used in FEA</b>	<b>31</b>
<b>3.5. Definitions And Terminology</b>	<b>31</b>
<b>3.5.1 Steps</b>	<b>31</b>
<b>3.5.2 Displacement Function</b>	<b>32</b>

<b>3.5.3 Choice of Element Type for Metal Structures</b>	<b>32</b>
<b>3.5.4 Shell element (Abaqus)</b>	<b>33</b>
<b>3.5.5 Definition of The Strain-displacement and Stress-strain Relationships</b>	<b>33</b>
<b>3.5.6 Material Modelling</b>	<b>34</b>
<b>3.5.7 Modelling the material nonlinearity</b>	<b>34</b>
<b>3.5.8 Modelling of Initial Imperfections</b>	<b>34</b>
<b>3.6 Nonlinear FEA</b>	<b>35</b>
<b>3.6.1 General</b>	<b>35</b>
<b>3.6.2 Geometrically Nonlinear Analysis</b>	<b>36</b>
<b>3.7 Linear Eigenvalue Buckling Analysis</b>	<b>36</b>
<b>3.8 Inelastic buckling analysis</b>	<b>37</b>
<b>3.8.1 General</b>	<b>37</b>
<b>CHAPTER 4 : SOFTWARE USED</b>	
<b>4.1. Abaqus Software For Elastic And Inelastic Buckling</b>	<b>42</b>
<b>4.1.1 Introduction</b>	<b>42</b>
<b>4.1.2 Applications</b>	<b>43</b>
<b>4.1.3 General on ABAQUS Software Modules</b>	<b>43</b>
<b>4.1.4 Solution sequence</b>	<b>44</b>
<b>4.1.5 Elements in ABAQUS</b>	<b>45</b>
<b>4.1.6 Examples</b>	<b>47</b>
<b>4.2 Modulistaion Using Abaqus Software</b>	<b>47</b>
<b>4.2.1 Create Sketch</b>	<b>47</b>
<b>4.2.2 Define Property</b>	<b>48</b>
<b>4.2.3 Assembly</b>	<b>49</b>
<b>4.2.4 Step</b>	<b>49</b>
<b>4.2.5 Load</b>	<b>50</b>
<b>4.2.6 Create Mesh</b>	<b>52</b>
<b>4.2.7 Job</b>	<b>53</b>
<b>4.2.8 Results</b>	<b>54</b>
<b>4.3 EBPlate For Elastic Buckling Analysis</b>	<b>54</b>
<b>4.3.1 General</b>	<b>54</b>
<b>4.3.2 Scope of EBPlate</b>	<b>54</b>
<b>4.3.3 Applications</b>	<b>55</b>
<b>4.3.4 Brief presentation of the capabilities</b>	<b>55</b>
<b>4.3.5 Menus</b>	<b>55</b>
<b>4.3.6 Toolbars</b>	<b>56</b>
<b>4.3.7 Examples</b>	<b>57</b>
<b>CHAPTER 5 VALIDATION AND VERIFICATION OF MODELS NON-PERFORATED AND PERFORATED THIN PLATES</b>	
<b>5.1 Introduction</b>	<b>59</b>
<b>5.2 Validation Of Models</b>	<b>59</b>
<b>5.2.1 Compression</b>	<b>59</b>
<b>5.2.1.1 Case of rectangular plate without cut-out (in compression)</b>	<b>59</b>

<b>5.2.1.2 Case of Rectangular plates with different circular cut-out diameter (in compression)</b>	<b>63</b>
<b>5.2.1.3 Case of Square Plate without Hole</b>	<b>66</b>
<b>5.2.2 Compression and Shear</b>	<b>73</b>
<b>CHAPTER 6</b>	
<b>PARAMETRIC ELASTIC AND INELASTIC BUCKLING ANALYSIS OF SQUARE PLATES</b>	
<b>6.1 Modelling of the studied cases</b>	<b>75</b>
<b>6.2 Elastic buckling analysis results and discussion</b>	<b>80</b>
<b>6.3 Inelastic RIKS FEA</b>	<b>83</b>
<b>6.3.1 General consideration of the model</b>	<b>89</b>
<b>6.3.2 Characteristic of the model</b>	<b>91</b>
<b>6.4 Results and discussion</b>	<b>93</b>
<b>6.5 General discussion</b>	<b>95</b>
<b>Conclusion general</b>	<b>100</b>
<b>References</b>	<b>101</b>

## ABSTRACT

*Plated structures are important in a variety of marine- and land-based applications, including ships, offshore platforms, box girder bridges, power/chemical plants, and box girder cranes. It is very likely in many cases to have holes in the plate elements for inspection, maintenance, and service purposes, and the size of these holes could be significant. In such cases, the presence of these holes redistributes the membrane stresses in the plate and may cause significant reduction in its strength in addition to changing its buckling characteristics. In fact, buckling analysis assesses the stability characteristics of a structure. The behaviour of a plate under applied loads may be classified into five regimes: pre-buckling, buckling, post-buckling, ultimate strength, and post-ultimate strength. In the pre-buckling regime, the structural response between loads and displacements is usually linear, and the structural component is stable. As the predominantly compressive stress reaches a critical value, buckling occurs. This dissertation presents a comprehensive parametric study on the elastic and inelastic buckling ultimate strength of intact and perforated square steel plates using the Finite Element package ABAQUS and EBPLATE. Finite element models are built-up under several loadings that is uniaxial compressive pressure, shear stressed  $s$  and combined stresses for the elastic buckling Eigen values analysis. For the inelastic buckling analysis carried out with Abaqus concerns the exclusive case of compression pressure. Modelling issues such as boundary conditions, meshing, initial imperfections, material models, and non-linear solution controls in FEA were addressed. It is vital to first develop a reliable and efficient FE model capable of producing realistic and accurate results particularly for elastic buckling, non-linear buckling and even post-buckling models. Buckling analysis assesses the stability characteristics of a structure. An accurate solution to a buckling problem requires more efforts than just following a numerical procedure, there are a number of factors to consider before a buckling solution can be accepted with confidence. So, the FEA models were first validated against some published research work taken from literature before adaptation of these models. The validation of the linear FEA model has been successfully done with the data available in literature, which gives a more confidence in the models which will be used as initial condition for more complex buckling analysis of plate with and without cut-out. Nonlinear problems pose the difficulty of describing phenomena by realistic mathematical and numerical models and the difficulty of solving nonlinear equations. In fact, the effort required of the analyst increases substantially when a problem becomes nonlinear. The main results coming up from the elastic buckling is that the most severe loading type for a intact or perforated square plate is the compression. For that reason, it has been decided to exclusively, for the inelastic buckling behaviour, to carry out the parametric analysis on unstiffened square intact and perforated plate. The thickness of the plate is of prime importance as it influences the elastic and inelastic buckling. The emphasize on the input imperfection sensitivity value in the inelastic behaviour should not only be a proportion of the width of the plate but also in terms of the thickness of plates.*

*Keywords: plate; intact; perforated; buckling; finite element analysis, elastic; inelastic; steel; Abaqus; EBPLATE.*

## ملخص

تعتبر الهياكل المطلوبة مهمة في مجموعة متنوعة من التطبيقات البحرية والبرية ، بما في ذلك السفن ، والمنصات البحرية ، وجسور العارضة أغراض الفحص والصيانة والخدمة ، وقد يكون حجم هذه الثقوب ، ومحطات الطاقة / الكيماويات ، ورافعات العارضة الصندوقية في مثل هذه الحالات ، يؤدي وجود هذه الثقوب إلى إعادة توزيع ضغوط الغشاء في اللوحة وقد يؤدي إلى انخفاض كبير في قوتها .كبيرًا يمكن تصنيف سلوك الصفيحة تحت الأحمال .في الواقع ، يقيم تحليل الالتواء خصائص ثبات الهيكل .بالإضافة إلى تغيير خصائص الالتواء في نظام ما قبل الالتواء ، تكون .المطبقة إلى خمسة أنظمة: ما قبل الالتواء ، والتواء ، وما بعد الالتواء ، والقوة النهائية ، والقوة اللاحقة النهائية عندما يصل الضغط الضاغظ في الغالب إلى قيمة .الاستجابة الهيكلية بين الأحمال وعمليات الإزاحة عادةً خطية ، ويكون المكون الهيكلية مستقرًا تقدم هذه الرسالة دراسة بارامترية شاملة حول القوة المطلقة للربط المرن وغير المرن للصفائح الفولاذية المربعة السليمة .حرجة ، يحدث التواء يتم بناء نماذج العناصر المحدودة في ظل العديد من عمليات التحميل التي .EBPLATE و ABAQUS والمتقبة باستخدام حزمة العناصر المحدودة بالنسبة .الانبساطية المرنة eigen هي عبارة عن ضغط انضغاطي أحادي المحور ، وضغط إجهاد القص ، والضغط المشتركة لتحليل قيم تمت معالجة قضايا النمذجة مثل .، يتعلق الأمر بالحالة الحصرية لضغط الانضغاط Abaqus لتحليل الالتواء غير المرن الذي تم إجراؤه مع من الأهمية بمكان أولاً تطوير .FEA شروط الحدود ، والتشابك ، والعيوب الأولية ، ونماذج المواد ، وعناصر التحكم في الحلول غير الخطية في موثوق وفعال قادر على إنتاج نتائج واقعية ودقيقة خاصة بالنسبة لنماذج الانحناء المرن والالتواء غير الخطي وحتى نماذج ما بعد FE نموذج يتطلب الحل الدقيق لمشكلة الانحناء جهودًا أكثر من مجرد اتباع إجراء رقمي ، فهناك .يقيم تحليل التواء خصائص الاستقرار للهيكل .الانحناء لأول مرة مقابل بعض الأعمال البحثية FEA لذلك ، تم التحقق من صحة نماذج .عدد من العوامل التي يجب مراعاتها قبل قبول حل الالتواء بثقة الخطي بنجاح باستخدام البيانات المتوفرة في الأدبيات ، FEA تم التحقق من صحة نموذج .المنشورة المأخوذة من الأدبيات قبل تكيف هذه النماذج تشكل المسائل غير الخطية .مما يعطي ثقة أكبر في النماذج التي سيتم استخدامها كشرط أولي لتحليل التواء أكثر تعقيدًا للوحة مع وبدون انقطاع في الواقع ، يزداد الجهد المطلوب من المحلل .صعوبة وصف الظواهر بنماذج رياضية وعددية واقعية وصعوبة حل المعادلات غير الخطية تتمثل النتائج الرئيسية الناتجة عن الالتواء المرن في أن الضغط هو أشد أنواع التحميل خطورة .بشكل كبير عندما تصبح المشكلة غير خطية لهذا السبب ، فقد تقرر حصرًا ، لسلوك الالتواء غير المرن ، إجراء التحليل المعياري على لوحة مربعة سليمة .اللوحة مربعة سليمة أو مثقوبة التأكيد على قيمة حساسية عيوب الإدخال في السلوك غير .سمك الصفيحة له أهمية قصوى لأنه يؤثر على الالتواء المرن وغير المرن .ومثقبة تحليل العناصر .الكلمات الرئيسية: لوحة؛ متصل؛ مثقب؛ التواء .المرن يجب ألا يكون فقط نسبة من اللوح ولكن أيضًا من حيث سماكة الألواح EB .المحدودة ، المرونة ؛ غير مرن؛ فولاذ؛ عباوقس



## RESUME

*Les plaques sont d'une importance capitale dans une variété d'applications marines et terrestres, y compris les constructions navales, les plates-formes offshore, les ponts à poutres-caissons, les centrales électriques/chimiques et les grues à poutres-caissons. Il est très probable dans de nombreux cas d'avoir des trous dans les éléments de plaque pour à des fins d'inspection, d'entretien et de service, et la taille de ces trous pourrait être importante. Dans de tels cas, la présence de ces trous redistribue les contraintes membranaires dans la plaque qui peut, éventuellement, entraîner une réduction significative de sa résistance en plus de modifier ses caractéristiques au voilement. L'analyse du voilement estime les caractéristiques de stabilité d'une structure. Le comportement d'une plaque sous des charges appliquées peut être classé en cinq régimes : pré-voilement, voilement, post-voilement, la résistance critique et la résistance postcritique. Dans le régime de précritique, la réponse structurelle la relation entre les forces et les déplacements est généralement linéaire et le composant structurel est ainsi stable. Lorsque la contrainte de compression prédominante atteint une valeur critique, un voilement se produit. Cette thèse présente une étude paramétrique complète sur la résistance ultime au voilement élastique et inélastique de plaques d'acier carrées intactes et perforées en utilisant du package d'éléments finis ABAQUS et EBPLATE. Les modèles d'éléments finis sont conçus en considérant plusieurs cas de chargements qui sont la compression uni-axiale, les contraintes de cisaillement et les contraintes combinées pour extraire les valeurs propres de voilement élastique. L'analyse de voilement inélastique réalisée avec Abaqus concerne le cas exclusif de la compression. Les problèmes de modélisation tels que les conditions aux limites, le maillage, les imperfections initiales, les modèles de matériaux et les contrôles de solutions non linéaires dans FEA ont été abordés. Il est essentiel de développer d'abord un modèle EF fiable et efficace capable de produire des résultats réalistes et précis, en particulier pour les modèles de voilement élastique, de voilement non linéaire et même en post-critique. L'analyse de voilement évalue les caractéristiques de stabilité d'une structure. Une solution précise à un problème de voilement nécessite plus d'efforts que de simplement suivre une procédure numérique, il y a un certain nombre de facteurs à considérer avant qu'une solution de voilement puisse être acceptée avec confiance. Ainsi, les modèles FEA ont d'abord été validés par rapport à certains travaux de recherche publiés tirés de la littérature avant l'adaptation de ces modèles. La validation du modèle FEA linéaire a été effectuée avec succès avec les données disponibles dans la littérature, ce qui donne une plus grande confiance dans les modèles qui seront utilisés comme condition initiale pour une analyse de voilement plus complexe de plaque avec et sans découpe centrale. Les problèmes non linéaires posent la difficulté de décrire des phénomènes par des modèles mathématiques et numériques réalistes et la difficulté de résoudre des équations non linéaires. En fait, l'effort demandé à l'analyste augmente considérablement lorsqu'un problème devient non linéaire. Les principaux résultats issus du flambement élastique sont que le type de chargement le plus sévère pour une plaque carrée intacte ou perforée est la compression. Pour cette raison, il a été décidé d'effectuer exclusivement, pour le comportement de voilement inélastique, l'analyse paramétrique sur une plaque intacte carrée non raidie et perforée. L'épaisseur de la plaque est primordiale dans l'étude du voilement, car elle influence à la fois le voilement élastique et inélastique. L'importance mise sur la valeur de sensibilité aux imperfections comme donnée de départ dans le comportement inélastique ne doit pas seulement être prise comme une proportion de la largeur de la plaque mais également en termes d'épaisseur des plaques.*

*Mots-clés : plaque ; intact ; perforé ; voilement ; analyse par éléments finis, élastique ; inélastique ; acier ; Abaqus ; EBPLATE*

## LIST OF FIGURES

<b>Figure 1.1 Compression or flexural members Section shapes (Galambos, 1998)</b>	<b>4</b>
<b>Figure 1.2 Flowchart of buckling of like-column and like-plate</b>	<b>6</b>
<b>Figure 2.1 Structural design considerations based on the ultimate limit state</b>	<b>16</b>
<b>Fig. 2.2 Local plate buckling coefficient, k for plates in compression with varied boundary conditions (ref.)</b>	<b>18</b>
<b>Fig.2.3 Plate buckling coefficients for long plates under compression and bending (ref.)</b>	<b>18</b>
<b>Fig. 2.4 Plate buckling coefficients for unstiffened elements in compression and bending, after (Bambach and Rasmussen 2004a)</b>	<b>19</b>
<b>Fig. 2.5 Plate buckling coefficients for plates in pure shear. (Side b is the short side.)</b>	<b>20</b>
<b>Fig. 2.6 Interaction curve for buckling of flat plates under shear and uniform compression.</b>	<b>21</b>
<b>Fig. 2.7. Buckling coefficients for plates in combined bending and shear.</b>	<b>22</b>
<b>Fig. 2.8 Interaction curve for buckling of flat plates under shear, compression, and bending.</b>	<b>23</b>
<b>Fig. 2.9 Simple model for post-buckling of a flat plate in uniform compression (after AISI 2007)</b>	<b>25</b>
<b>Figure 3.1 Shell element types: (A) conventional shell elements and (B) continuum shell elements.</b>	<b>33</b>
<b>Figure 3.2 Load-Displacement curve used in Riks method</b>	<b>39</b>
<b>Figure 3.3 Critical load vs. in plane deformation loading history</b>	<b>39</b>
<b>Figure 4.1 Components of the main window.</b>	<b>44</b>
<b>Figure 4.2. Abaqus FEA software products used in Finite Element Analysis and their order of use.</b>	<b>45</b>
<b>Figure 4.3. Family of finite elements in Abaqus software.</b>	<b>45</b>
<b>Figure 4.4 An element's number of nodes in Abaqus software.</b>	<b>46</b>
<b>Figure 4.5. Square plate without hole: elastic buckled shape.</b>	<b>47</b>
<b>Figure 4.6. Square plate with hole: inelastic buckled shape.</b>	<b>47</b>
<b>Figure 4.7 creating a sketch</b>	<b>48</b>
<b>Figure 4.8 Defining Property</b>	<b>48</b>
<b>Figure 4.9 creating the section</b>	<b>49</b>
<b>Figure 4.10 Creating instance</b>	<b>49</b>
<b>Figure 4.11 creating a step</b>	<b>50</b>
<b>Figure 4.12 Creating boundary condition</b>	<b>50</b>
<b>Figure 4.13 Selection the boundary condition</b>	<b>51</b>
<b>Figure 4.14 the boundary condition</b>	<b>51</b>
<b>Figure 4.15 Creating load</b>	<b>51</b>
<b>Figure 4.16 Selection the value of load</b>	<b>52</b>
<b>Figure 4.17 Presentation of Load</b>	<b>52</b>
<b>Figure 4.18 Selection the value of the mesh</b>	<b>52</b>
<b>Figure 4.19 Selection the type of element and technique in mesh control</b>	<b>53</b>
<b>Figure 4.20 the presentation of meshing in the plate</b>	<b>53</b>
<b>Figure 4.21 creating the job and submitted it</b>	<b>53</b>

<b>Figure 4.22 Results</b>	<b>54</b>
<b>Figure 4.23 Main window of EBPlate and its areas</b>	<b>56</b>
<b>Figure 4.24. Square plate with hole: elastic buckled shape under compression.</b>	<b>57</b>
<b>Figure 4.25. Square plate with hole: elastic buckled shape under shear</b>	<b>57</b>
<b>Figure 5.1. Non-perforated plate model and boundary conditions</b>	<b>60</b>
<b>Figure 5.2. Finite element mesh of the plate without hole by Abaqus.</b>	<b>61</b>
<b>Figure 5.3. Ultimate deformation configuration at the last stage of buckled shape. (a) Author's results; (b).</b>	<b>62</b>
<b>Figure 5.4. Ultimate deformation configuration at the last stage of buckled shape. (a) Author's results; (b).</b>	<b>63</b>
<b>Figure 5.5. Perforated plate model and boundary conditions under</b>	<b>64</b>
<b>Figure 5.6. Ultimate deformation configuration at the last stage of buckled shape for plates with different cut-out diameters. Author's results; (b).</b>	<b>65-66</b>
<b>Figure 5.7. Non-perforated square plate model and boundary condition</b>	<b>67</b>
<b>Figure 5.8 Ultimate deformation configuration at the last stage of buckled shape. (a) Author's results; (b).</b>	<b>68</b>
<b>Figure 5.9. Ultimate deformation configuration at the last stage of buckled shape. (a) Author's results; (b).</b>	<b>69</b>
<b>Figure 5.10. Non-perforated square plate model and boundary condition</b>	<b>70</b>
<b>Figure 5.11. Ultimate deformation configuration at the last stage of buckled shape. (a) Abaqus; (b) EBPLATE.</b>	<b>71</b>
<b>Figure 5.12. Ultimate deformation configuration at the last stage of buckled shape. (a) Abaqus; (b) EBPLATE.</b>	<b>72</b>
<b>Figure 6.1. Square plate model with boundary conditions</b>	<b>75</b>
<b>Figure 6.2 Dimensional parameters of the perforated plate on the side.</b>	<b>76</b>
<b>Figure 6.3 Types of loading used in the parametric elastic buckling analysis by FEA</b>	<b>76</b>
<b>Figure 6.4 modelling the intact plates</b>	<b>76</b>
<b>Figure 6.5 Plane view of square plate models with circle and square hole shapes used for inelastic buckling analysis by FEA by Abaqus.</b>	<b>77</b>
<b>Figure 6.6. The first modal vibration mode shapes for an intact square plate by Abaqus</b>	<b>79</b>
<b>Figure 6.7. The first modal vibration mode shapes for an intact square plate by EBPLATE</b>	<b>80</b>
<b>Figure 6.8. Plate with hole R=50 mm Buckled shape in compression, shear and combined.</b>	<b>83</b>
<b>Figure 6.9 Plate with circular hole R=200 mm Buckled shape in compression, shear and Combined.</b>	<b>83</b>
<b>Figure 6.10 Plate with Square hole A =100 mm Buckled shape in compression, shear and Combined.</b>	<b>84</b>
<b>Figure 6.11 Plate with Square hole A =400 mm Buckled shape in compression, shear and Combined.</b>	<b>84</b>
<b>Figure 6.12 Dimensional parameters of the perforated plate on the side.</b>	<b>85</b>
<b>Figure 6.13 Elastic and inelastic load- in plane deflection of intact plate square with different thicknesses</b>	<b>87</b>
<b>Figure 6.14 Elastic and inelastic load- in plane deflection of square perforated plate with <math>t = 10</math> mm</b>	<b>88</b>

<b>Figure 6.15 Elastic and inelastic load- in plane deflection of square perforated plate with <math>t = 20</math> mm</b>	<b>88</b>
<b>Figure 6.16 Elastic and inelastic load- in plane deflection of square perforated plate with <math>t = 40</math> mm</b>	<b>88</b>
<b>Figure 6.17 Elastic and inelastic load- in plane deflection of square perforated plate with <math>t = 10</math> mm</b>	<b>89</b>
<b>Figure 6.18 Elastic and inelastic load- in plane deflection of square perforated plate with</b>	<b>89</b>
<b><math>t = 20</math> mm</b>	<b>89</b>
<b>Figure 6.19 Elastic and inelastic load- in plane deflection of square perforated plate with <math>t = 40</math> mm</b>	<b>90</b>
<b>Figure 6.20 Different hole shape same size 100 mm with thickness <math>t = 10</math> mm</b>	<b>90</b>
<b>Figure 6.21 Different hole shape same size 100 mm with thickness <math>t = 20</math> mm</b>	<b>90</b>
<b>Figure 6.22 Different hole shape same size 100 mm with thickness <math>t = 40</math> mm</b>	<b>90</b>
<b>Figure 6.23. Different hole shape same size 100 mm with thickness <math>t = 10</math> mm</b>	<b>91</b>
<b>Figure 6.24 Different hole shape same size 100 mm with thickness <math>t = 20</math> mm</b>	<b>91</b>
<b>Figure 6.25 Different hole shape same size 100 mm with thickness <math>t = 40</math> mm</b>	<b>91</b>
<b>Figure 6.26 Ratio between critical buckling load and the displacement for plates with the thickness <math>t = 10</math>mm</b>	<b>92</b>
<b>Figure 6.27 Ratio between critical buckling load and the displacement for plates with the thickness <math>t = 20</math>mm</b>	<b>92</b>
<b>Figure 6.28 Ratio between critical buckling load and the displacement for plates with the thickness <math>t = 40</math>mm</b>	<b>93</b>
<b>Figure 6.29 Contours of Von Mises stress and deformed shape <math>t = 10</math> mm</b>	<b>93</b>
<b>Figure 6.30 Contours of Von Mises stress distribution and deformed shape <math>t = 20</math> mm</b>	<b>93</b>
<b>Figure 6.31 Contours of Von Mises stress distribution and deformed shape <math>t = 40</math> mm</b>	<b>93</b>
<b>Figure 6.32 Contours of Von Mises stress distribution and deformed shape <math>t = 10</math> mm</b>	<b>94</b>
<b>Figure 6.33 Contours of Von Mises stress distribution and deformed shape <math>t = 20</math> mm</b>	<b>94</b>
<b>Figure 6.34 Contours of Von Mises stress distribution and deformed shape <math>t = 40</math> mm</b>	<b>94</b>
<b>Figure 6.35 Contours of Von Mises stress distribution and deformed shape <math>t = 10</math> mm</b>	<b>94</b>
<b>Figure 6.36 Contours of Von Mises stress distribution and deformed shape <math>t = 20</math> mm</b>	<b>95</b>
<b>Figure 6.37 Contours of Von Mises stress distribution and deformed shape <math>t = 40</math> mm</b>	<b>95</b>
<b>Figure 6.38 Contours of Von distribution Mises stress and deformed shape <math>t = 10</math> mm</b>	<b>95</b>
<b>Figure 6.39 Contours of Von Mises stress distribution and deformed shape <math>t = 20</math> mm</b>	<b>95</b>
<b>Figure 6.40 Contours of Von Mises stress distribution and deformed shape <math>t = 40</math> mm</b>	<b>95</b>
<b>Figure 6.41 Contours of Von Mises stress distribution and deformed shape <math>t = 10</math> mm</b>	<b>96</b>

---

<b>Figure 6.42 Contours of Von Mises stress distribution and deformed shape t = 20 mm</b>	<b>96</b>
<b>Figure 6.43 Contours of Von Mises stress distribution and deformed shape t = 40 mm</b>	<b>96</b>

## LIST OF TABLES

<b>Table 5.1 Geometrical and material characteristics of the implanted models</b>	<b>60</b>
<b>Table 5.2. Comparison of critical buckling load for plate non-perforated.</b>	<b>62</b>
<b>Table 5.3. Comparison of critical buckling load for plate non-perforated.</b>	<b>63</b>
<b>Table 5.4. Comparison of critical buckling load for plate with centred circular hole.</b>	<b>65</b>
<b>Table 5.5 Geometrical and material Characteristics of the implanted model</b>	<b>67</b>
<b>Table 5.6. Comparison of critical buckling load for plate non-perforated.</b>	<b>68</b>
<b>Table 5.7. Comparison of critical buckling load for plate non-perforated.</b>	<b>69</b>
<b>Table 5.8 Geometrical and material Characteristics of the implanted model</b>	<b>70</b>
<b>Table 5.9. Comparison of critical buckling load for plate non-perforated.</b>	<b>71</b>
<b>Table 5.10. Comparison of critical buckling load for plate non-perforated.</b>	<b>72</b>
<b>Table 6.1 Geometric dimensions and material properties of the perforated plate.</b>	<b>76</b>
<b>Table 6.2 Values of the first mode eigenvalue for intact square plate in terms of plate's thickness.</b>	<b>77</b>
<b>Table 6.3. Comparison of the calculated critical buckling load of an intact square in terms of plate's thickness.</b>	<b>78</b>
<b>Table 6.5 Values of the first mode eigenvalue for perforated square plate in terms of plate's thickness.</b>	<b>78</b>
<b>Table 6.6 Values of the first mode eigenvalue for perforated square plate in terms of plate's thickness.</b>	<b>79</b>
<b>Table 6.7 Values of the first mode eigenvalue for perforated square plate in terms of plate's thickness.</b>	<b>79</b>
<b>Table 6.8 Critical buckling load for perforated square plates</b>	<b>80</b>
<b>Table 6.9. Geometric dimensions and material properties of the perforated plate.</b>	<b>81</b>
<b>Table 6.1 Geometric dimensions and material properties of the perforated plate.</b>	<b>82</b>
<b>Table 6.2 Values of the first mode eigenvalue for intact square plate in terms of plate's thickness.</b>	<b>83</b>
<b>Table 6.3. Comparison of the calculated critical buckling load of an intact square in terms of plate's thickness.</b>	<b>83</b>
<b>Table 6.5 Values of the first mode eigenvalue for perforated square plate in terms of plate's thickness.</b>	<b>84</b>
<b>Table 6.6 Values of the first mode eigenvalue for perforated square plate in terms of plate's thickness.</b>	<b>84</b>
<b>Table 6.7 Values of the first mode eigenvalue for perforated square plate in terms of plate's thickness.</b>	<b>85</b>
<b>Table 6.8 Critical buckling load for perforated square plates</b>	<b>86</b>

### List of symbols

$\sigma$ :Normal (perpendicular) stress
$\tau$ :Shear (parallel) stress
t :Thickness of plate
d: Diameter of circular hole
W:Height dimension of a plate
W:Half Height dimension of a plate
L:Length of plate
a,b: Dimensions of elliptical hole
b,a: Dimensions of a rectangle hole
r:Fillet in rectangular hole
r :Distance between the center of the hole and the calculated point position for a Circular hole
$\theta$ :Angle of the inclination of distance (r) with respect to the x axis
a :Hole radius
Kt :Elastic or theoretical equivalent stress concentration factor
E:Modulus of elasticity
$\epsilon$ :Strain
$\nu$ :Poisson's ratio
K Abaqus: Coefficient of concentration of the stress of the simulation in Abaqus
$\sigma_{nom}$ :Nominal stress
$\sigma_{max}$ :Maximum stress (real)
$\sigma_{min}$ :Minimal stress
$\sigma$ :Stress far from hole to infinity

## GENERAL INTRODUCTION

### Buckling of plated structures with and without cut-out

Plated structures are important in a variety of marine- and land-based applications, including ships, offshore platforms, box girder bridges, power/chemical plants, and box girder cranes. Compared to steel structures of rolled profiles, plated structures are more prone to local buckling and therefore require design rules to cover such phenomena. Plate buckling related problems in steel structures are inherently linked to complex solution strategies and design procedures. They involve stability analysis in the post-critical state, interaction of different failure modes, imperfection sensitivity, etc.

It is very likely in many cases to have holes in the plate elements for inspection, maintenance, and service purposes, and the size of these holes could be significant. In such cases, the presence of these holes redistributes the membrane stresses in the plate and may cause significant reduction in its strength in addition to changing its buckling characteristics.

The behaviour of a plate under applied loads may be classified into five regimes: pre-buckling, buckling, post-buckling, ultimate strength, and post-ultimate strength. Two methods have been used extensively for determining the buckling load (or stress) in plates subjected to uniaxial, biaxial, and shear loadings, namely the finite element method (FEM).

In the pre-buckling regime, the structural response between loads and displacements is usually linear, and the structural component is stable. As the predominantly compressive stress reaches a critical value, buckling occurs. Unlike columns, in which buckling is meant to cause collapse, plates that buckle in the elastic regime may have sufficient redundancy to remain stable in the sense that further loading can be sustained until the ultimate strength is reached, even if the in-plane stiffness significantly decreases after the inception of buckling.

### Buckling under loadings

Slender plates in compression possess significant post critical resistance that can be utilized in design procedures for plated structural. For geometrically perfect plates pre- and post-critical behaviour is very evident, while for imperfect plates the transition between pre- and post-critical behaviour is gradual and for larger imperfections nearly imperceptible. It is important that after reaching the elastic critical stress the resistance is not exhausted, but it increases further until plastic collapse occurs.

As for plates subjected to direct compressive stress, slender plates under shear possess a post-critical reserve. After buckling, the plate reaches the post-critical stress state, while a shear buckle forms in the direction of the principal tensile stresses 1. Due to buckling, no significant increase of the stresses in the direction of the principal compressive stresses is possible, whereas the principal tensile stresses can still increase. As a result, stress values of different magnitude occur (tension > compression), which lead to a rotation of the stress field for equilibrium reasons and which is denoted tension field action.

In an imperfect plate out-of-plane deformations begin immediately upon loading, such deformations lead to second order (geometrically nonlinear) forces (and strains) that must be accounted for throughout the loading/deformation, and thus the notions of buckling and post-buckling are not definitively distinct.

Currently, inelastic buckling, post-buckling, and the strength of thin plates analyses are examined through the use of numerical methods such as finite element analysis modelling. The nonlinear numerical models include the material stress-strain relation the yield criterion the hardening



law (isotropic hardening is the most common for static loading, but is inadequate if large strain reversals are present).

### **Motivation and objective of the present work**

Exploring the impact of different buckling phenomenon on the elastic and inelastic behaviour of steel plates with and without cut-out under several static loadings is quite interesting by considering parameters that are believed to greatly influence the elastic and inelastic buckling. These parameters are: thickness of the plates; kind and size of the cut-out. The numerical modelling of the plates has been developed through well-known software: EBPLATE for elastic buckling analysis and ABAQUS for both elastic and inelastic buckling behaviours of plates. By performing this task, the author of this dissertation has learned how to deal with complex analyses in 3D models.

### **Structure of the thesis**

This dissertation has been structured into six chapters as follows:

- **An introduction** providing a brief information on the work undertaken in this study and its objectives.
- **Chapter 1:** This chapter presents an overview on general introduction to buckling of steel plates the behaviour of steel plates including the buckling of perforated steel plates.
- **Chapter 2:** This chapter is aimed at giving a brief account elastic and inelastic analytical buckling of steel thin plates under several loading cases.
- **Chapter 3:** This chapter deals with the use of the analysis of steel structures elastic and inelastic buckling of plates using finite element.
- **Chapter 4:** This chapter presents ample information on the software used in this research work: EBPLATE and Abaqus. Examples on performing the buckling analyses are also given.
- **Chapter 5:** Explains the operation of validation and verification of models on non-Perforated and perforated thin plates by comparing results.
- **Chapter 6** This chapter details the personal work done in this thesis which is a parametric elastic and inelastic FEA.
- **Conclusions:** conclusions and suggestions for further work: Main conclusions are drawn with some suggestions for further work.

**CHAPTER 1**  
**GENERAL INTRODUCTION TO BUCKLING OF**  
**STEEL PLATES**

This chapter concerns a general presentation of the steel thin plates accompanied with a succinct literature review on the topic of this dissertation. The buckling behaviour is also highlighted.

### **1.1. General**

In many ways structural steel is an ideal material for the design of resistant structures. It is strong, light weight, ductile, and tough, capable of dissipating extensive energy through yielding when stressed into the inelastic range. Steel is a mixture of iron and carbon, with trace amounts of other elements, including principally manganese, phosphorus, sulphuric, and silicon. In addition, as with all structural materials, it is very important to assure that the structures are actually constructed as designed, that quality is maintained in fabrication and field welding operations, and that the structure is maintained over its life.

Most of structural steel members are composed of flat plate elements, which form flanges and webs of the cross sections. The performance of these members to carry loads depends mainly upon the properties of the members as a whole as well as the properties and the behaviour of the plate elements. [1]

### **1.2. Plate Elements in Steel Members**

Large varieties of structural steel shapes are manufactured. The cross-sectional shape and the size are governed by the arrangement of the material for an optimum structural efficiency, functional requirements, dimensional and weight capacity of rolling mills, and material properties. These four sets of criteria lead for most cases, to use steel sections, as stated in EC3, as an assembly of flat rectangular plates joined at right angle to form flanges and webs of their cross sections.

In Fig.1.1 several cross-sectional shapes for metal compression or flexural members are presented. Excluding the hollow cylinders, all members are composed of connected elements which, for purposes analysis and design, can be treated as flat plates. Use steel sections consist of an assembly of flat rectangular plates joined at right angle to form flanges and webs of their cross sections. [1]

When a plate element is under direct compression, bending, shear, or a combination of these stresses in its plane, theoretical critical loads may be assessed and signifying that the plate may buckle locally before the member, as a whole, becomes unstable or before the yield stress of the material is reached. Such behaviour is characterized by distortion of the cross section of the member. The almost inevitable presence of initial out-of-straightness may result in a gradual

development of cross-sectional distortion with no sudden discontinuity in real behaviour at the theoretical critical load.

A number of metal cross-sectional shapes for metal compression or flexural members are shown in Figure.1.1. All members are composed of connected elements which, for purposes analysis and design, can be treated as flat plates, except for the hollow cylinders. When a plate element is subjected to direct compression, bending, shear, or a combination of these stresses in its plane, theoretical critical loads may be evaluated indicating that the plate may buckle locally before the member as a whole becomes unstable or before the yield stress of the material is reached. Such behaviour is characterized by distortion of the cross section of the member. The almost inevitable presence of initial out-of-straightness may result in a gradual growth of cross-sectional distortion with no sudden discontinuity in real behaviour at the theoretical critical load.

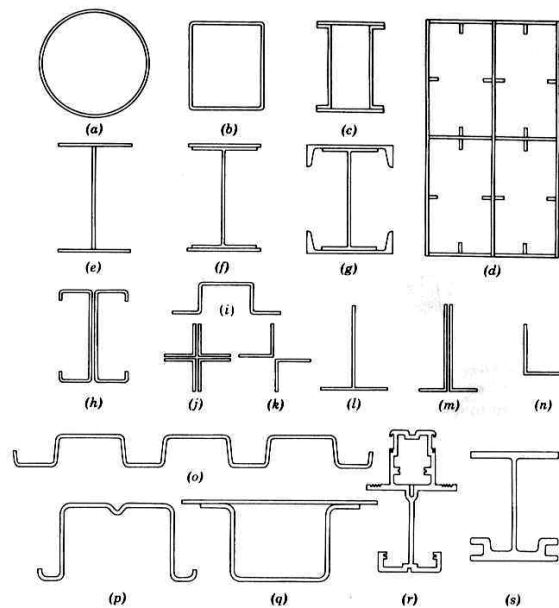


**Figure 1.1 Compression or flexural members Section shapes (Galambos, 1998)**

The theoretical critical load for a plate is not necessarily a satisfactory basis for design, since the ultimate strength can be much greater than the critical buckling load. For example, a plate loaded in uniaxial compression, with both longitudinal edges supported, will undergo stress redistribution as well as develop transverse tensile membrane stresses after buckling that provide post-buckling support. Thus, additional load may often be applied without structural damage. Initial imperfection in such a plate may cause bending to begin below the buckling load, yet unlike an initially imperfect column, the plate may sustain loads greater than the theoretical buckling load. [2]

### 1.3. Buckling of steel members

Buckling is caused by in-plane stresses exceeding the buckling stability of the structure, causing local yield and permanent deformation of the structure. The buckling capacity is a property of the plate, depending on many factors. Two cases of instability may occur, that is overall or global column instability and plate element local instability. Local buckling of plate elements in a steel column can cause premature failure of the entire section and reduce the overall strength. The mode of failure and load carrying capacity of steel columns are affected by the behaviour of plate elements and the interaction between local and overall buckling.

Buckling can be classified into three states:

1. Elastic buckling: occurs only in the elastic regime of the stress -strain material graph.
2. Elastic - plastic buckling: occurs when a local region inside the plate experiences a plastic deformation.
3. Plastic buckling: happens after the plate has yielded over large regions.

Many factors affect the buckling behaviour of panels, including geometric or material properties, loading characteristics, boundary conditions, initial geometrical imperfections, and material nonlinearity.

### 1.4. Buckling of steel thin plates

The behaviour of a plate under applied loads may be classified into five regimes: pre-buckling, buckling, post-buckling, ultimate strength, and post-ultimate strength. In the pre-buckling regime, the structural response between loads and displacements is usually linear, and the structural component is stable. As the predominantly compressive stress reaches a critical value, buckling occurs. Unlike columns, in which buckling is meant to cause collapse, plates that buckle in the elastic regime may have sufficient redundancy to remain stable in the sense that further loading can be sustained until the ultimate strength is reached, even if the in-plane stiffness significantly decreases after the inception of buckling. In this regard, the elastic buckling of a plate between stiffeners may in some design cases be allowed to reduce the structural weight associated with efficient and economic design.

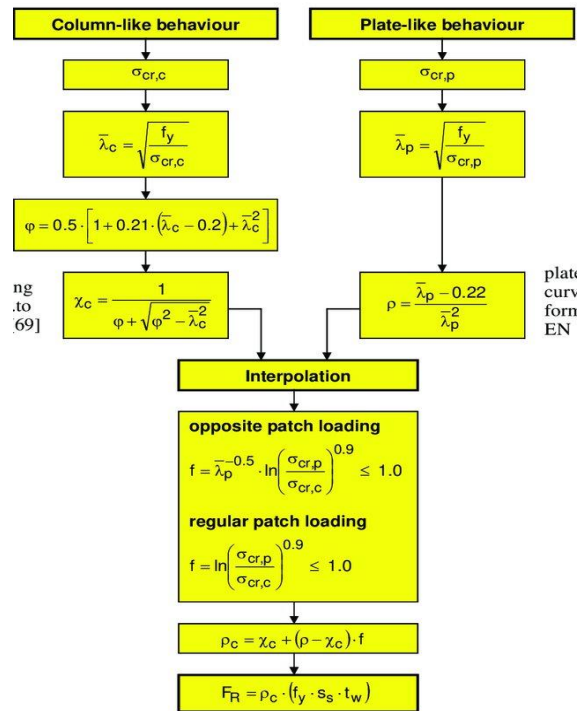


Figure 1.2 Flowchart of buckling of like-column and like-plate

As reported in (Wang et.al 2009), the stability of plates is one of the most important design considerations to ensure that the plated structures do not fail prematurely. Much research studies on the elastic-buckling of plates have been done and are well documented in text books, monographs, and handbooks such as Timoshenko and Gere 1961; Bulson 1970; Shanmugam and Wang 2006; and Handbook for Structural Stability 1971.

The effect of local plate buckling on the strength of the entire member depends upon the location of the buckled element, its buckling and post-buckling strength, and the type of the member.

### 1.5. Local Buckling

Thin-walled steel structures are susceptible to local buckling if the in-plane stresses, that is that stresses in the plane of the plate elements reach their critical value. If this occurs, the geometry of the cross-section of the structure changes. However, if a thin-walled column is made sufficiently slender (class 4 to EC3) it may suffer overall buckling before it buckles locally. This means that thin-walled structures must be designed against both local and overall buckling with, eventually an interaction of two phenomena. When this happens, the buckling load can be depressed below the value of the individual buckling loads (Murray, 1986). [3]

Slender compression members that are not susceptible to torsional, or flexural- torsional buckling will lose their stability by flexural buckling. Doubly symmetric sections and closed sections, axially loaded, do not have any tendency to twist if they are of dimensions commonly used in structures.

Due to different load cases, the structure is subjected to a variety of phenomena, which can be accounted for by the non-linear behaviour. It also accounts for the possible interactions between those forces and phenomena, and this interaction may be difficult to formulate. Moreover, problems become non-linear when stiffness and loads become a function of displacement and deformation. Those phenomena in structures may be material yielding, plastic strain local buckling of members, and holes in the geometry.

### 1.6. Non-linear buckling capacity

Nonlinear problems induce the difficulty of describing phenomena by realistic mathematical and numerical models and the difficulty of solving nonlinear resultant equations. The effort required of the analyst increases substantially when a problem becomes nonlinear. Computational cost may also be a concern, despite the growing capability of computers.

Problems become non-linear when stiffness and loads become a function of displacement and deformation, in buckling structures. Nonlinear problems pose the difficulty of describing phenomena by realistic mathematical and numerical models and the difficulty of solving nonlinear equations. The effort required of the analyst increases substantially when a problem becomes nonlinear. Computational cost may also be a concern, despite the growing capability of computers. (Cook et al 1989). Nonlinearity include the following:

**Material nonlinearity:** where material properties are functions of stress strain relation, including the elastic, plastic, and creep phases.

**Contact nonlinearity,** in which a gap between adjacent parts may open or close, the contact area between parts changes as the contact force changes, or there is sliding contact with frictional forces.

**Geometrical nonlinearity:** when the displacement and the alteration in the geometry become large enough to influence the equilibrium equations so that they must include the deformed geometry. In addition to loads, directions that might change as they increase and the geometry deform (Cook et al 1989).

For buckling analyses, it is necessary to introduce equivalent geometric imperfections in order to predict the buckling capacity. This will be discussed further in the next chapters. The non-linear buckling analysis is not intended to replace the determination of structural buckling resistance according to traditional standards but to cover the cases that are not within the limitations of the standards.

When using FE methods to analyse buckling resistance, it is critical to account for the statistical

variation of the different parameters. This is done so that the results reflect a safe estimate when compared to the results acquired, if physical testing could be performed. When the statistical variance is uncertain, the best engineering judgment must be applied to choose the regulating parameters. [1]

## **1.7. Perforated Steel Plates**

### **1.7.1. General**

Thin steel plate elements constitute very important structural components in many structures, such as ship grillages and hulls, dock gates, plate and box girders of bridges, platforms of offshore structures, and structures used in aerospace industries. In many cases, these plates are subjected to axial compressive forces which make them prone to instability or buckling. If the plate is slender, the buckling is elastic. However, if the plate is sturdy, it buckles in the plastic range causing the so-called inelastic (or elasto-plastic) buckling.

It is very likely in many cases to have holes in the plate elements for inspection, maintenance, and service purposes, and the size of these holes could be significant. In such cases, the presence of these holes redistributes the membrane stresses in the plate and may cause significant reduction in its strength in addition to changing its buckling characteristics. Two methods have been used extensively for determining the buckling load (or stress) in plates subjected to uniaxial, biaxial, and shear loadings, namely the finite element method (FEM).

Many thin-walled structures contain holes. In marine and offshore structures, the perforated panels are used to make a way of access or to reduce the total weight of the structure. When these plates are subject to compression loads, the structure could buckle if the load exceeds the critical load. Thus, to know how this phenomenon occurs and to analyse the buckling behavior of these perforated panels has great importance for an efficient structural design. An example of a ship hull with circular holes is shown in FIGURE 1.

### **1.7.2. Buckling of perforated steel plates**

The elastic buckling is an instability phenomenon that can occur if a slender and thin-walled plate (plane or curved) is subjected to axial compression. At a certain given critical-loads, the plate will suddenly bend in the out-of-plane transverse direction. However, if the plate is sturdy, it buckles in the plastic range causing the so-called inelastic (or Elasto-plastic) buckling. Although the elastic buckling of such thin perforated plates has received the attention of many researchers over the past two decades, very little has been reported on the inelastic buckling of thicker plates.

The problem of elastic and inelastic buckling of a simply supported perforated plate subjected to uniaxial end compression along its longitudinal direction is considered.



## 1.8. Succinct literature review of the buckling of thin plates

In studies of a numerical character, such as this, it is essential to deploy a satisfactory foundation of previous research within the field of buckling – hence the need of an adequate literature survey. The synthesis of the survey's outcome will then form the theoretical background to the first part of the dissertation.

The aim of the first part is to perform parametric studies where the impact on the buckling load of variables such as geometry, load cases, thicknesses of plates along with the kind and positions of the cut-outs. Are studied. [2]

### Plate in general

Early works on the buckling problems can be found in the literature including those relative to Timoshenko (1910), Leggett (1937), Zetlin (1955), White and Cottingham (1962), Bulson (1969), Hopkins (1969), Khan and Walker (1972), Khan et al. (1977), and Young and Lui (2005). The first work in this area was perhaps reported [4]

Shakerley and Brown (1996) investigated elastic buckling of simply supported and fully fixed plates with eccentrically placed rectangular cut-outs using conjugate method. Their results were given for uniaxial compression and shear loading. Bert and Devarakonda (2003) studied the buckling of rectangular plates subjected to non-linearly distributed in-plane loading using analytical solution method. They considered a rectangular plate subjected to parabolic loads along with the removal of some deficiencies of earlier reported work. Zhong and GU (2006) reported a study on the buckling analysis of simply supported rectangular plates subjected to linearly varying edge loads. An analytical solution to buckling problem was developed and the effect of load intensity variation on the critical load was investigated.

Recently, Mijušković et al. (2014) presented an accurate buckling analysis for thin rectangular plates under locally-distributed compressive stresses. Interestingly, Wang et al.'s (2007) and Wang's (2015) studies have also shown that the differential quadrature method can yield accurate buckling loads for rectangular plates under uniformly or non-uniformly distributed edge compressions. It is also noteworthy that some other researchers have conducted comprehensive research, most recently, on the buckling of shells and plates, e.g. McCann et al. (2016), Riahi et al. (2017 and 2018), and Vu et al. (2019).

### - On perforated steel plates

Daniel Helbig et al. Study About Buckling Phenomenon in Perforated Thin Steel Plates Employing Computational Modeling and Constructal Design Method

For the particular case of perforated thin-walled, there are several studies focused in analysing the buckling behaviour of plates with openings. In the elastic buckling behaviour, El-Sawy and Nazmy (2001) investigated the effect of aspect ratio on the elastic buckling critical loads of uniaxially loaded rectangular plates with eccentric circular and rectangular (with curved corners) holes. Also, El-Sawy and Martini (2007) used the FEA to determine the elastic buckling stresses of biaxially loaded perforated rectangular plates with longitudinal axis located circular holes. Alternatively, Moen and Schafer (2009) developed, validated and summarised analytical expressions for estimating the influence of single or multiple holes on the elastic buckling critical stress of plates in bending or compression. In Rocha et al. (2012), Isoldi et al. (2013) and Rocha et al. (2013a) the constructal design method was employed to determine the best shape and size of centred cut-out in a plate, aiming to maximize the critical buckling load. Regarding the researches dedicated to the elasto-plastic buckling, El-Sawy et al. (2004) investigated the elasto-plastic buckling of uniaxially loaded square and rectangular plates with circular cut-outs by the use of the finite element method, including some recommendations about hole size and location for perforated plates of different aspect ratios and slenderness ratios.

Afterwards, Paik (2007a), Paik (2007b) and Paik (2008) studied the ultimate strength characteristics of perforated plates under edge shear loading, axial compressive loading, combined biaxial compression and edge shear loads. Moreover, Paik proposed closed-form empirical formulae for predicting the ultimate strength of perforated plates based on the regression analysis of the nonlinear finite element analyses results. Maiorana et al. (2008) and Maiorana et al. (2009) focused on the linear and nonlinear finite element analyses of perforated plates subjected to localized symmetrical load.

More recently, in Helbig et al. (2014) and in Lorenzini et al. (2016a, 2016b) the elastic and elasto-plastic buckling of perforated plates were analysed, applying the computational modelling allied to the constructal design method. These last authors investigated the influence of shape and type of centred cut-outs in the plate buckling, defining a stress limit curve to avoid the buckling occurrence in each studied case. [5]

## 1.9. Conclusion

Details on buckling of steel plates has been succinctly presented in this chapter.

In structural engineering, thin-walled structures play an important role in the design of the lightweight structural model. It carries different loading conditions when it exists in any model, and it is designed with thin plates or thin shells. Penetrating thin-walled structures with different kinds of holes can decrease their weight and facilitate repair and maintenance operations, such as those carried out for the wing of an airplane. In such applications, cut-outs are often employed as part of the design of composite plates.

In order to improve the knowledge about how the buckling load of plates is affected when geometrical parameters, different types of load, and geometrical cases are changed, a parametric study will be presented in the following chapters.

**CHAPTER 2**  
**ELASTIC AND INELASTIC ANALYTICAL**  
**BUCKLINGS OF STEEL THIN PLATES**

## **2.1 Plate Theory Development and Buckling**

### **2.1.1 Introduction**

A beam is a bar, possessing length significantly greater than the depth and width. While plates and shells are initially flat and curved surface structures, respectively, whose thicknesses are slight compared to their other dimensions. Beams are usually loaded in a direction normal to the longitudinal axis, while bars are axially loaded or twisted. Because of the one-, two-, and three-dimensional (3D) load-carrying capacity, the foregoing members are extensively used in various applications in all fields of engineering.

Load-supporting action of plates resembles, to a certain extent, that of beams. However, the load-carrying mechanism of a shell differs from that of other structural forms.

Because of the distinct advantages discussed below, thin plates are extensively used in all fields of engineering. Plates are used in architectural structures, bridges, hydraulic structures, pavements

The classical theory of plates or shells, which formulates and solves problems from the point of view of rigorous mathematical analysis, is an important application of the theory of elasticity. The study of mechanics of materials and the theory of elasticity is based on an understanding of equilibrium of bodies under action of forces. While statics treats the external behaviour of bodies that are assumed to be ideally rigid and at rest, mechanics of materials and the theory of elasticity are concerned with the relationships between external loads and internal forces and deformations induced in the body.

Mechanics of materials and theory of elasticity methods are used to determine strength, stiffness, and stability of variously loaded members, or possible modes of failure. In most general terms, failure refers to any action resulting in an inability on the part of the structure to function in the manner intended. The ability of a member to resist yielding or fracture is called strength. The stiffness refers to the ability of a member to resist deformation. It is often necessary to limit the magnitude of displacement in the member for it to function in normal service. The ability of the structure to retain its equilibrium configuration under loading is termed stability. Instability occurs if the loading produces an abrupt shape change of a member.

### **2.1.2 Definition and terminology**

Once again, thin plates are initially flat structural members bounded by two parallel planes, called faces, and a cylindrical surface, called an edge or boundary. The generators of the cylindrical surface are perpendicular to the plane faces. The distance between the plane faces is called the thickness ( $h$ ) of the plate. It will be assumed that the plate thickness is small compared with other characteristic dimensions of the faces (length, width, diameter, etc.). Geometrically, plates are

bounded either by straight or curved boundaries. It must be noted that the static or dynamic loads carried by plates are predominantly perpendicular to the plate faces.

- **Loadings**

Steel-plated structures are likely to be subjected to various types of loads and deformations arising from service requirements that may range from the routine to the extreme or accidental. The mission of the structural designer is to design a structure that can withstand such demands throughout its expected lifetime. [6]

- **Classification of plates:**

According to (Mesmar 2016), plates are generally classified as:

- **Thick plates:**

When the plate minimum dimension to thickness ratio ( $b/h$ ) is less than 10. While thick plates develop internal load resultants, governed by three-dimensional elasticity to counterbalance the applied load.

- **Thin plates:**

When  $b/h$  ranges from 10 to 100. Thin plates behave as plane stress members provided that the plate maximum deflection to plate thickness ratio ( $w/h$ ) is less than 0.2. In this case, the plate develops internal load resultants, governed by two-dimensional elasticity to counterbalance the applied loading.

- **Membranes:**

When the  $b/h$  ratio approaches 100 and  $w/h > 0.2$ . Membranes are only capable of developing internal tensile stress resultants, namely, membrane tensile force resultants acting within the plate middle plane (Yamaguchi and Wai-Fah, 1999; Ventsel and Krauthammer, 2001; Stephen et al. 2010). [6]

### 2.1.3 General behaviour of plates

When a certain structural member undergoes buckling, its load-carrying capacity decreases. This causes redistribution of internal forces in unbuckled structural members and increases the internal forces in these structural members, which may lead to the progressive occurrence of buckling failure of these structural members. If the load increases further, progressive buckling may result in the collapse of a whole structure. This was the reason why occurrence of buckling was not allowed in any members in ship structures in old classification societies' rules.

In a strict sense, buckling is a bifurcation phenomenon that stable deformation changes from in-plane (or axial) deformation to in-plane (or axial) plus out-of-plane deformations.

Therefore, to have buckling in a strict sense, the structural member has to be completely flat (or straight) before it is loaded; that is, it has to be completely free from initial distortion/deflection

#### 2.1.4. Brief history of theory of plates [9]

Bellow, a very brief survey summary, taken from [9] of the historical background of the plate bending theory and its application is given.

The first impetus to a mathematical statement of plate problems, was probably done by Euler, who in 1776 performed a free vibration analysis of plate problems. Chladni, a German physicist, discovered the various modes of free vibrations. In experiments on horizontal plates, he used evenly distributed powder, which formed regular patterns after induction of vibration. The powder accumulated along the nodal lines, where no vertical displacements occurred. J. Bernoulli attempted to justify theoretically the results of these acoustic experiments. Bernoulli's solution was based on the previous work resulting in the Euler–D.Bernoulli's bending beam theory. J. Bernoulli presented a plate as a system of mutually perpendicular strips at right angles to one another, each strip regarded as functioning as a beam. But the governing differential equation, as distinct from current approaches, did not contain the middle term.

The French mathematician Germain developed a plate differential equation that lacked the warping term. Lagrange was the first person to present the general plate equation properly. Cauchy and Poisson were first to formulate the problem of plate bending on the basis of general equations of theory of elasticity. Expanding all the characteristic quantities into series in powers of distance from a middle surface, they retained only terms of the first order of smallness. In such a way they obtained the governing differential equation for deflections that coincides completely with the well-known Germain–Lagrange equation. In 1829 Poisson expanded successfully the Germain–Lagrange plate equation to the solution of a plate under static loading. In this solution, however, the plate flexural rigidity  $D$  was set equal to a constant term. [8]

In 1850 Kirchhoff published an important thesis on the theory of thin plates. In this thesis, Kirchhoff stated two independent basic assumptions that are now widely accepted in the plate-bending theory and are known as “Kirchhoff's hypotheses.” Kirchhoff's theory contributed to the physical clarity of the plate bending theory and promoted its widespread use in practice.

Lord Kelvin (Thomson) and Tait provided an additional insight relative to the condition of boundary equations by converting twisting moments along the edge of a plate into shearing forces. Thus, the edges are subject to only two forces: shear and moment.

Saint-Venant also pointed out that the series proposed by Cauchy and Poisson as a rule, are divergent. The solution of rectangular plates, with two parallel simple supports and the other two supports arbitrary, was successfully solved by Levy in the late 19th century.

Timoshenko made a significant contribution to the theory and application of plate bending analysis. Among Timoshenko's numerous important contributions are solutions of circular plates

considering large deflections and the formulation of elastic stability problems. Timoshenko and Woinowsky-Krieger published a fundamental monograph that represented a profound analysis of various plate bending problems.

A differential equation of motion of thin plates may be obtained by applying either the D’Alambert principle or work formulation based on the conservation of energy. The first exact solution of the free vibration problem for rectangular plates, those two opposite sides are simply supported, was achieved by Voight. Ritz used the problem of free vibration of a rectangular plate with free edges to demonstrate his famous method for extending the Rayleigh principle for obtaining upper bounds on vibration frequencies. Poisson analysed the free vibration equation for circular plates. The monographs by Timoshenko and Young, Den

Hartog, Thompson, etc., contain a comprehensive analysis and design considerations of free and forced vibrations of plates of various shapes. A reference book by Leissa presents a considerable set of available results for the frequencies and mode shapes of free vibrations of plates could be provided for the design and for a researcher in the field of plate vibrations.

The recent trend in the development of plate theories is characterized by a heavy reliance on modern high-speed computers and the development of the most complete computer-oriented numerical methods, as well as by introduction of more rigorous theories with regard to various physical effects, types of loading, etc. [9]

## **2.2 Analytical Elastic Local Buckling of Flat Plates**

### **2.2.1 General**

Thin plates or sheets, although quite capable of carrying tensile loadings, are poor in resisting compression. Usually, buckling or wrinkling phenomena observed in compressed plates (and shells) take place rather suddenly and are very dangerous. Fortunately, there is close correlation between theory and experimental data concerned with buckling of plates subjected to various types of loads and edge conditions.

When a plate is compressed in its midplane, it becomes unstable and begins to buckle at a certain critical value of the in-plane force. It must be recalled that the behaviour of flat plates after buckling is of considerable interest. The post-buckling analysis of plates is usually difficult to assess since it is basically a nonlinear problem. As mentioned earlier, buckling of plates is qualitatively similar to some extent to column buckling. Classical buckling problems are solved by the so-called equilibrium method and the conditions that result in the lowest eigenvalue, or the actual buckling load, are not at all obvious in many situations.



Indeed, the structural design criteria to prevent the ULS are based on plastic collapse or ultimate strength. The simplified ULS design of many types of structures including merchant ship structures has in the past tended to rely on estimates of the buckling strength of components, usually from their elastic buckling strength adjusted by a simple plasticity correction.

This is represented by point A in Figure 2.1. In such a design scheme based on strength at point A, the structural designer does not use detailed information on the post-buckling behavior of component members and their interactions. The true ultimate strength represented by point B in Figure 2.1 may be higher although one can never be sure of this since the actual ultimate strength is not being directly evaluated.

The plate, being originally flat, develops shear forces, bending and twisting moments to resist transverse loads. Because the loads are generally carried in both directions and because the twisting rigidity in isotropic plates is quite significant, a plate is considerably stiffer than a beam of comparable span and thickness. So, thin plates combine light weight and a form efficiency with high load-carrying capacity, economy, and technological effectiveness.

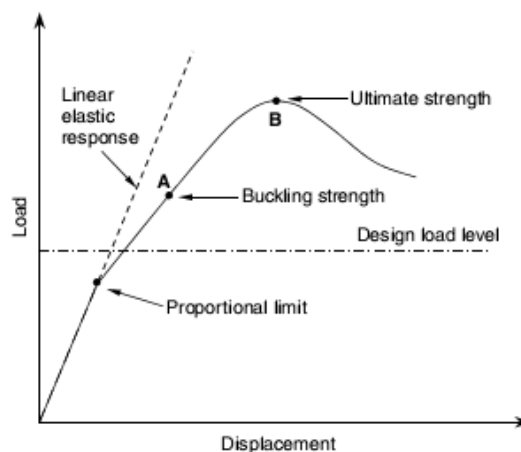


**Figure 2.1 Structural design considerations based on the ultimate limit state**

### 2.2.2 Loadings [10]

- **Uniform compression**

**Long plates:** in 1891, Bryan (1891) presented the analysis of the elastic critical stress for a rectangular plate simply supported along all edges and subjected to a uniform longitudinal compressive stress. The elastic critical stress of a long plate segment is determined by the plate width-to-thickness ratio  $b/t$ , by the restraint conditions along the longitudinal boundaries, and by the elastic material properties (elastic modulus,  $E$ , and Poisson's ratio  $\nu$ ). In the following, only finally results will be given for the elastic critical stress,  $\sigma_c$  is expressed as

$$\sigma_c = k \frac{\pi^2 E}{12(1-\nu^2)(b/t)^2}$$

In which  $k$  is a plate buckling coefficient determined by a theoretical critical-load analysis;  $k$  is a function of plate geometry and boundary conditions such as those shown in Fig. 2.2 bellow.

For short plates, that is when a plate element is relatively short in the direction of the compressive stress, there may exist an influence in the elastic buckling stress due to the fact that the buckled half waves which take integer values are forced into a finite length plate.

Fig. 2.2 demonstrates how  $k$  varies as a function of normalized plate length; the variation is a function of the plate boundary conditions and the loading. Full analytical solutions for  $k$  as a function of  $a/b$  and  $m$  may be found in Timoshenko and Gere (1961),

Allen and Bulson (1980) and others. When a plate element is very short in the direction of the compressive stress (i.e.  $a/b \ll 1$ ), the critical stress may be conservatively estimated by assuming that a unit width of plate behaves like a column.

- **Compression and Bending**

When compression plus bending loads are applied to a structural member, plate elements of the member can be subjected to in-plane stresses which vary along the loaded edges of the plate, from a maximum compressive stress,  $\sigma_1$ , to a minimum stress,  $\sigma_2$ , as shown in Fig. 4.4. For this situation, elastic critical plate stresses are dependent on the edge-support conditions and the ratio of bending stress to uniform compression stress. Long plate values of  $kc$  that can be substituted for  $k$  in Eq. 4.1 are tabulated in Fig. 2.3 for several cases. For plates with a free edge the  $kc$  values vary slightly with Poisson's ratio.

Beyond the  $k$  values provided in Fig. 2.3 closed-form expressions also exist for the compression and bending case. For plates simply supported on all four sides  $k$  may be found based on the work of Peköz (1987) to be:

$$kc = 4 + 2(1 - \psi)3 + 2(1 - \psi)c$$

Where  $\psi = \sigma_1 / \sigma_2$ . For plates with one longitudinal edge free Bambach and Rasmussen (2004a) provide a series of solutions summarized in Fig. 2.4. These closed-form expressions for  $k$  are employed in the AISI (2007) Specification. Diagrams for buckling coefficients for rectangular plates under combined bending and compressive stresses in two perpendicular directions are given by Yoshizuka and Naruoka (1971).

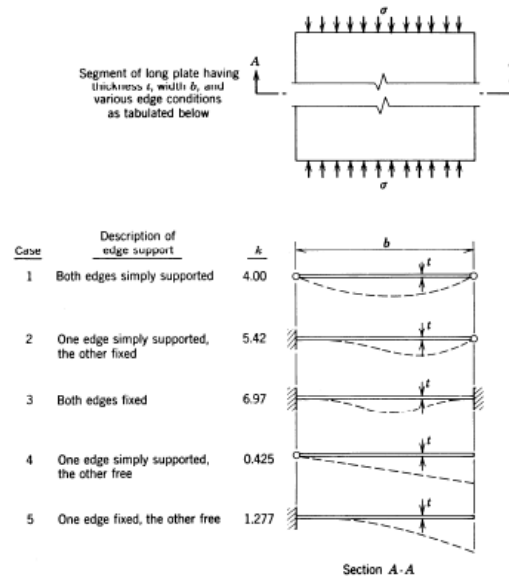


Fig. 2.2 Local plate buckling coefficient, k for plates in compression with varied boundary conditions [10]

Loading	Ratio of Bending Stress to Uniform Compression Stress $\sigma_2/\sigma_1$	Minimum Buckling Coefficient, $k_c$					
		Unloaded Edges Simply Supported	Unloaded Edges Fixed	Top Edge Free		Bottom Edge Free	
				Bottom Edge Simply Supported	Bottom Edge Fixed	Top Edge Simply Supported	Top Edge Fixed
	= (pure bending)	23.9	39.6	0.85	2.15		
	5.00	15.7					
	2.00	11.0					
	1.00	7.8	13.6	0.57	1.61	1.70	5.93
	0.50	5.8					
	0.0 (pure compression)	4.0	6.97	0.42	1.33	0.42	1.33

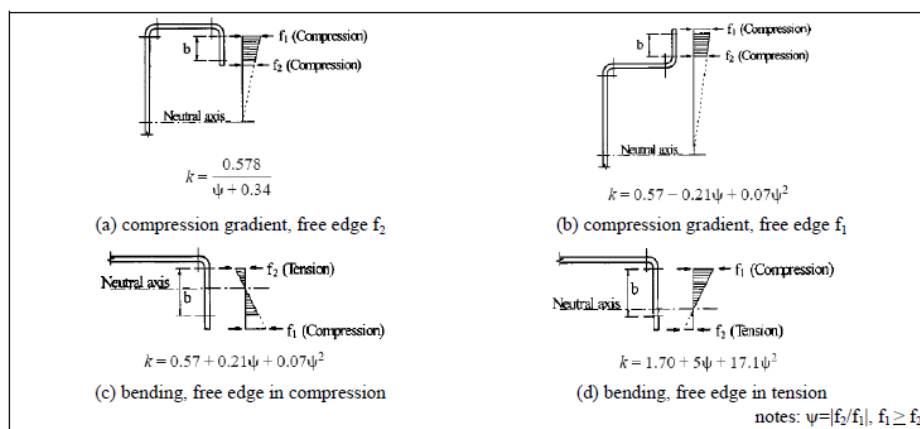
\*Values given are based on plates having loaded edges simply supported and are conservative for plates having loaded edges fixed.

Fig.2.3 Plate buckling coefficients for long plates under compression and bending.

Beyond the  $k$  values provided in Fig. 2.3 closed-form expressions also exist for the compression and bending case. For plates simply supported on all four sides  $k$  may be found based on the work of Peköz (1987) to be:

$$kc = 4 + 2(1 - \psi)3 + 2(1 - \psi)c$$

Where  $\psi = \sigma_1 / \sigma_2$ . For plates with one longitudinal edge free Bambach and Rasmussen (2004a) provide a series of solutions summarized in Fig. 2.4. These closed-form expressions for  $k$  are employed in the AISI (2007) Specification. Diagrams for buckling coefficients for rectangular plates under combined bending and compressive stresses in two perpendicular directions are given by Yoshizuka and Naruoka (1971).



**Fig. 2.4 Plate buckling coefficients for unstiffened elements in compression and bending, after (Bambach and Rasmussen 2004a)**

- **Shear**

When a plate is subjected to edge shear stresses as shown in Fig. 2.5, it is said to be in a state of pure shear. The critical shear buckling stress can be obtained by substituting  $\tau_c$  and  $k_s$ , for  $\sigma_c$  and  $k$  in the equation, in which  $k_s$  is the buckling coefficient for shear buckling stress.

Critical stress coefficients,  $k_s$  for plates subjected to pure shear have been evaluated for three conditions of edge support. These are plotted with the side  $b$ , as used in the equation, always assumed to be shorter than side  $a$ . Thus  $\alpha$  is always greater than 1 and by plotting  $k_s$  in terms of  $1/\alpha$ , the complete range of  $k_s$  can be shown and the magnitude of  $k_s$  remains manageable for small values of  $\alpha$ .

However, for application to plate-girder design it is convenient to define  $b$  (or  $h$  in plate girder applications) as the vertical dimension of the plate-girder web for a horizontal girder.

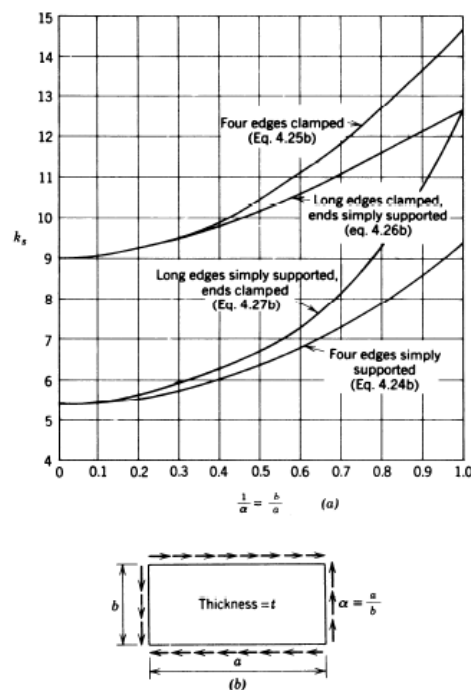
Then  $\alpha$  may be greater or less than unity and empirical formulas for  $k_s$  together with source data are as follows:

Plate Simply Supported on Four Edges. Solutions developed by Timoshenko (1910), Bergmann and Reissner (1932), and Seydel (1933) are approximated by equations in which  $\alpha = a/b$ :

$$k_s = \begin{cases} 4.00 + \frac{5.34}{\alpha^2} & \text{for } \alpha \leq 1 \\ 5.34 + \frac{4.00}{\alpha^2} & \text{for } \alpha \geq 1 \end{cases}$$

Plate Clamped on Four Edges. In 1924, Southwell and Skan obtained  $k_s = 8.98$  for the case of the infinitely long rectangular plate with clamped edges. For the finite-length rectangular plate with clamped edges, Moheit (1939) obtained

$$k_s = \begin{cases} 5.6 + \frac{8.98}{\alpha^2} & \text{for } \alpha \leq 1 \\ 8.98 + \frac{5.6}{\alpha^2} & \text{for } \alpha \geq 1 \end{cases}$$



**Fig. 2.5 Plate buckling coefficients for plates in pure shear. (Side b is the short side.)**

Plate Clamped on Two opposite Edges and Simply Supported on the Other

$$k_s = \begin{cases} \frac{8.98}{\alpha^2} + 5.61 - 1.99\alpha & \text{for } \alpha \leq 1 \\ 8.98 + \frac{5.61}{\alpha^2} - \frac{1.99}{\alpha^3} & \text{for } \alpha \geq 1 \end{cases}$$

and for short edges clamped,

$$k_s = \begin{cases} \frac{5.34}{\alpha^2} + \frac{2.31}{\alpha} - 3.44 + 8.39\alpha & \text{for } \alpha \leq 1 \\ 5.34 + \frac{2.31}{\alpha} - \frac{3.44}{\alpha^2} + \frac{8.39}{\alpha^3} & \text{for } \alpha \geq 1 \end{cases}$$

Curves for  $\alpha \geq 1$  are plotted in Fig. 2.5. Tension and compression stresses exist in the plate, equal in magnitude to the shear stress and inclined at  $45^\circ$ . The destabilizing influence of compressive stresses is resisted by tensile stresses in the perpendicular direction, often referred to as ‘tension field action’ in the literature. Unlike the case of edge compression, the buckling mode is composed of a combination of several waveforms and this is part of the difficulty in the buckling analysis for shear.

- **Combined Shear and Compression**

The case of shear combined with longitudinal compression, with all sides simply supported, was treated by Iguchi (1938). His results are approximated by the following interaction equation, also shown graphically in:

$$\frac{\sigma_c}{\sigma_c^*} + \left( \frac{\tau_c}{\tau_c^*} \right)^2 = 1$$

Where  $\sigma_c$  and  $\tau_c$  denote critical stress, respectively, under compression or shear alone.

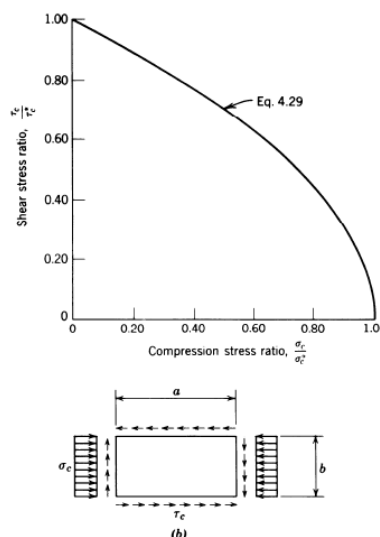


**Fig. 2.6 Interaction curve for buckling of flat plates under shear and uniform compression.**

The Equation shown in Fig. 2.6, is for ratios of  $a/b$  greater than unity. Batdorf and associates (Batdorf and Houbolt, 1946; Batdorf and Stein, 1947) have shown that when the loaded side  $b$  is more than twice as long as  $a$ , Eq. 4.29 becomes overly conservative. This situation is the exception in actual practice, and the equation may be accepted for engineering design purposes.

- **Combined Shear and Bending**

For a plate simply supported on four sides, under combined bending and pure shear, Timoshenko

(1934) obtained a reduced  $k_c$  as a function of  $\tau_c^*/\tau_c^*$  for values of  $\alpha = 0.5, 0.8, \text{ and } 2.0$ , where  $\tau_c$  is

The actual shearing stress and  $\tau_c$  is the buckling stress for pure shear. This problem was also solved by Stein (1936) and Way (1936), whose results for four values of  $\alpha$  are plotted in Fig. 2.7.

Chwalla (1936a) suggested the following approximate interaction formula, which agrees well with the graphs of Fig. 2.7.

$$\left(\frac{\sigma_{cb}}{\sigma_{cb}^*}\right)^2 + \left(\frac{\tau_c}{\tau_c^*}\right)^2 = 1$$

For a plate simply supported on four sides, under combined bending and direct stress at the ends (of dimension  $b$ ), combined with shear, an approximate evaluation of the critical combined load is obtained by use of a three-part interaction formula, next equation (Gerard and Becker, 1957/1958).

$$\frac{\sigma_c}{\sigma_c^*} + \left(\frac{\sigma_{cb}}{\sigma_{cb}^*}\right)^2 + \left(\frac{\tau_c}{\tau_c^*}\right)^2 = 1$$

The foregoing problem, with the further addition of vertical compressive force along the top and bottom edges of length  $a$ , has been treated by McKenzie (1964) with results given in the form of interaction graphs. The results are in good agreement with the special case of previous equation. Interaction previous equation, valid when  $a/b$  is greater than unity, is shown graphically in Fig. 2.8, as presented in Brockenbrough and Johnston (1974).

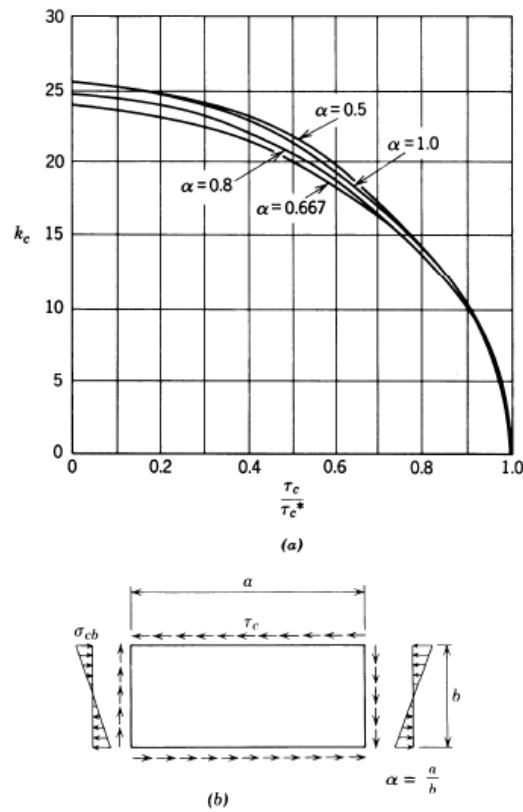


Fig. 2.7. Buckling coefficients for plates in combined bending and shear.

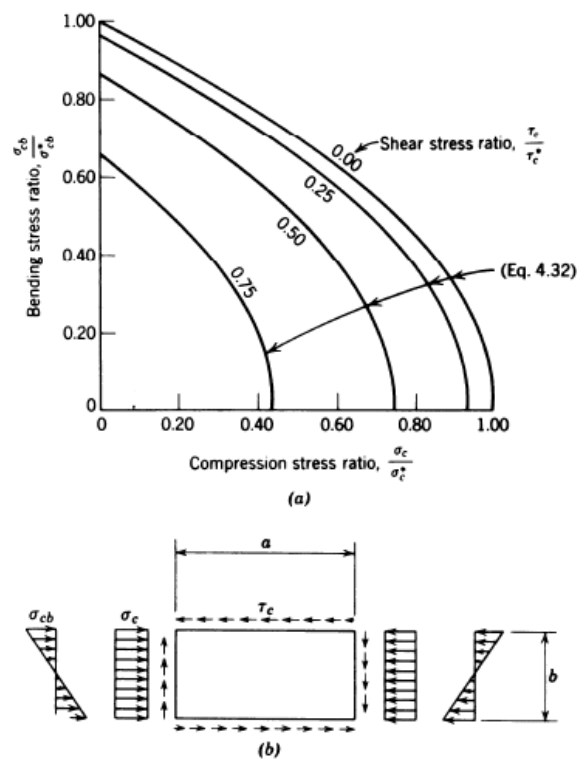


Fig. 2.8 Interaction curve for buckling of flat plates under shear, compression, and bending.



- **Biaxially Compressed**

Pavlovic and Baker (1989) presented an exact solution for the stability of a rectangular plate under biaxial compression. The case when both longitudinal and transverse stresses were uniform was used as a starting point to investigate the much more complex problem of partial loading on two opposite edges. A parametric study was carried out covering different plate geometrics, load ratios, and varying edge lengths over which the applied load acted. The limiting cases of very long and very wide plates were considered in the study, as was the problem in which two opposite edges were subjected to concentrated forces.

## 2.3 Inelastic Buckling, Post-Buckling and Strength of Flat Plates

- **General**

The elastic critical plate buckling stresses, or corresponding plate buckling coefficients ( $k$ 's), provided in the previous section represent an important benchmark for understanding the behaviour of thin plates. However, such elastic critical buckling stresses do not directly indicate the actual behaviour that may occur in such a thin plate. In thin plates loaded to failure material and geometric effects complicate the response.

Actual plate response under load is more complicated than the simple notions of inelastic buckling and post-buckling, this is due in part to unavoidable imperfections. In an imperfect plate out-of-plane deformations begin immediately upon loading, such deformations lead to second order (geometrically nonlinear) forces (and strains) that must be accounted for throughout the loading/deformation, and thus the notions of buckling and post-buckling are not definitively distinct.

These are the focus of this section. In particular, the effective width method, has wide use as an approximate technique for determining ultimate strength of plates that accounts for inelastic buckling and post-buckling and is discussed in detail.

- **Design approximations Inelastic buckling**

The notion of “inelastic buckling” is an attempt to extend the elastic critical buckling approximations to situations where material yielding has already occurred. Bleich (1952) generalized the expression for the critical stress of a flat plate under uniform compressive stress in either the elastic or inelastic range in the following manner:

$$\sigma_c = k \frac{\pi^2 E \sqrt{\eta}}{12(1-\nu^2)(b/t)^2}$$

In which  $\eta = Et/E$ . This modification of the equation to adapt it to a stress higher than the proportional limit is a conservative approximation to the solution of a complex problem that involves a continuous

updating of the constitutive relations depending on the axial stress carried (Stowell, 1948; Bijlaard, 1949, 1950).

In combined loading the work of Stowell (1949) and Peters (1954) suggest that the inelastic buckling interaction is not the same as the elastic buckling interaction. Under combined compressive and shear stress for loads applied in constant ratio Peters found that a circular stress-ratio interaction formula as expressed by the equation was conservative and agreed better with test results than the equation which was provided for elastic buckling interaction.

$$\left(\frac{\sigma_c}{\sigma_c^*}\right)^2 + \left(\frac{\tau_c}{\tau_c^*}\right)^2 = 1$$

- **Post-buckling**

Post-buckling of plates may readily be understood through an analogy to a simple grillage model, as shown in Fig. 2.2. In the grillage model the continuous plate is replaced by vertical columns and horizontal ties. Under edge loading the vertical columns will buckle, if they were not connected to the ties they would buckle at the same load and no post-buckling reserve would exist. However, the ties are stretched as the columns buckle outward, thus restraining the motion and providing post-buckling reserve. [10]

In an actual plate the tension in the transverse ties is represented by membrane tension and shear. Note also that the columns nearer to the supported edge are restrained by the ties more than those in the middle. This too occurs in a real plate, as more of the longitudinal membrane compression is carried near the edges of the plate than in the centre. Thus, the grillage model provides a working analogy for both the source of the post-buckling reserve and its most important result, re-distribution of longitudinal membrane stresses.

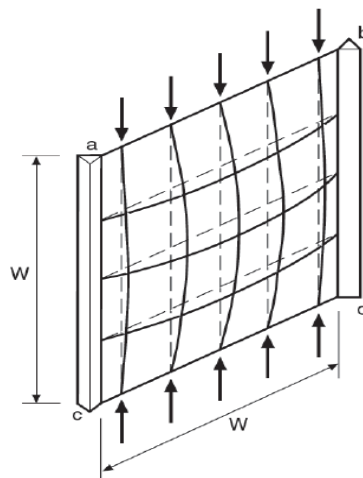


**Fig. 2.9 Simple model for post-buckling of a flat plate in uniform compression (after AISI 2007)**

Elastic post-buckling stiffness may be measured in terms of the apparent modulus of elasticity  $E^*$  (the ratio of the average stress carried by the plate to average strain). The values of  $E^*$  for long plates ( $a \gg b$ ) for some typical longitudinal edge conditions are given by Allen and Bulson (1980). The values given below are sufficiently accurate up to twice the critical stress.

Elastic post-buckling stiffness may be measured in terms of the apparent modulus of elasticity  $E^*$  (the ratio of the average stress carried by the plate to average strain). The values of  $E^*$  for long plates ( $a \gg b$ ) for some typical longitudinal edge conditions are given by Allen and Bulson (1980). The values given below are sufficiently accurate up to twice the critical stress.

*Simply supported longitudinal edges.*

Sides straight but free to move laterally:

$$E^* = 0.5E$$

Sides free to move:

$$E^* = 0.408E$$

*Clamped longitudinal edges.*

Sides straight but free to move laterally:

$$E^* = 0.497E$$

*One longitudinal edge simply supported, the other free*

$$E^* = 0.444E$$

**N.B.** Information on the post-buckling strength of plate elements subjected to the combined action of shear and compression is limited. A semi-empirical method for the determination of stress levels at which permanent buckles occur in a long plate with simply supported edges under the combined action of uniform axial compression and shear has been suggested by Zender and Hall (1960).

## 2.4 Interaction between Plate Elements

In the preceding sections, attention has been confined to the behaviour of a single plate element supported along one or both of its longitudinal edges with or without stiffeners. The structural sections employed in practice are composed of plate elements arranged in a variety of configurations. It is clear that the behaviour of an assembly of plates would be governed by an interaction between the plate components.

In this section the mechanics of such an interaction and its implication in design are discussed briefly. [10]

### - **Buckling Modes of a Plate Assembly**

Unlike a single plate element supported along the unloaded edges, a plate assembly can buckle in one of several possible modes. For the case of axial compression, the buckling mode can take one of the following forms:

- **Mode I / local.** This is the purely local buckling mode discussed earlier. The mode involves out-of-plane deformation of the component plates with the junctions remaining essentially straight, and it has a half-wavelength of the same order of magnitude as the widths of the plate elements.
- **Mode II / distortional.** The buckling process may involve in-plane bending of one or more of the constituent plates as well as out-of-plane bending of all the elements, as in a purely local mode. Such a buckling mode is referred to as a distortional buckling mode, stiffener buckling mode, local torsional mode, or orthotropic mode, depending on the context. The associated wavelengths are considerably greater than those of mode I (local buckling) but there is a half wavelength at which the critical stress is a minimum.
- **Mode III / global.** The plate structure may buckle as a column in flexural or flexural-torsional mode with or without interaction of local buckling.

### - **Local Buckling of a Plate Assembly**

A prismatic plate structure is often viewed simply as consisting of stiffened and unstiffened plate elements. The former are plate elements supported on both of their longitudinal edges by virtue of their connection to adjacent elements, while the latter are those supported only along one of their longitudinal edges. Thus, the critical local buckling stress of a plate assembly may be taken as the smallest of the critical stresses of the plate elements, each treated as simply supported along its junctions with other plates. [10]

This stress will be conservative because the element providing the lower bound will be restrained by the more stable adjoining plate elements if longitudinal edge joints provide effective continuity. More complete information on k-factors as influenced by the interaction between plates components can be found in a number of classic references (Bleich, 1952); (Stowell et al., 1952; Gerard and Becker, 1957/1958; Timoshenko and Gere, 1961). However, such a calculation must be used with caution for the following reasons:

1. The results can be unduly conservative when the plate structure consists of elements with widely varying slenderness. This is the result of neglecting the rotational restraints at the functions.
2. The results are inapplicable unless it is ensured that all the plate elements buckle locally (i.e., the junctions remain essentially straight). If, on the other hand, mode II or III type of buckling is critical, the result of such a simplified calculation would be on the unsafe side.

The intervention of distortional, or stiffener buckling (mode II) may be averted in practice by designing “out” the stiffener buckling mode by the provision of stiffeners (edge or intermediate) of adequate rigidity. This may be advantageous because of the limited post-buckling resistance associated with the mode II type of buckling. However, it is not always practical or economical, designs where distortional buckling must be considered are discussed gives the variations of the local buckling coefficients  $k_w$  for a wide-flange I section, a box section and a Z- or channel section, respectively, with respect to the geometrical properties of the member. Each of these charts is divided into two portions by a dashed line running across it (Kroll et al., 1943). In each portion, buckling of one of the elements dominates over the other, but the proportions exactly on the dashed line represent the case where the buckling stress of the elements are equal.

**CHAPTER 3**  
**ANALYSIS OF STEEL STRUCTURES BUCKLING**  
**USING FINITE ELEMENT**

### 3.1. Introduction

Steel-plated structures are likely to be subjected to various types of loads and deformations arising from service requirements that may range from the routine to the extreme or accidental. The mission of the structural designer is to design a structure that can withstand such demands throughout its expected lifetime.

Buckling occurs as an instability when a structure can no longer support the existing compressive load levels. Buckling Analysis is an FEA routine that can solve all the difficult buckling problems that cannot be solved by hand calculations. Linear Buckling (LBA) is the most common Buckling Analysis. The nonlinear approach, on the other hand, offers more complex solutions than Linear Buckling.

The present chapter presents a brief review of the finite element method for application on buckling steel structures. This chapter is to provide a general review of the main steps of finite element analysis of structures, specifically for steel structures. It also the necessary background of the FEM that was used to write most of the special and general-purpose programs available in the literature. Furthermore, it reviews different finite element types used to analyse metal structures.

### 3.2. General Concept of FEA

The present section highlights the very beginning of the FEA development of the finite element modelling of metal structures.

In fact, the Finite Element Analysis (FEA) method, originally introduced by Turner et al. (1956), is a powerful computational technique for approximate solutions to a variety of "real-world" engineering problems having complex domains subjected to general boundary conditions. FEA has become an essential step in the design or modelling of a physical phenomenon in various engineering disciplines. A physical phenomenon usually occurs in a continuum of matter (solid, liquid, or gas) involving several field variables. The field variables vary from point to point, thus possessing an infinite number of solutions in the domain. Within the scope of this book, a continuum with a known boundary is called a domain.

The basis of FEA relies on the decomposition of the domain into a finite number of subdomains (elements) for which the systematic approximate solution is constructed by applying the Variational or weighted residual methods. In effect, FEA reduces the problem to that of a finite number of unknowns by dividing the domain into elements and by expressing the unknown field variable in terms of the assumed approximating functions within each element. These functions (also called interpolation functions) are defined in terms of the values of the field variables at specific points, referred to as nodes. Nodes are usually located along the element boundaries, and they connect adjacent elements.

The ability to discretize the irregular domains with finite elements makes the method a valuable and practical analysis tool for the solution of boundary, initial, and eigenvalue problems arising in various engineering disciplines. Since its inception, many technical papers and books have appeared on the development and application of FEA. The books by Desai and Abel (1971), Oden (1972), Gallagher (1975), Huebner (1975), Bathe and Wilson (1976), Ziekiewicz (1977), Cook (1981), and Bathe (1996) have influenced the current state of FEA.

### **3.3. Experimental Investigations and its Role for Finite Element Modelling**

Experimental investigation plays a major role in finite element analysis. It is important to verify and validate the accuracy of finite element models using test data, particularly nonlinear finite element models.

### **3.4. Review of the General Steps of Finite Element Analysis**

#### **3.4.1. General**

Finite element analysis can provide a good insight into the behaviour of metal structural elements outside the ranges covered by specifications. In addition, finite element analysis can check the validity of the empirical equations for sections effected by nonlinear material and geometry, which may be ignored in the specifications.

The finite element method is based on modelling the structure using small interconnected elements called finite elements with defined points forming the element boundaries called nodes. There are numerous finite elements analysed in the literature such as bar, beam, frame, solid, and shell elements. The use of any element depends on the type of the structure, geometry, type of analysis, applied loads and boundary conditions, computational time, and data required from the analysis. Each element has its own displacement function that describes the displacement within the element in terms of nodal displacement. Every interconnected element has to be linked to other elements simulating the structure directly by sharing the exact boundaries or indirectly through the use of interface nodes, lines, or elements that connect the element with the other elements. The element stiffness matrices and finite element equations can be generated by making use of the commonly known stress-strain relationships and direct equilibrium equations. By solving the finite element equations, the unknown displacements can be determined and used to predict different straining actions such as internal forces and bending moments. [11]

In matrix notation, the global system of equations can be cast into

$$\mathbf{Ku} = \mathbf{F}$$

Where  $\mathbf{K}$  is the system stiffness matrix,  $\mathbf{u}$  is the vector of unknowns, and  $\mathbf{F}$  is the force vector. Depending on the nature of the problem,  $\mathbf{K}$  may be dependent on  $\mathbf{u}$ , i.e.,  $\mathbf{K} = \mathbf{K}(\mathbf{u})$  and  $\mathbf{F}$  may be time dependent, i.e.,  $\mathbf{F} = \mathbf{F}(t)$ .



Briefly, the solution for structural problems typically refers to determining the displacements at each node and the stresses within each element making up the structure that is subjected to applied loads. In non- structural problems, the nodal unknowns may, for instance, be temperatures or fluid pressures due to thermal or fluid fluxes.

### 3.4.2. Approaches used in FEA

Getting an exact solution sometimes becomes very complicated and even impossible in some cases that involve highly nonlinear material and geometry analyses. However, experimental investigations are also costly and time consuming, which require specialized laboratory and expensive equipment as well as highly trained and skilled technician. [11]

There are three main approaches to constructing an approximate solution based on the concept of FEA:

**Direct Approach:** This approach is used for relatively simple problems, and it usually serves as a means to explain the concept of FEA and its important steps.

**Weighted Residuals:** This is a versatile method, allowing the application of FEA to problems where the functional cannot be constructed. This approach directly utilizes the governing differential equations, such as those of heat transfer and fluid mechanics.

**Variational Approach:** This approach relies on the calculus of variations, which involves extremizing a functional. This functional corresponds to the potential energy in structural mechanics.

Furthermore, design guides specified in current codes of practice contain some assumptions based on previous measurements, e.g., assuming values for initial local and overall imperfections in metal structural elements. Also, finite element modelling can investigate the validity of these assumptions.

## 3.5. Definitions and Terminology

### 3.5.1. Steps

The finite element analysis method requires the following major steps:

- Discretization of the domain into a finite number of subdomains (elements).
- Selection of interpolation functions.
- Development of the element matrix for the subdomain (element).
- Assembly of the element matrices for each subdomain to obtain the global matrix for the entire domain,
- Imposition of the boundary conditions.
- Solution of equations.
- Additional computations (if desired).

### 3.5.2. Displacement Function

The displacement function is defined as the function that describes the displacement within the element in terms of the nodal values of the element. The functions that can be used as shape functions are polynomial functions and may be linear, quadratic, or cubic polynomials. However, trigonometric series can be also used as shape functions. The same displacement function can be used to describe the displacement behaviour within each of the remaining finite elements of the structure. Hence, the finite element method treats the displacement throughout the whole structure approximately as a discrete model composed of a set of piecewise continuous functions defined within each finite element of the structure.

### 3.5.3. Choice of Element Type for Metal Structures

There are three commonly known cross section classifications that are compact, noncompact, and slender sections. Compact sections have a thick plate thickness and can develop their plastic moment resistance without the occurrence of local buckling. Slender sections are those sections in which local buckling will occur in one or more parts of the cross section before reaching the yield strength. Compact sections in 3D can be modelled either using solid elements or shell elements that are able to model thick sections. However, no compact and slender sections are only modelled using shell elements that are able to model thin sections.

Numerical integration is normally used to predict the behaviour within the shell element. Conventional shell elements can use full or reduced numerical integration, as shown in Figure 3.1. Reduced integration shell elements use lower order integration to form the element stiffness. However, the mass matrix and distributed loadings are still integrated exactly. Reduced integration usually provides accurate results provided that the elements are not distorted or loaded in in-plane bending. Reduced integration significantly reduces running time, especially in three dimensions.

Shell elements are commonly identified based on the number of element nodes and the integration type. Hence, a shell element S8 means a stress-displacement shell having eight nodes with full integration while a shell element S8R means a stress-displacement shell having eight nodes with reduced integration. On the other hand, continuum shell elements are general-purpose shells that allow finite membrane deformation and large rotations and, thus, are suitable for nonlinear geometric analysis. These elements include the effects of transverse shear deformation and thickness change.

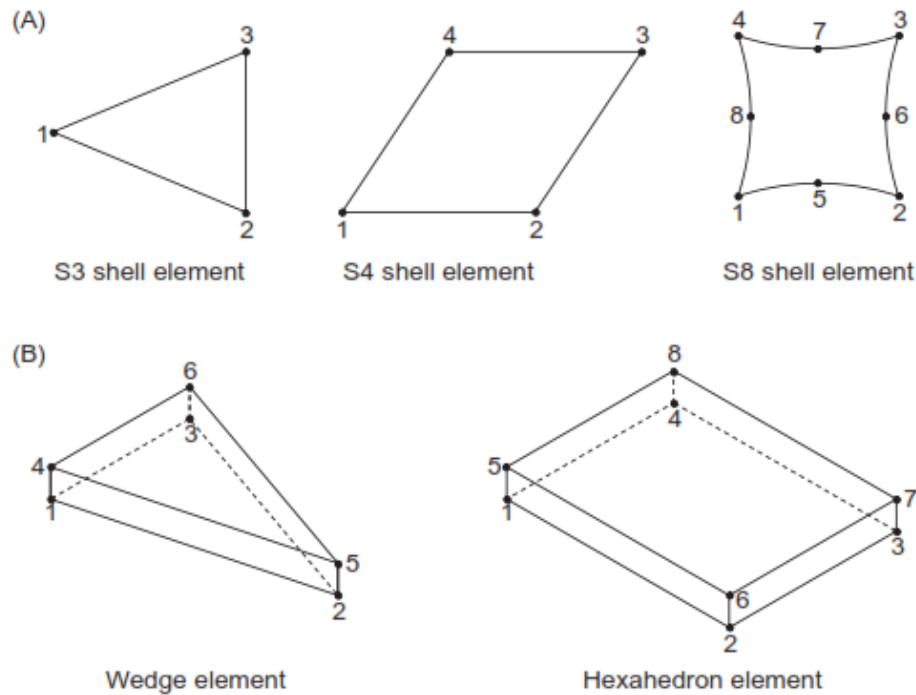


**Figure 3.1 Shell element types: (A) conventional shell elements and (B) continuum shell elements.**

### 3.5.4. Shell element (Abaqus)

Element type S8R5 may give inaccurate results for buckling problems of doubly curved shells due to the fact that the internally defined integration point may not be positioned on the actual shell surface. Element type S4 is a fully integrated, general-purpose, finite-membrane-strain shell element. Element type S4 has four integration locations per element compared with one integration location for S4R, which makes the element computation more expensive. S4 is compatible with both S4R and S3R. S4 can be used in areas where greater solution accuracy is required, or for problems where in-plane bending is expected. In all of these situations, S4 will outperform element type S4R.

### 3.5.5. Definition of the Strain-displacement and Stress-strain Relationships

The next step, following the selection of a displacement function, is to define the strain-displacement and stress-strain relationships. The relationships depend on the element type and are used to derive the governing equations of each finite element. Assuming that the axial displacement is  $u$ , then the axial strain associated with this deformation  $\epsilon_x$  can be evaluated as follows:

$$\epsilon_x = du/dx$$

To evaluate the stresses in the element, the stress-strain relationship or constitutive law has to be used. The relationship is also characteristic to the element type and in this simple 1D finite element, Hooke's law can be applied to govern the stress-strain relationship throughout the element as follows:

$$\sigma_x = E \epsilon_x$$

Where  $\sigma_x$  is the stress in direction  $x$ , which is related to the strain  $\epsilon_x$  and  $E$  is the modulus of elasticity.

### 3.5.6. Material Modelling

Most metal structures have nonlinear stress/strain curves or linear nonlinear stress/strain curves. The stress/strain curves can be determined from tensile coupon tests or stub column tests specified in most current international specifications. The stress - strain curves are characteristic to the construction materials and differ considerably from a material to another. The main important parameters needed from the stress/ strain curve are the measured initial Young's modulus ( $E_0$ ), the measured proportional limit stress ( $\sigma_p$ ), the measured static yield stress ( $\sigma_y$ ) that is commonly taken as the 0.1% or 0.2% proof stress ( $\sigma_{0.1}$  or  $\sigma_{0.2}$ ) for materials having a rounded stress- strain curve with no distinct yield plateau, the measured ultimate tensile strength ( $\sigma_u$ ), and the measured elongation after fracture ( $\epsilon$ ).

### 3.5.7. Modelling the material nonlinearity

Materially nonlinear analysis (with or without consideration of geometric nonlinearity) of metal structures is done to determine the overall response of the structures. From a numerical viewpoint, the implementation of a nonlinear stress/strain curve of a construction metal material involves the integration of the state of the material at an integration point over a time increment during a materially nonlinear analysis. The implementation of a nonlinear stress/strain curve must provide an accurate material stiffness matrix for use in forming the nonlinear equilibrium equations of the finite element formulation. [11]

### 3.5.8. Modelling of Initial Imperfections

In a strict sense, buckling is a bifurcation phenomenon that stable deformation changes from in-plane (or axial) deformation to in-plane (or axial) plus out-of-plane deformations. Therefore, to have buckling in a strict sense, the structural member has to be completely flat (or straight) before it is loaded; that is, it has to be completely free from initial distortion/deflection.

Initial geometric imperfections can be classified into two main categories, which are local and overall (bow, global, or out-of-straightness) imperfections. Initial local geometric imperfections can be found in any region of the outer or inner surfaces of metal structural members and are in the perpendicular directions to the structural member surfaces. On the other hand, initial overall geometric imperfections are global profiles for the whole structural member along the member length in any direction.

Initial local and overall geometric imperfections can be predicted from finite element models by conducting eigenvalue buckling analysis to obtain the worst cases of local and overall buckling modes. Accurate finite element models must incorporate initial local and overall geometric imperfections in the analysis; otherwise, the results will not be accurate. Even in most axially loaded metal long column tests, the columns tend to buckle in the direction of the maximum initial overall geometric imperfection.

## 3.6. Nonlinear FEA

### 3.6.1. General

Nonlinear finite element analysis is an essential component of computer-aided design. Testing of prototypes is increasingly being replaced by simulation with nonlinear finite element method because this provides a more rapid and less expensive way to evaluate design concepts and design details.

For both users and developers of nonlinear finite element programs, an understanding of the fundamental concepts of nonlinear finite element analysis is essential. Without an understanding of the fundamentals, a user must treat the finite element program as a black box that provides simulations. However, even more so than linear finite element analysis, nonlinear finite element analysis confronts the user with many choices and pitfalls. Without an understanding of the implication and meaning of these choices and difficulties, a user is at a severe disadvantage. Nonlinear analysis consists of the following steps:

1. Development of a model;
3. Formulation of the governing equations;
3. Discretization of the equations;
3. Solution of the equations;
5. Interpretation of the results.

Modelling is a term that tends to be used for two distinct tasks in engineering. The older definition emphasizes the extraction of the essential elements of mechanical behaviour. The objective in this approach is to identify the simplest model which can replicate the behaviour of interest. In this approach, model development is the process of identifying the ingredients of the model which can provide the qualitative and quantitative predictions.

A second approach to modelling, which is becoming more common in industry, is to develop a detailed, single model of a design and to use it to examine all of the engineering criteria which are of interest. The impetus for this approach to modelling is that it costs far more to make a model or mesh for an engineering product than can be saved through reduction of the model by specializing it for each application.

Nonlinear finite element analysis represents a nexus of three fields:

1. Linear finite element methods, which evolved out of matrix methods of structural analysis;
3. Nonlinear continuum mechanics; and
3. Mathematics, including numerical analysis, linear algebra and functional analysis.

In each of these fields a standard notation has evolved. Unfortunately, the notations are quite different, and at times contradictory or overlapping. We have tried to keep the variety of notation to a minimum and both consistent within the book and with the relevant literature.

To begin with, in the buckling analysis, when using a software, all nonlinear or inelastic material properties are ignored during an eigenvalue buckling analysis. Any structural finite elements can be used in an eigenvalue buckling analysis. The values of the eigenvalue load multiplier (buckling loads) will be printed in the data files after the eigenvalue buckling analysis. The buckling mode shapes can be visualized using the software. Any other information such as values of stresses, strains, or displacements can be saved in files at the end of the analysis. [11]

### 3.6.2. Geometrically Nonlinear Analysis

Geometrically nonlinear analysis of metal structures is a general nonlinear analysis step. The analysis can be also called load-displacement nonlinear geometry analysis and normally follows the linear eigenvalue buckling analysis step or initial condition stress analysis. The initial overall and local geometric imperfections and residual stresses are included in the load-displacement nonlinear geometry analysis. If the stress-strain curve of the construction metal material is nonlinear, the analysis will be called combined materially and geometrically nonlinear analysis or load-displacement nonlinear material and geometry analysis.

A full geometrically nonlinear (GNL) analysis, if appropriately perturbed, will take account of any pre-buckling displacements of the structure and, moreover, provide a complete response of the structure at all stages of the analysis.

The geometrically nonlinear functionality depends on the element type proposed, but the general available options are as follows:

- Total Lagrangian
- Updated Lagrangian
- Eulerian
- Co-rotational

The buckling load is not given directly in this method; rather a complete deformation history is obtained. A graph of force-displacement (stress-strain) at any point or for the structure will enable the buckling load to be determined. See later section on buckling load output for further information.

If a perturbation load is not specified and if the applied load on its own does not induce buckling due to its nature and its direction, then when the buckling load has been exceeded a negative pivot will be found in the iterative log output. This is after the increment has converged (negative pivots that occur during the iterative procedure, i.e. at un-converged configurations, can be ignored).

### 3.7. Linear Eigenvalue Buckling Analysis

Eigenvalue buckling analysis is generally used to estimate the critical buckling (bifurcation) load of structures. The analysis is a linear perturbation procedure.

The analysis can be the first step in a global analysis of an unloaded structure or it can be performed after the structure has been preloaded. It can be used to model measured initial overall and local geometric imperfections or in the investigation of the imperfection sensitivity of a structure in case of lack of measurements. Eigenvalue buckling is generally used to estimate the critical buckling loads of stiff structures. [11]

The fundamental assumptions of such an analysis are as follows

- The linear stiffness matrix does not change prior to buckling;
- The stress stiffness matrix is simply a multiple of its initial value.

The buckling loads are calculated relative to the original state of the structure. If the eigenvalue buckling procedure is the first step in an analysis, the buckled (deformed) state of the model at the end of the eigenvalue buckling analysis step will be the updated original state of the structure. The eigenvalue buckling can include preloads such as dead load and other loads. The preloads are often zero in classical eigenvalue buckling analyses. An incremental loading pattern is defined in the eigenvalue buckling prediction step.

The magnitude of this loading is not important; it will be scaled by the load multipliers that are predicted by the eigenvalue buckling analysis. The buckling mode shapes (eigenvectors) are also predicted by the eigenvalue buckling analysis. The critical buckling loads are then equal to the preloads plus the scaled incremental load. Normally, the lowest load multiplier and buckling mode are of interest. The buckling mode shapes are normalized vectors and do not represent actual magnitudes of deformation at critical load. They are normalized so that the maximum displacement component has a magnitude of 1.0. If all displacement components are zero, the maximum rotation component is normalized to 1.0. These buckling mode shapes are often the most useful outcome of the eigenvalue buckling analysis, since they predict the likely failure modes of the structure. [11]

### 3.8. Inelastic buckling analysis

#### 3.8.1. General

Buckling occurs as an instability when a structure can no longer support the existing compressive load levels. Many structural components are sufficiently stiff that they will never suffer any form of instability. At the other extreme, structures that are slender could fail at load levels well below what is required to cause compressive yielding. The failing mode tends to be toward the classic Euler buckling mode.

Buckling analysis assesses the stability characteristics of a structure. An accurate solution to a buckling problem requires more efforts than just following a numerical procedure, there are a number of factors to consider before a buckling solution can be accepted with confidence. In fact, a starting step should be a linear buckling analysis. Nonlinear buckling analysis capability can be performed restart the linear buckling analysis. While serving the purpose of a nonlinear buckling analysis following a static nonlinear analysis, this buckling analysis procedure is cumbersome to the user because it requires a restart. [12]

(Riks) analysis must be performed to investigate the structures accurately. The Riks method provided by ABAQUS is an efficient method that is generally used to predict unstable, geometrically nonlinear collapse of a structure. The method can include nonlinear materials and boundary conditions. The method commonly follows an eigenvalue buckling analysis to provide complete information about a structure's collapse. The Riks method can be used to speed convergence of unstable collapse of structures.

Geometrically nonlinear static metal structures sometimes involve buckling or collapse behaviour. Several approaches are possible for modelling such behaviour. One of the approaches is to treat the buckling response dynamically, thus actually modelling the response with inertia effects included as the structure snaps. This approach is easily accomplished by restarting the terminated static procedure and switching to a dynamic procedure when the static solution becomes unstable. In some simple cases, displacement control can provide a solution, even when the conjugate load (the reaction force) is decreasing as the displacement increases.

The Riks method can be used to speed convergence of unstable collapse of structures. It also treats the load magnitude as an additional unknown and solves loads and displacements simultaneously.

### **Riks step procedure details using ABAQUS**

The Riks method works well with structures having a smooth equilibrium path in load-displacement domain. The Riks method can be used to solve post-buckling problems, both with stable and unstable post-buckling behaviour. In this way, the Riks method can be used to perform post-buckling analyses of structures that show linear behaviour prior to (bifurcation) buckling.

The method can provide solutions even in cases of complex, unstable response such as that shown in Figure 3.3. [12]

A structure's behavior under loading is usually studied with the use of load-displacement plots. This applies also to studying the structural behavior in the post-buckling region (past the bifurcation point). In simple structures, linear eigenvalue buckling analysis may be sufficient for design evaluation. However, in complex structures involving material nonlinearity, geometric nonlinearity prior to buckling, or unstable post-buckling behaviour, a load/displacement (Riks) analysis must be



performed to investigate the structures accurately. When performing a load-displacement analysis using the Riks method, important nonlinear effects can be included. Imperfections based on linear buckling modes can be also included in the analysis of structures using the Riks method.

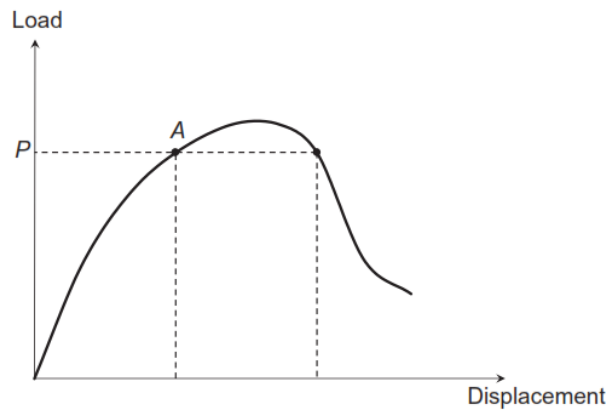


**Figure 3.2 Load-Displacement curve used in Riks method**

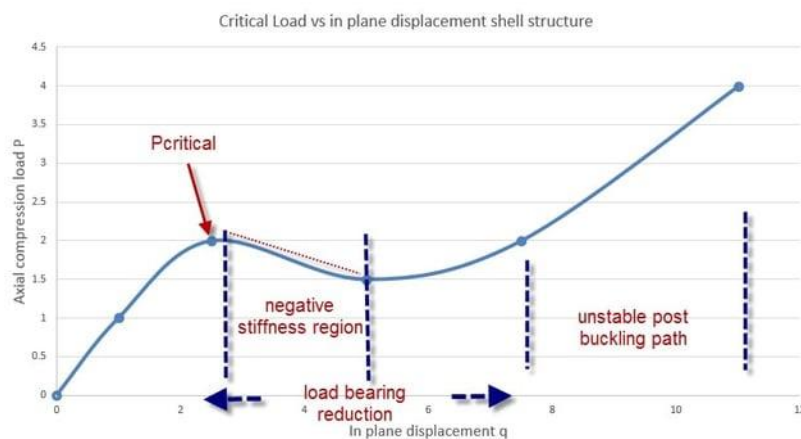


**Figure 3.3 Critical load vs. in plane deformation loading history**

The Riks method treats the load magnitude as an additional unknown and solves loads and displacements simultaneously. Therefore, another quantity must be used to measure the progress of the solution, see Figure 3.5.

ABAQUS uses the arc length along the static equilibrium path in load-displacement domain. This approach provides solutions regardless of whether the response is stable or unstable. If the Riks step is a continuation of a previous history, step is referred to as a reference load. All prescribed loads are ramped from the initial (dead load) value to the reference values specified. ABAQUS uses Newton's method to solve the nonlinear equilibrium equations. [12]

The Riks procedure uses very small extrapolation of the strain increment. Modellers can provide an initial increment in arc length along the static equilibrium path when defining the step. After that, ABAQUS computes subsequent steps automatically. Since the loading magnitude is part

of the solution, modellers need a method to specify when the step is completed. It is common that one can specify a maximum displacement value at a specified degree of freedom. The step will terminate once the maximum value is reached. Otherwise, the analysis will continue until the maximum number of increments specified in the any loads that exist at the beginning of the step are treated as dead loads with constant magnitude. A load whose magnitude is defined in the Riks step definition is reached.

It should be noted that the Riks method cannot obtain a solution at a given load or displacement value since these are treated as unknowns. Termination of the analysis using the Riks method occurs at the first solution that satisfies the step termination criterion.

To obtain solutions at exact values of load or displacement, the analysis must be restarted at the desired point in the step and a new, non-Riks step must be defined. Since the subsequent step is a continuation of the Riks analysis, the load magnitude in that step must be given appropriately so that the step begins with the loading continuing to increase or decrease according to its behaviour at the point of restart. Initial values of stresses such as residual stresses can be inserted in the analysis using the Riks method. Also, boundary conditions can be applied to any of the displacement or rotation degrees of freedom (six degrees of freedom). Concentrated nodal forces and moments applied to associated displacement or rotation degrees of freedom (six degrees of freedom) as well as distributed loads at finite element faces can be inserted in the analysis using the Riks method.

Nonlinear material models that describe mechanical behaviour of metal structures can be incorporated in the analysis using the Riks method. [12]

**CHAPTER 4**  
**SOFTWARE USED**

Dealing with buckling problems, designer has been provided with practical tools to calculate with more accuracy the value of elastic critical buckling stresses in plates, in both linear and nonlinear behaviour and without neglected favourable effects.

Plate buckling checks are of the utmost importance in the design of steel plated structures. They often govern the steel weight by imposing the plate thicknesses and/or the use of stiffeners which are generally expensive to work out. Plate buckling checks are treated in EN 1993-1-5 and involve elastic critical stresses (or plate buckling coefficients) which may have a major influence on the assessment of plate buckling resistances. Elastic critical stresses are also needed for checking web breathing for plated structures with rolling loads.

For very common cases, elastic critical stresses may be obtained from formulas, or specific charts, often in the frame of simplified assumptions which can be sometimes far from the reality and very conservative. Moreover these charts deal with a limited number of configurations (geometry, stiffener positions and properties, stress distribution, ...) and can not always be used because practical cases are often beyond their limits. Beside this, numerical simulations using Finite Element Codes may be used but they are complex to carry out and time consuming.

As this dissertation is mainly concerned by the study of the elastic and inelastic buckling of steel thin plates the FEA was used through some very famous software: ABAQUS and EBPLATE. The software EBPlate has been used to verify some results obtained in ABAQUS.

In this chapter, a succinct and brief description of the software being used in this dissertation will be given. Two different software namely, the general purpose ABAQUS software and EBPLATE have been used for the validation of the obtained results. This is concern only the elastic buckling study of both steel plate with and without holes. The inelastic buckling analysis has been performed using exclusive ABAQUS, as it give the opportunity to do so.

In the following the features of each software will be presented in some details.

Firstly, Abaqus will be presented, then EBPLATE.

## **4.1. ABAQUS Software for elastic and inelastic buckling**

### **4.1.1 Introduction**

Abaqus Company was founded in 1978 by Dr. David Hibbitt, Dr. Bengt Karlsson, and Dr. Paul Sorensen with the original name Hibbitt, Karlsson & Sorensen, Inc., (HKS). Later on, the company name was changed to ABAQUS Inc. before the acquisition by Dassault Systems in 2005. After that, it became part of Dassault Systems Simulia Corp. The headquarters of the company was located in Providence, Rhode Island until 2014. Since 2014, the headquarters of the company are located in Johnston, Rhode Island, United States.

ABAQUS/CAE is a complete ABAQUS environment that provides a simple, consistent interface for creating, submitting, monitoring, and evaluating results from ABAQUS/Standard and ABAQUS/Explicit simulations. ABAQUS/CAE is divided into modules, where each module defines a logical aspect of the modelling process; for example, defining the geometry, defining material properties, and generating a mesh. As you move from module to module, each module contributes keywords, parameters, and data to form an input file that you submit to the ABAQUS/Standard or ABAQUS/Explicit solver. The solver reads the input file generated by ABAQUS/CAE, performs the analysis, sends information to ABAQUS/CAE to allow you to monitor the progress of the job, and generates an output database. Finally, you use ABAQUS/CAE to read the output database and view the results of your analysis. [12]

#### **4.1.2 Applications**

Abaqus covers many fields including: structures, automotive, aerospace, and industrial products industries. The product is popular with non-academic and research institutions in engineering due to the wide material modelling capability, and the program's ability to be customized. Abaqus also provides a good collection of Multiphysics capabilities, such as coupled acoustic-structural, piezoelectric, and structural-pore capabilities, making it attractive for production-level simulations where multiple fields need to be coupled.

Abaqus was initially designed to address non-linear physical behaviour; as a result, the package has an extensive range of material models such as elastomeric (rubberlike) and hyperplastic (soft tissue) material capabilities.

#### **4.1.3 General on ABAQUS Software Modules**

ABAQUS/CAE is divided into modules, where each module defines an aspect of the modelling process; for example, defining the geometry, defining material properties, and generating a mesh. As you move from module to module, each module contributes keywords, parameters, and data to form an input file that you submit to the ABAQUS/Standard or ABAQUS/Explicit solver for analysis. For example, you use the Property module to define material and section properties and the Step module to choose an analysis procedure; the ABAQUS/CAE postprocessor is called the Visualization module. [12]

The modules are:

1. Part – defines the geometry of a structural element or model to be used in the analysis.
2. Property – defines materials and cross sections.
3. Assembly – assembles a number of parts to form the global geometry of a model.
4. Step – defines the different analyses to be carried out.
5. Interaction – defines connections and interface conditions between different parts.

6. Load – defines the boundary conditions of the model.
7. Mesh – provides the discretization of the model into finite elements.
8. Job – defines the jobs to be carried out by the analysis program.
9. Visualization – is utilized for viewing and post processing the results.
10. Sketch – can be used as a simple CAD program for making additional drawings.

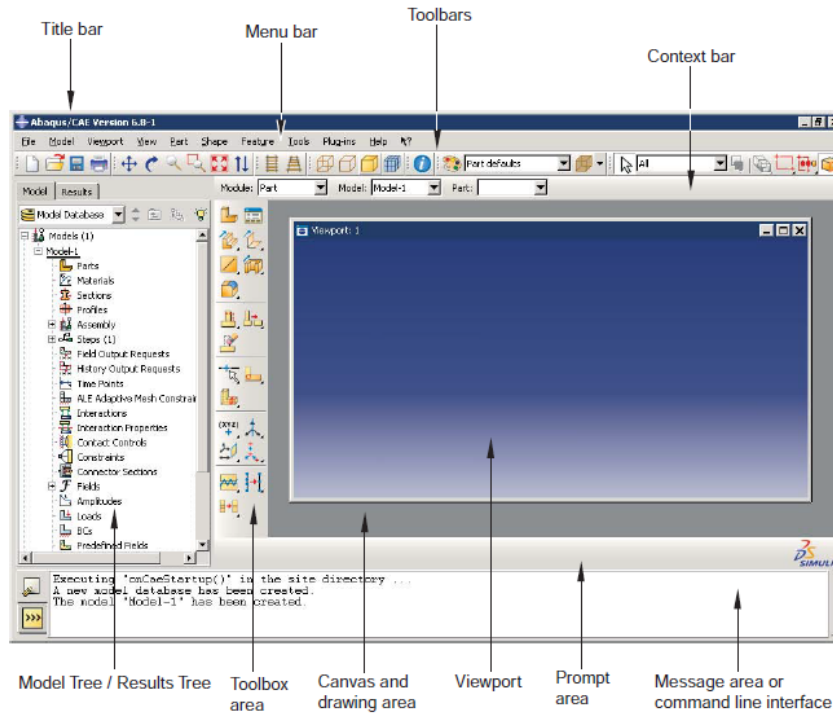


**Figure 4.1 Components of the main window.**

#### 4.1.4 Solution sequence

Generally speaking, every complete finite-element analysis consists of 3 separate stages:

- Pre-processing or modelling: This stage involves creating an input file for a finite-element analyser (also called "solver").
- Processing or finite element analysis: This stage produces an output visual file.
- Post-processing or generating report, image, animation, etc. from the output file: This stage is a visual rendering stage.

Abaqus/CAE is capable of pre-processing, post-processing, and monitoring the processing stage of the solver; however, the first stage can also be done by other compatible CAD software, or even a text editor. Abaqus/Standard, Abaqus/Explicit or Abaqus/CFD are capable of accomplishing the processing stage. Dassault Systems also produces Abaqus for CATIA for adding advanced processing and post processing stages to a pre-processor like CATIA. [12]

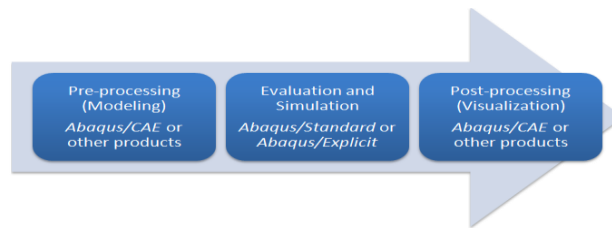


**Figure 4.2. Abaqus FEA software products used in Finite Element Analysis and their order of use.**

### 4.1.5 Elements in ABAQUS

The wide range of elements in the ABAQUS element library provides flexibility in modeling different geometries and structures. [1]

–Each element can be characterized by considering the following:

- Family
- Number of nodes
- Degrees of freedom
- Formulation
- Integration

#### Family

A family of finite elements is the broadest category used to classify elements. [1]

- Elements in the same family share many basic features.
- There are many variations within a family.

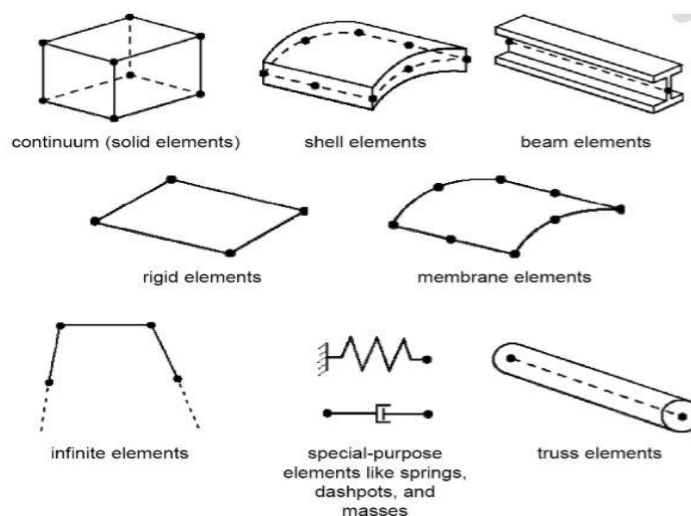


**Figure 4.3. Family of finite elements in Abaqus software.**

### Number of nodes (interpolation)

- An element's number of nodes determines how the nodal degrees of freedom will be interpolated over the domain of the element.
- ABAQUS includes elements with both first and second-order interpolation.

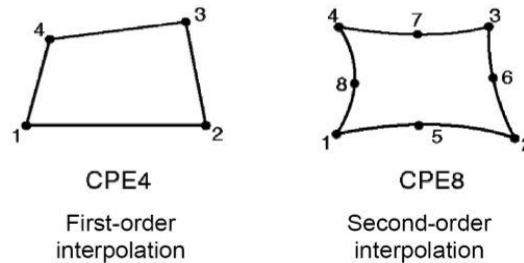


**Figure 4.4** An element's number of nodes in Abaqus software.

### Degrees of freedom

–The primary variables that exist at the nodes of an element are the degrees of freedom in the finite element analysis.

–Examples of degrees of freedom are:

- Displacements
- Rotations
- Temperature
- Electrical potential

–Some elements have internal degrees of freedom that are not associated with the user-defined nodes.

### Formulation

–The mathematical formulation used to describe the behaviour of an element is another broad category that is used to classify elements.

–Examples of different element formulations:

- |                              |                        |
|------------------------------|------------------------|
| - Plane strain               | - Small-strain shells  |
| - Plane stress               | - Finite-strain shells |
| - Hybrid elements            | - Thick shells         |
| - Incompatible-mode elements | - Thin shells          |

### Integration

–The stiffness and mass of an element are calculated numerically at sampling points called “integration points” within the element.

–The numerical algorithm used to integrate these variables influences how an element behaves.



## 4.1.6 Examples

### • 4.1.6.1 Elastic eigen values analysis

#### Compression

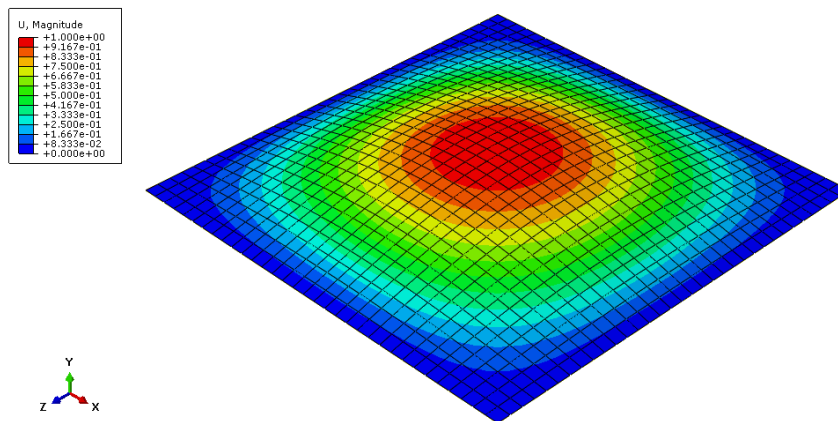


Figure 4.5. Square plate without hole: elastic buckled shape.

### • Inelastic

#### Compression

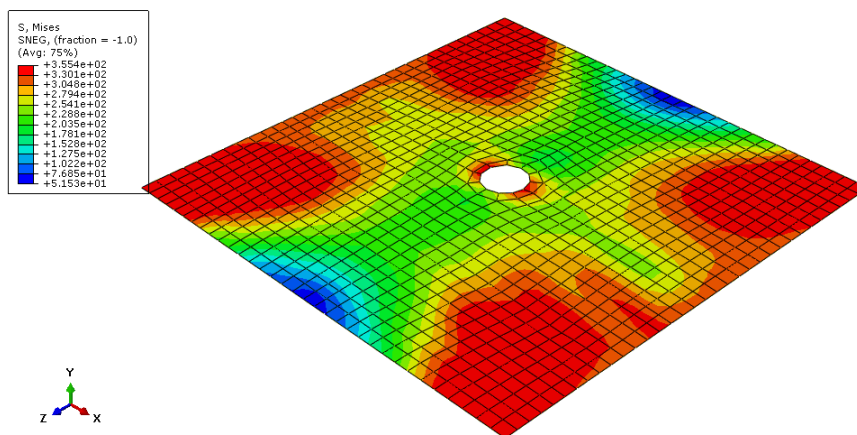


Figure 4.6. Square plate with hole: inelastic buckled shape.

## 4.2 Modulation using ABAQUS software:

In the following, an example of modelling a flat plate with a circular hole using ABAQUS. In this appendix, some details on modelling a perforated plate using ABAQUS is provided. The simplest concentration case of a thin plate loaded in tension where the plate contains a centrally located hole.

### 4.2.1 Create Sketch

ABAQUS has prepared a set of tools to create easy parts. In our case which is a very simple one, there is no need to go back and forth with other advanced modeler. From the module menu choose Part and assign a name for it. The model is planner and we are going to study its deformation characteristics, see Figure 4.7.

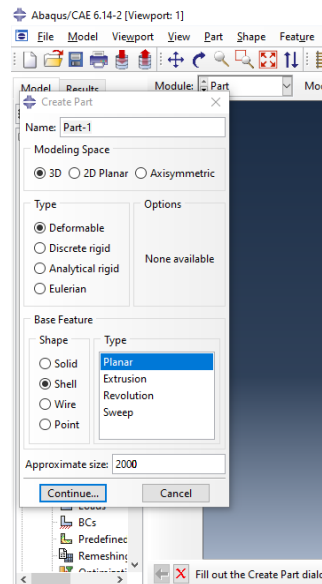


**Figure 4.7** creating a sketch

#### 4.2.2 Define Property

Keep following the ABAQUS order in Module Menu. The second module is Property. In this step it is not only necessary to define the material properties of the Part but assigning it to the Part as well. This will add more flexibility in complex analyses when we should study different properties of the same model with minimum effort.

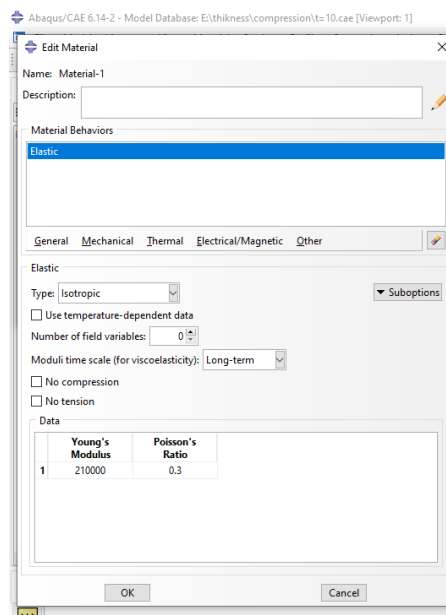


**Figure 4.8** Defining Property

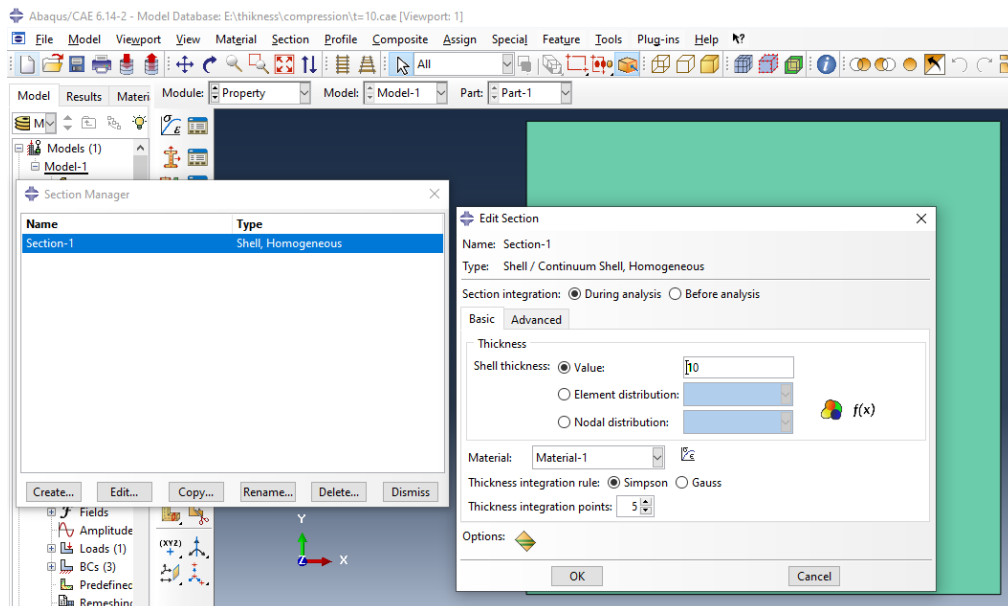


Figure 4.9 creating the section

### 4.2.3 Assembly

Select Assembly module and create an Instance by double clicking on Instances. Choose the Part to Instance in the box, and depending on mesh dependency choose right one. In the current case use independent and click Ok. Figure 4.10.

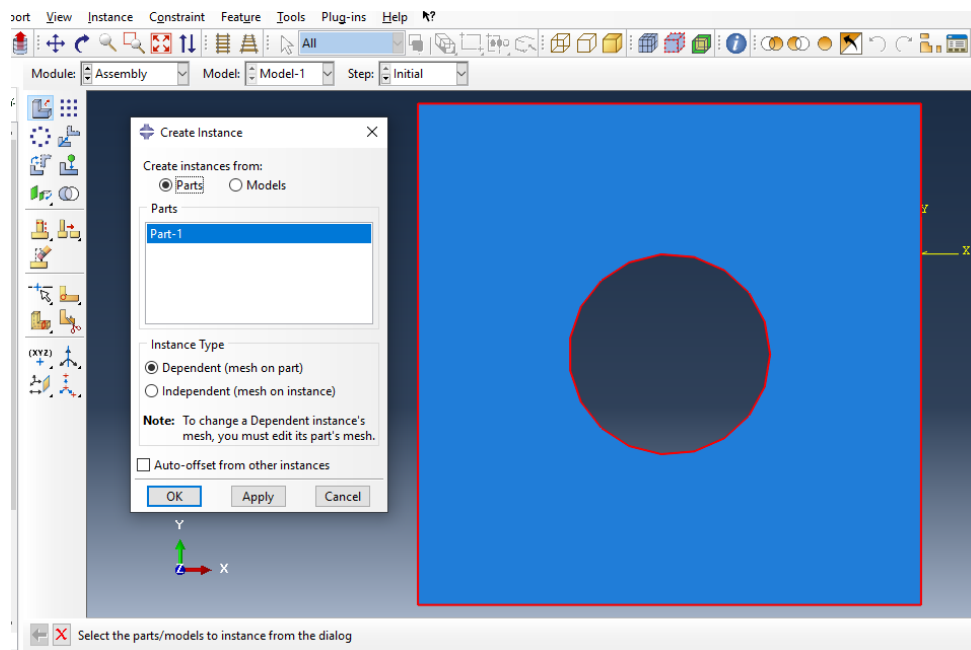


Figure 4.10 Creating instance

### 4.2.5 Step

Select Step module to create and configure analysis steps and associated output requests, Figure 4.11. Step module provides a convenient way to capture changes in model; the output requests can vary as necessary between steps. Make sure to set OFF the Nlgeom parameter when creating the step-1 this parameter is related to nonlinear analysis of materials.

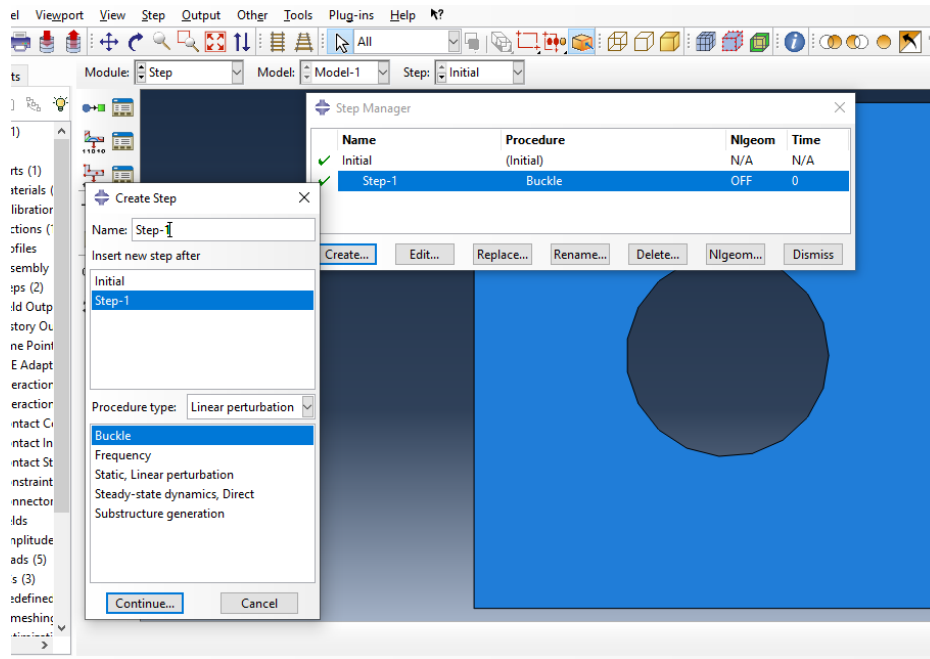


Figure 4.11 creating a step

#### 4.2.5 Load

Choose Load module from the Load Manager. Create a load case and fill the box with compression as General and Magnitude=355. Define the positive direction of X as direction of the load. Select the edges of the geometry for assigning the load to the model. From the same module define the boundary conditions of the model.

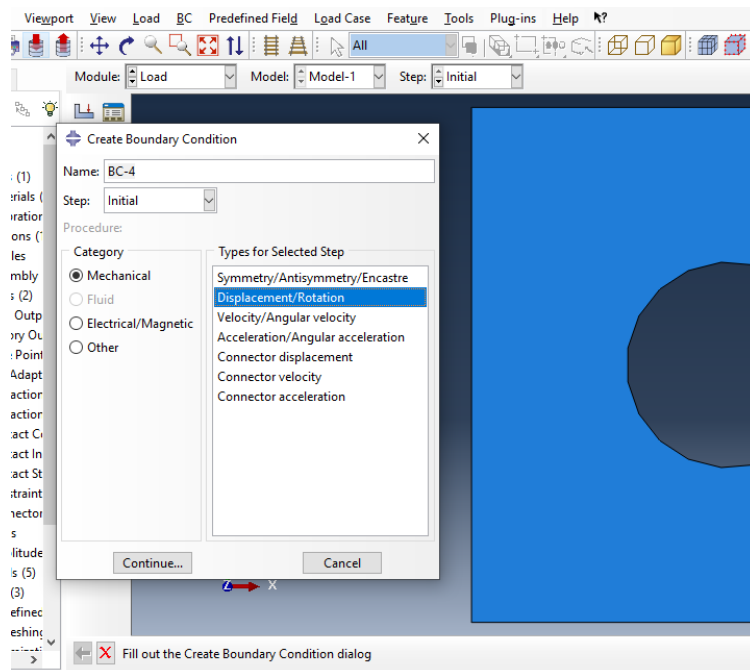


Figure 4.12 Creating boundary condition

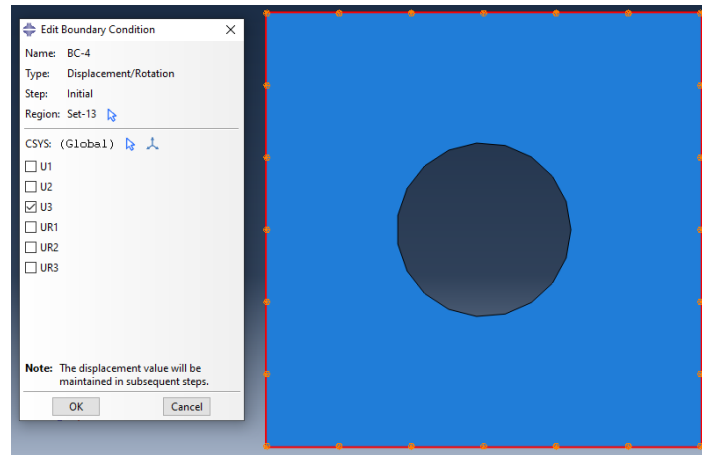


Figure 4.13 Selection the boundary condition

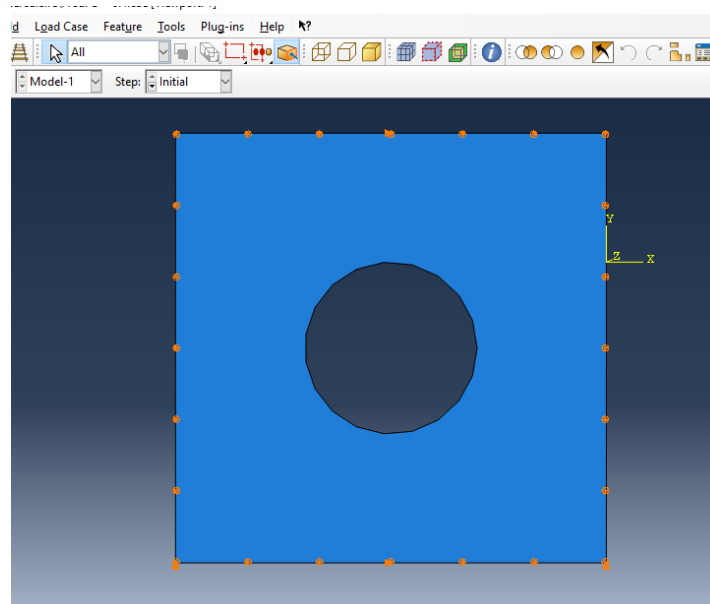


Figure 4.14 the boundary condition

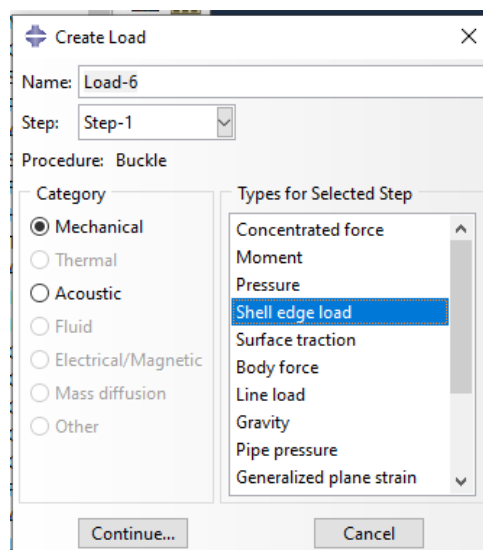


Figure 4.15 Creating load

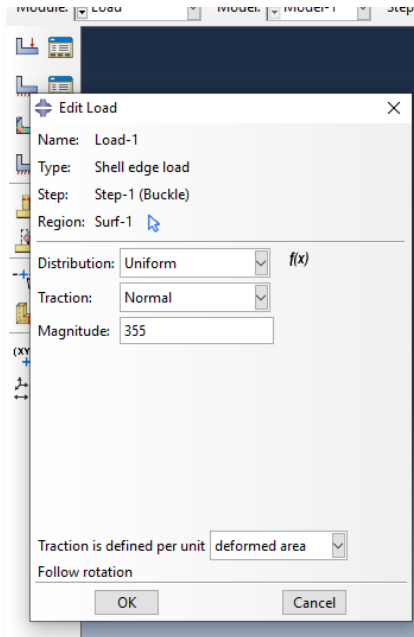


Figure 4.16 Selection the value of load

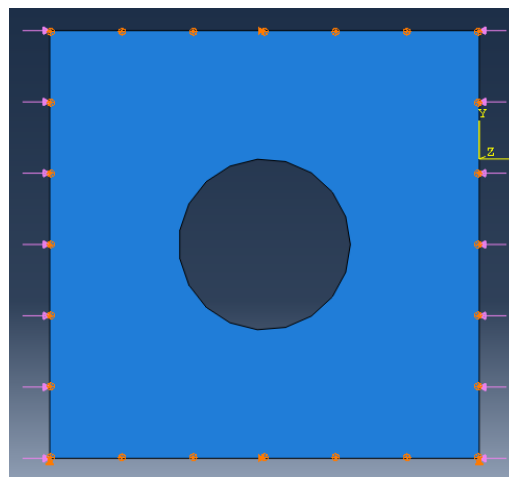


Figure 4.17 Presentation of Load

#### 4.2.6 Create Mesh

Select Mesh Module. From Seed Part make an approximation for global size of part and the number of nodes on each edge. Smaller values mean smaller finite element size and more execution time. Choose Mesh Part and click Ok. The mesh will be creating as Figure 4.18. This automatic mesh is good enough for our analysis and will produce reliable results, therefore keep it as it is and keep going to the next step.

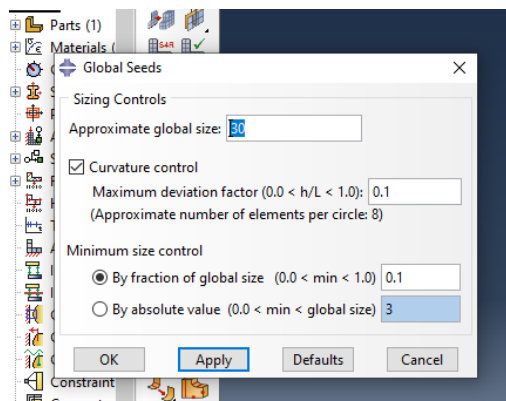


Figure 4.18 Selection the value of the mesh

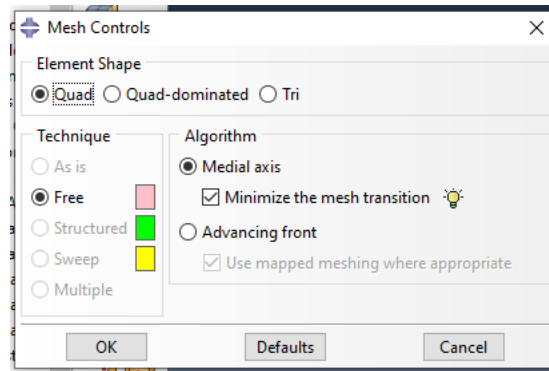


Figure 4.19 Selection the type of element and technique in mesh control

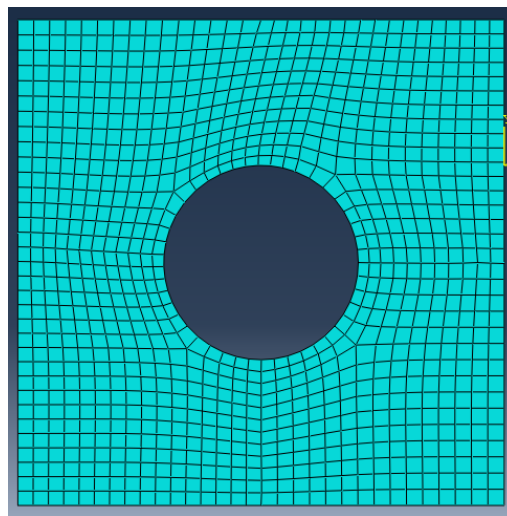


Figure 4.20 the presentation of meshing in the plate (1)

#### 4.2.7 Job

As soon as finishing the previous actions to define the model, use Job Module to involve the analysis tasks. This module allows submitting a job for analysis and monitoring its progress. Multiple models and runs may be submitted and monitored simultaneously. Follow the progress and wait to see the successful completion of job, Figure 4.21.

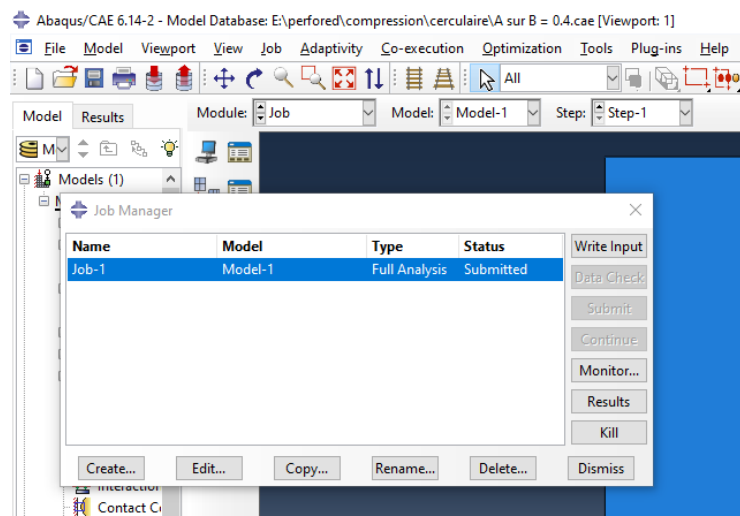


Figure 4.21 creating the job and submitted it

### 4.2.8 Results

Switch from Model to Results mode first. ABAQUS/CAE has provided sets of tools to display the results on finite element model. It can show deformed/undeformed plots and plots contours on deformed shape as well and so more, see Figure 4.22

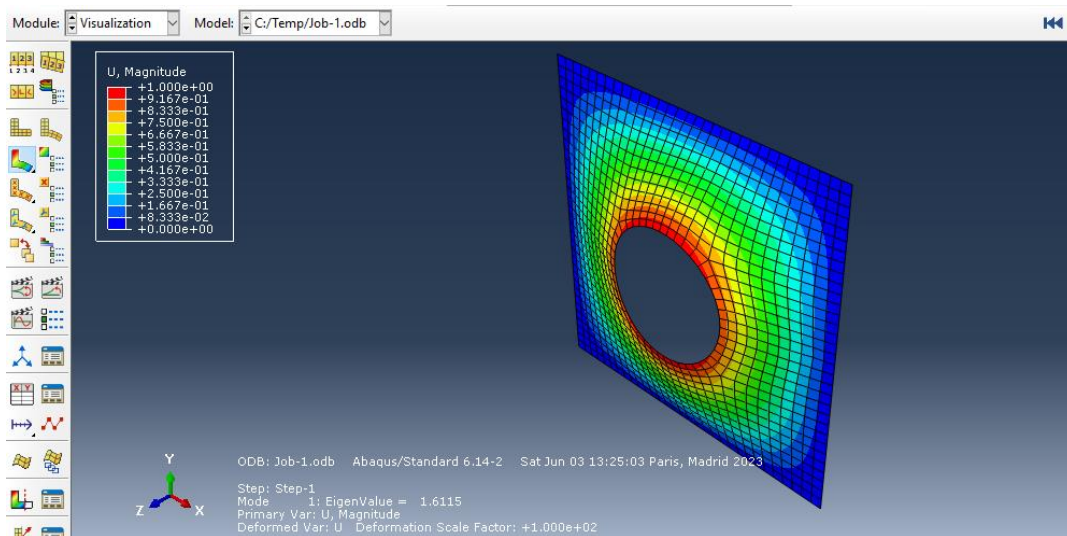


Figure 4.22 Results

## 4.3 EBPlate for elastic buckling analysis

### 4.3.1 General

EBPlate is a freeware program that is made primarily for with or without stiffeners. EBPLATE is a software literally **Elastic Buckling of Plate** (EBPlate) was designed and developed by the “Centre Technique Industriel de la Construction Métallique “in abbreviation CTICM, with a partial funding from European Research Fund for Coal (RFCS).and Steel to help with calculation of critical buckling stress of panels. EBPlate is a piece of software developed by CTICM with a partial funding of the European Research Fund for Coal and Steel.

### 4.3.2 Scope of EBPlate

EBPlate is designed to calculated critical buckling strength of rectangular plate with or without stiffeners subjected to in-plane load. Stiffeners can be assigned to the plate as longitudinal and/or transverse stiffeners of which EBPlate offers a number of different options. It assesses the critical stresses associated to the elastic buckling of plates loaded in their plan.

EBPlate software provides accurate values of elastic critical stresses for a wide field of practical cases of rectangular plates subject to in-plane loading. Plates can be either stiffened or unstiffened, the stiffening being provided by longitudinal and/or transverse stiffeners; orthotropic plates can also be treated. Complex stresses patterns can easily be defined, including patch loads. Numerous display possibilities are available for data and results

The User Graphical Interface is available in English, French, German and Spanish, whereas the Help file is provided only in English and in French. EBPlate V2. 01 has been validated and runs



on the following OS: Microsoft Windows XP, Microsoft Windows Vista et Microsoft Windows Seven.

### 4.3.3 Applications

When it comes to calculation of critical buckling stress for a panel without stiffeners or panel with stiffeners two different types of buckling should be consider, global buckling and local buckling. EBPlate is deigned to calculate the first buckling mode without considering the type of buckling (local buckling or global buckling) by taking into account separately or simultaneously the presence of discrete stiffeners and orthotropic behaviour of plates. [13]

### 4.3.4 Brief presentation of the capabilities

The scope of EBPlate may be summarized as follows :

**Plate:** . rectangular ( $a \times b$ ), uniform thickness  $t$

Possibly orthotropic ( $D_x, D_y$ ) due to smeared stiffeners

Plate stretching neglected

**Supports:**

laterally supported along its 4 edges (out-of-plane displacement  $w = 0$ )

support conditions in rotation at edges: hinged or restrained (full or elastic – rotational ( $K_r$ ) and/or torsional ( $J$ ) stiffnesses accounted for)

**Stiffeners:**

longitudinal and/or transverse, single or multiple, with different properties

axial (due to area  $A_s$ ), flexural (due to flexural inertia  $I_s$ ) and torsional (due to torsional constant  $J_s$ ) stiffnesses accounted for . smearing of identical and regularly spaced stiffeners ( $D_x, D_y$ ) automatic calculations of stiffener properties for commonly used cross-sections . special treatment for closed (trapezoidal) stiffeners, accounting for the distance between their junctions to the plate, their torsional stiffness, the flexibility of their cross-section

**Stresses:**

normally, generated by stress patterns acting along edges in the mid-plane . possibility of linear variation of longitudinal stress  $\sigma_x$  along the plate length . possibility of generating any stress distribution by defining directly stresses ( $\sigma_x, \sigma_y, \tau$ ) within the elements of a regular meshing of the plate possibility to impose one or more stresses at buckling state and to perform the buckling analysis on the remaining free stresses.

### 4.3.5 Menus

The following menus are available:

- “File” menu

The parameters of the study, but not the results, can be saved in an ASCII file, which extension is .EBP. The following operations are allowed: opening a file, saving or saving as a file and opening directly one of the last four files. [13]

- “Options” menu:

The options menus enable the user to modify several parameters of EBPlate:

- the language of the interface – French, English, German and Spanish are available;
- the default working directory, where files are opened or saved;
- the unit in which length are defined by the user (m, cm or mm);
- the table of colors with whom the results are displayed;
- The coefficient which defines the length of plate to be attached to a stiffener to calculate its second moment of inertia.

This menu give access to the “About” window and to the Help Files.

The “About” windows proposes email addresses to be contacted in case of troubles.

EBPlate is delivered with a French Help File, associated to the French interface and with an English Help File, associated to all other language of the interface.

#### 4.3.6 Toolbars

The most useful functions and the working areas of EBPlate can be activated directly by the buttons of the toolbars. The functions associated with the buttons of the main

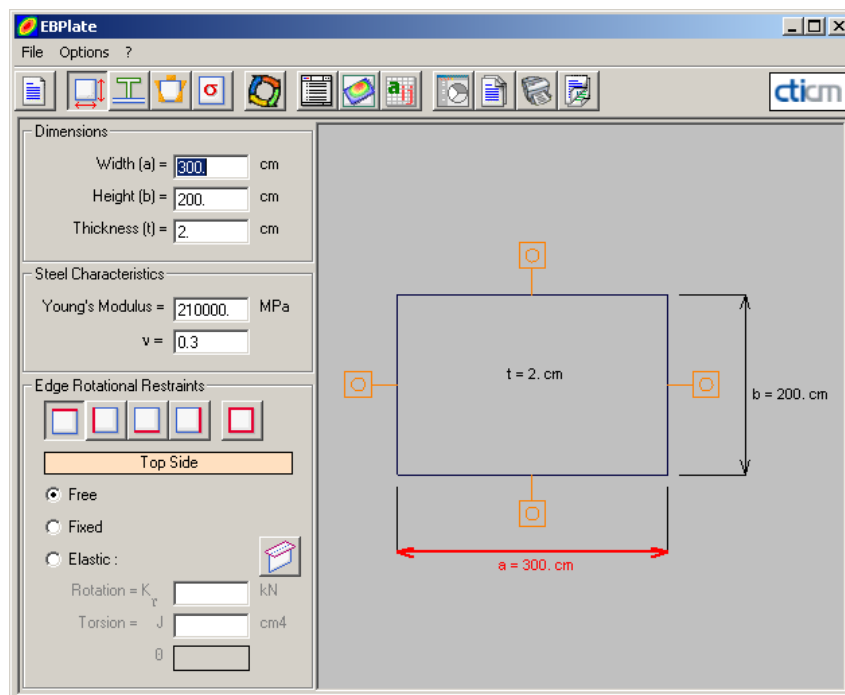


Figure 4.23 Main window of EBPlate and its areas

**Calculation's options:**

- The maximum number of half waves of the buckling mode has to be specified for each direction of the plate. This can be done automatically by EBPlate from a level of complexity defined by the user, from 1 for the simplest case to 3 for the most complicated one. But the user can also impose his own values.

A high maximal number of half wave's leads to more accurate results but in the other hands implies much longer calculation times.

- The number of modes to be searched: the first buckling mode by default, the twenty first ones or all the buckling modes.

- The contour lines of the first buckling mode can be calculated if requested.

**Calculation:**

The calculation process is divided in three steps: preparation of the matrices, resolution of the Eigen problem and calculation of the contour lines. For each step, a progress bar is displayed during the process and the calculation times are edited. [13]

**4.3.7 Examples****Elastic case:**

- **Compression case :**

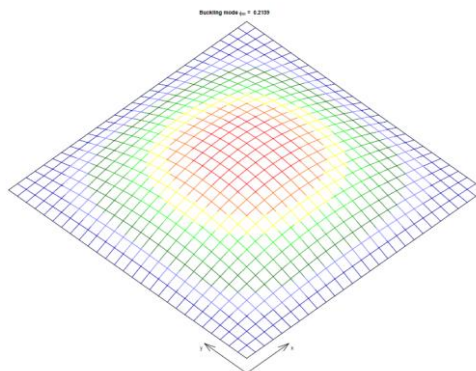


**Figure 4.24. Square plate with hole: elastic buckled shape under compression.**

- **Shear case :**

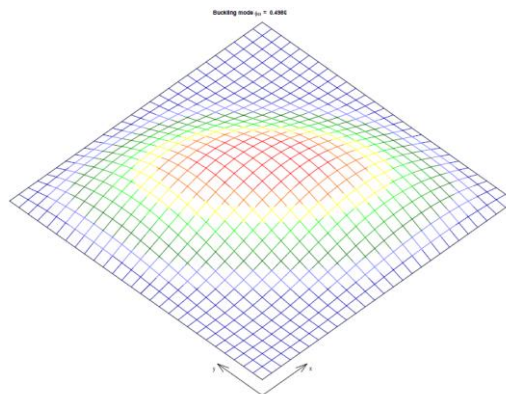


**Figure 4.25. Square plate with hole: elastic buckled shape under shear**

**CHAPTER 5**  
**VALIDATION AND VERIFICATION OF MODELS**  
**NON-PERFORATED AND PERFORATED THIN**  
**PLATES**

## 5.1 Introduction

In this chapter, a compressive FEA program models has been performed on thin steel plates. For the sake of validation, the FEA elastic models were executed and verified with some results available in literature and restart this linear buckling analysis in order to conduct nonlinear buckling analysis on the same models. The aim of this task is to have, obviously, more confidence in the numerical analysis in these models, as they will be used later, for more complicated analyses: nonlinear and inelastic buckling analysis.

As already mentioned in chapter 3, the numerical analyses are conducted by using two software: Abaqus and EBPlate.

In fact, the validation concerns models under different kind of loadings, that is: compression; shearing and combined compression associated to shearing loadings. Also, models are built-up for thin plates with and without cut-up, with variable sizes and shapes. The validation is done by comparing the obtained values of the elastic eigen buckling analysis.

For plates under compression, the validation addresses some results found from literature, under compression namely: (Real and al. 2013) for rectangular plates and (Uslu et al. 2022) for square plates. Also, the same operation was carried out using the two software of interest, as fully described in Chapter 3. As far as plates under shear loading are concerned, the comparison is made through the modelling build-up in two different software: ABAQUS and EBPLATE (see chapter 4 for more details).

## 5.2 Validation of Models

It is well known that the quality of the results obtained from FEA depends up on the density of the mesh, element type and the input properties of the element. Some preliminary analyses were conducted to study the effect of mesh refinement, and to determine whether reduced integration elements could be used to improve computational time without loss of significant accuracy.

The validation of elastic models will be presented according to the applied loads: compression, shear and combined.

### 5.2.1 Compression

In the following, the validation addresses some results found from literature, under compression namely: (Real and al. 2013) for rectangular plates and (Uslu et al. 2022) for square plates respectively.

#### 5.2.1.1 Case of rectangular plate without cut-out (in compression)

For the sake of validation and verification of the computational modelling, the first model concerns the basic case of rectangular plate under compression loading without hole). [14]

The general characteristics of the model, including geometry and material properties are summarised in Table 5.1 giving the essential of properties of the model to be used and compared using both Abaqus and EBPLATE software respectively.

So, the critical load of a non-perforated plate was numerically evaluated, and results are compared to the analytical solution given by Timoshenko and Gere.

**Table 5.1 Geometrical and material characteristics of the implanted models**

Characteristic	Value
Young's modulus ( $E$ ).	210.0 GPa
Poisson's ratio ( $\nu$ )	0.3
width of plate ( $H$ )	1.0 m
length of plate ( $L$ )	2.0 m
thickness ( $t$ )	0.01 m

- **Validation using Abaqus (see Chapter 3)**

A summary of how to proceed is given in the following.

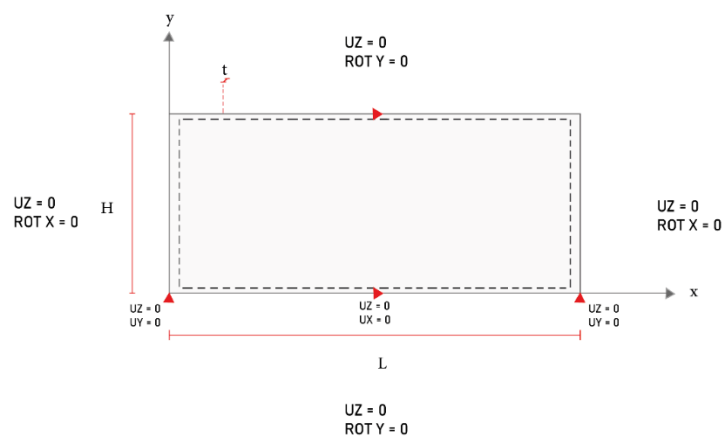


**Figure 5.1. Non-perforated plate model and boundary conditions**

### Type of Element

In all numerical simulations the ABAQUS, reduced integration eight-node thin shell element was employed. This element has six degrees-of-freedom at each node: three translations ( $u, v, w$ ) and three rotations ( $\theta_x, \theta_y, \theta_z$ ).

### Meshing

The plate was discretised adopting a rectangular element with side size of 30.00 mm, generating a mesh with 1814 finite elements. (See Figure 5.2)

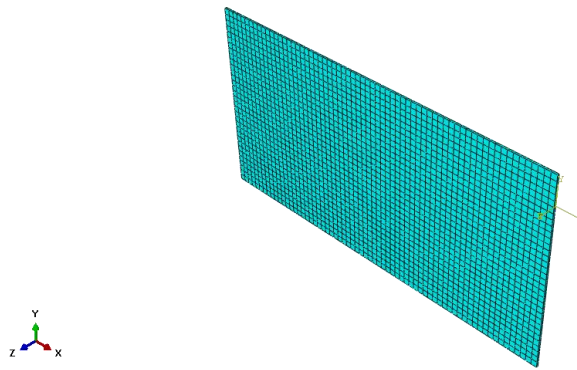


**Figure 5.2. Finite element mesh of the plate without hole by Abaqus.**

### Boundary conditions

Boundary conditions and general characteristics of the model are depicted in Figure 5.1. In the present study, plates are considered to be simply supported on all edges. As shown in Figure 5.1, it can be seen that freedom of the translational displacement in the plane of the plate and condition of non-occurrence of rigid body movement should be applied to the models. For this purpose, two joints at the bottom corners were fixed in the y direction and middle joint at the bottom edge was fixed in the x direction.

### Outcomes (results)

As previously mentioned in the previous section, the comparison will be made through the values of the obtained critical load.

The numerical results for the critical buckling load showed in the Table 5.2, while Figure 5.2 presents the buckled shape of the plate without hole.

**Table 5.2. Comparison of critical buckling load for plate non-perforated.**

<b>Hole diameter (mm)</b>	<b>Ncr (kN/m)</b>		<b>Difference</b>
	<b>Reference [16]</b>	<b>This study using ABAQUS</b>	
d = 0	759.20	752.60	-1.58%

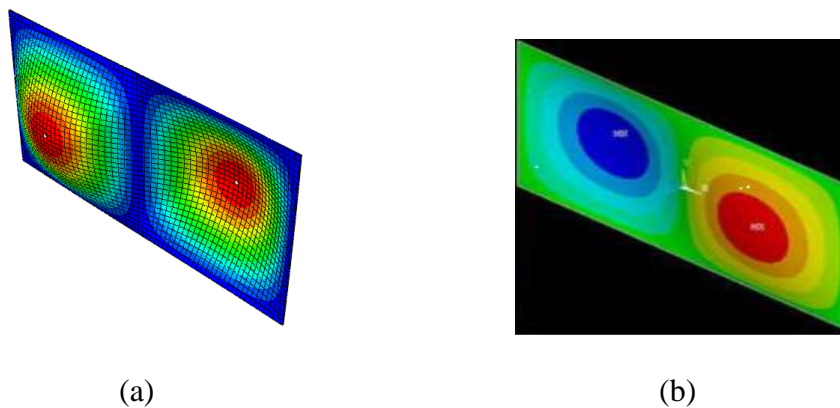


**Figure 5.3. Ultimate deformation configuration at the last stage of buckled shape. (a) Author's results; (b). [14]**

#### - Validation using EBPLATE (chapter 3)

The validation of the reference results follows the same manner as it was for Abaqus. In fact, the same data has been used as describe in the previous section for modelling using EBPLATE.

#### **Summary of the modelling procedure with (EBPLATE)**

##### **Outcomes (results)**

The numerical result for the critical buckling load showed in the table 5.1, (Figure 5.2) presents the buckled shape of the plate without hole.



**Table 5.3. Comparison of critical buckling load for plate non-perforated.**

Hole diameter (mm)	Ncr (kN/m)		Difference
	Previous research using ANAYSIS [16]	EBPLATE	
d = 0	759.20	759.34	0.01%

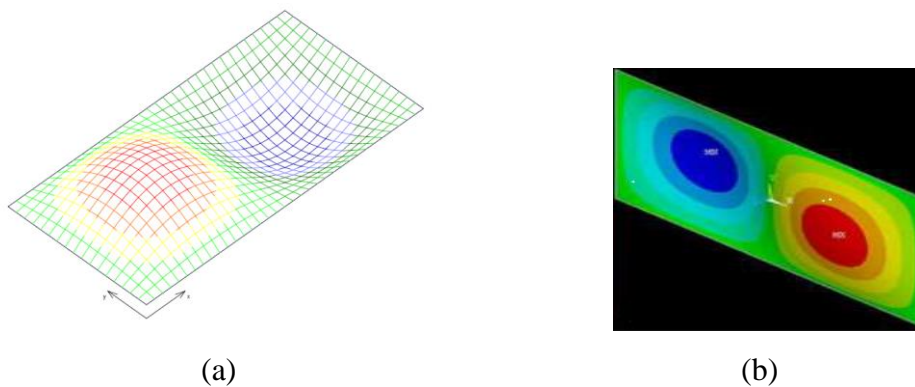


**Figure 5.4. Ultimate deformation configuration at the last stage of buckled shape. (a) Author's results; (b). [14]**

**Conclusion:** As can be seen from Tables 5.2 and 5.3, the results obtained in this work are very close to those given in the ref. However, the EBPlate outcomes seem to be more accurate compared to Abaqus outcomes. So, the model with its details seems to be correct.

### 5.2.1.2 Case of Rectangular plates with different circular cut-out diameter (in compression)

For plates with perforations there is no easy analytical solution available and the approach adopted for buckling analysis was the finite element eigenvalue buckling analysis. Here, the computational model previously presented was employed to analyse the buckling behaviour of thin perforated plates already studied by El-Sawy and Nazmy.

## - Using only Abaqus

### Summary of the modelling procedure

#### Type of Element, Meshing and Boundary conditions:

In the following, the same conditions have been used as describe in the previous section for modelling using ABAQUS (Figure 5.4).

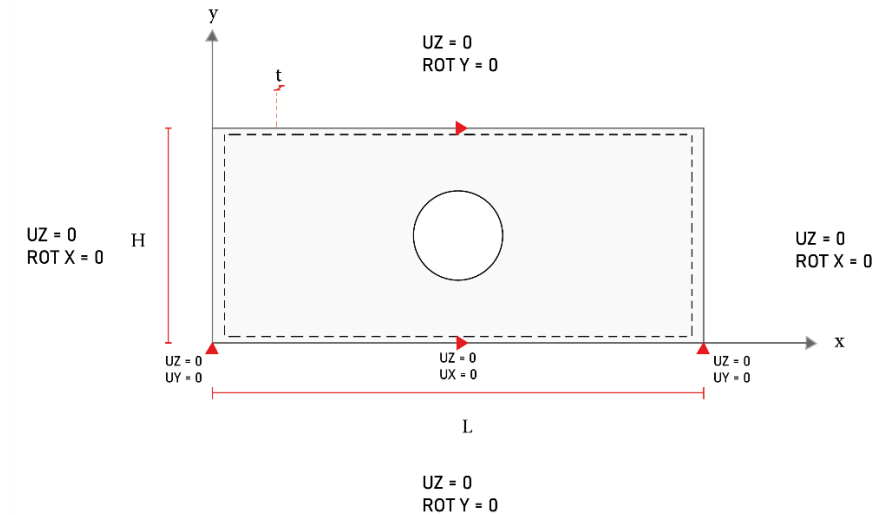


**Figure 5.5. Perforated plate model and boundary conditions**

#### Number of elements:

In this case we preformed 6 models which is a rectangular perforated plate under compression with a different hole diameter ( $d$ ).

#### Outcomes (results)

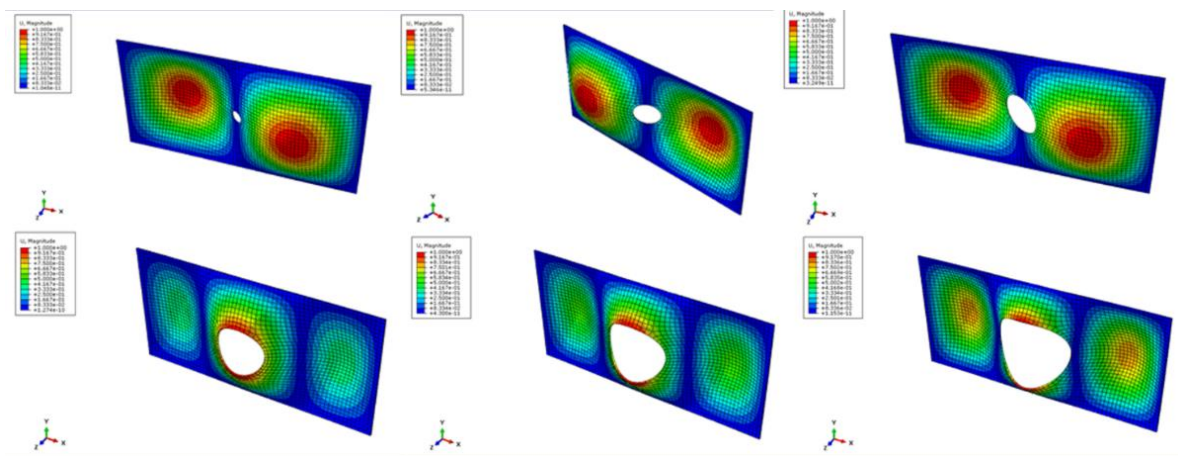
The same plate used in the previous section was once again studied with centred circular holes.

In table 5.4 the results for the critical buckling load were compared with those obtained by the numerical study developed by El-Sawy and Nazmy [16]. Once again, an excellent agreement was obtained, being -1.58% the maximal difference encountered as explicitly shown in the relative Table 5.4.

The Buckling modes for a perforated plate is presented by the following figures from 5.6.1 to 5.6.6 in order

**Table 5.4. Comparison of critical buckling load for plate with centred circular hole.**

Hole diameter (m)	Ncr (kN/m) Using ANAYSIS Reference [16]	Ncr (kN/m) Authors (Abaqus)	Difference (%)
0.10	766.19	758.72	-0.98%
0.20	789.36	781.05	-1.06%
0.30	825.08	814.31	-1.32%
0.40	849.26	841.38	-0.93%
0.50	901.54	890.47	-1.24%
0.60	986.46	971.11	-1.58%



(a)

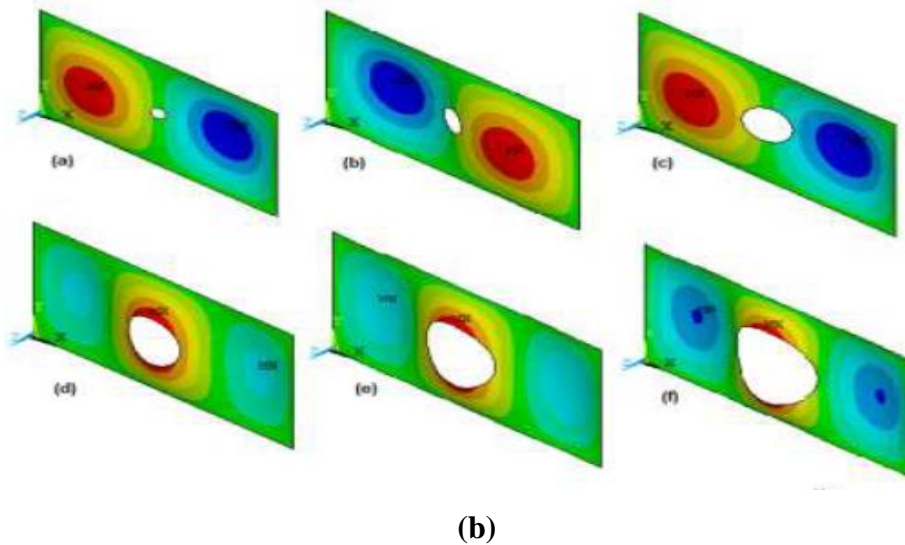


**Figure 5.6. Ultimate deformation configuration at the last stage of buckled shape for plates with different cut-out diameters. Author's results; (b). [14]**

In addition to the obtained  $N_{cr}$  values, it can be seen from the above figure, the deformed buckled shape of the analysed plates presents the same patterns and look like alike for all studied cases. This will give, once again, and obviously some confidence to the model built-up in Abaqus as it give very reasonable outcomes.

### 5.2.1.3 Case of Square Plate without Hole

In order to investigate the effect of slenderness ration ( $A/B$ ) of the plate on the modelling of the linear and nonlinear buckling behaviour of plates, a square thin plate under compression was considered. In the same way as explained in the previous section, models built-up in Abaqus and EBPlate software were considered.

The general characteristics of the model, including geometry and material properties. Table 5.5 summarises the essential of properties of the model to be compared using Abaqus and EBPLATE software. [15]

**Table 5.5 Geometrical and material Characteristics of the implanted model**

Characteristic	Value
Young's modulus ( $E$ )	200.0 GPa
Poisson's ratio ( $\nu$ )	0.3
width of plate ( $H$ )	300 mm
length of plate ( $L$ )	300 mm
Thickness ( $t$ )	2 mm

**- Using Abaqus**

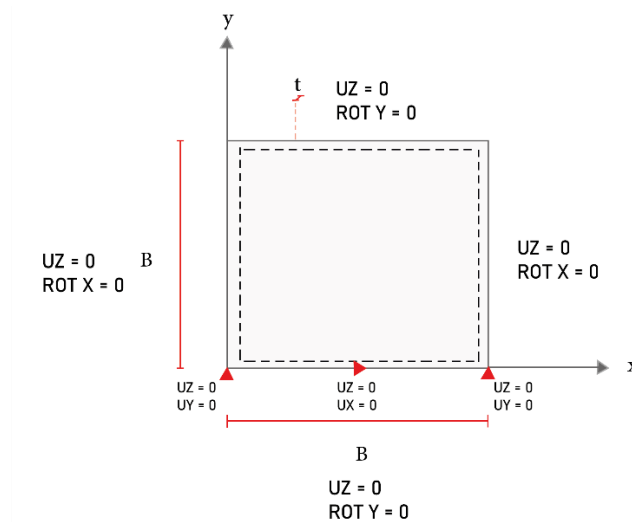


**Figure 5.7. Non-perforated square plate model and boundary condition**

**Outcomes (results)**

The numerical result for the critical buckling load showed in the table 5.6, (Figure 5.8) for buckled shape of the plate without hole.

**Table 5.6. Comparison of critical buckling load for plate non-perforated.**

Hole diameter (mm)	Ncr (kN/m)		Difference
	Reference [15]	ABAQUS	
d = 0	64.2790	64.2252	0.08%

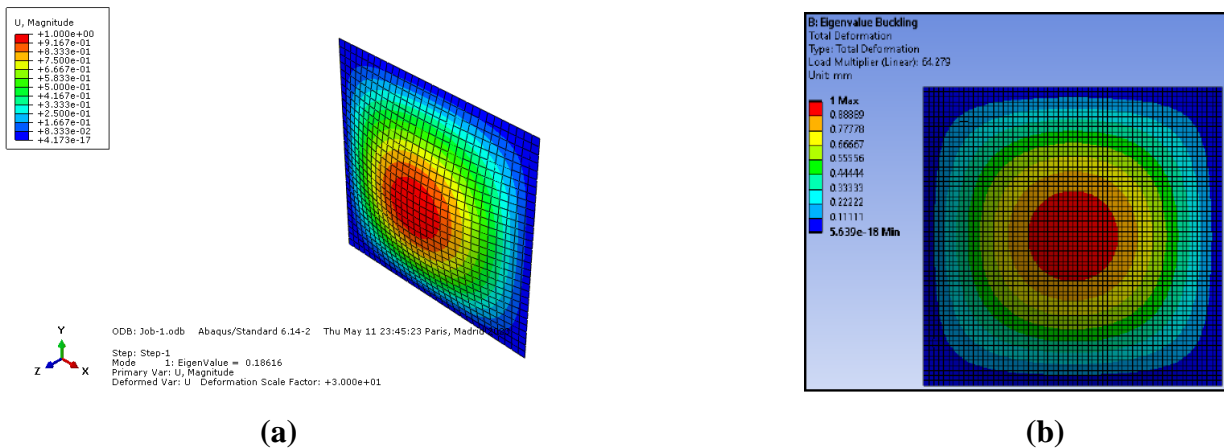


**Figure 5.8 Ultimate deformation configuration at the last stage of buckled shape. (a) Author's results; (b). [15]**

**- Using EBPLATE**

In the following, the same data has been used as describe in the previous section for modelling using EBPLATE.

**Outcomes (results)**

The numerical result for the critical buckling load showed in the table 5.7, (Figure 5.9) presents the buckled shape of the plate without hole.

**Table 5.7. Comparison of critical buckling load for plate non-perforated.**

Hole diameter (mm)	Ncr (kN/m)		Difference
	Reference [15]	EBPLATE	
d = 0	64.2790	64.2390	0.07%

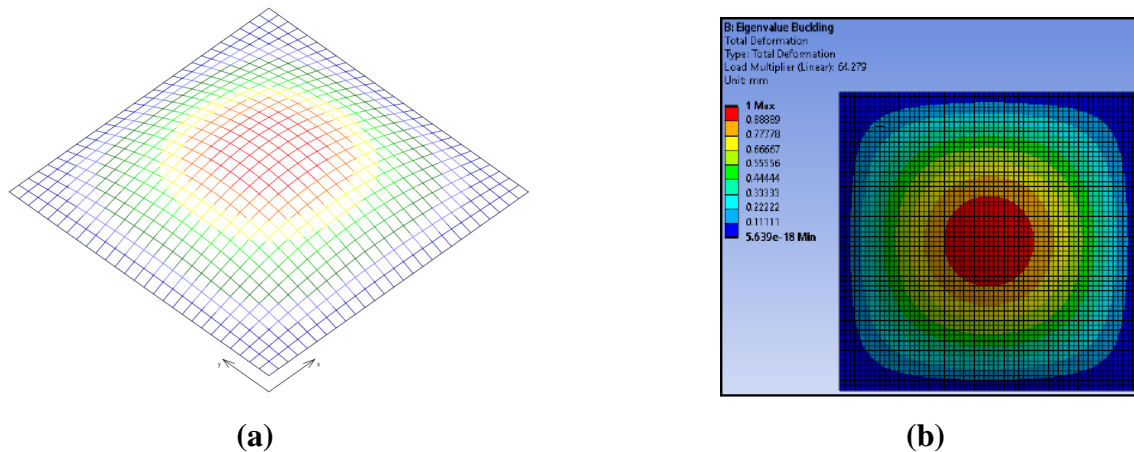


**Figure 5.9. Ultimate deformation configuration at the last stage of buckled shape. (a) Author's results; (b). [15]**

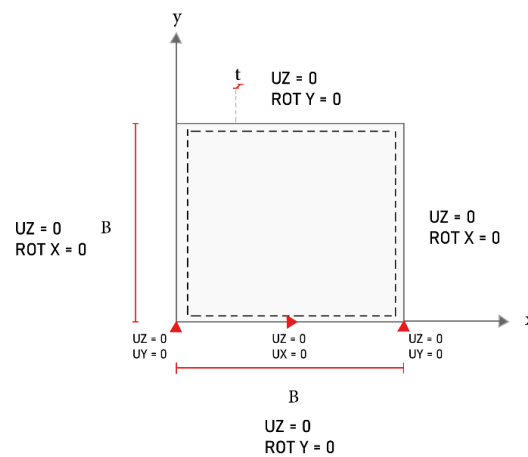
### 5.2.2 Shear

For the same objective as above, the validation and verification of the computational modelling, shear forces, the first model concerns the basic case of square plate under shear loading without hole.

The general characteristics used in the numerical models including geometry and material properties are summarised in Table 5.8. The comparison of results will be conducted between Abaqus and EBPLATE software.

**Table 5.8 Geometrical and material Characteristics of the implanted model**

Characteristic	Value
Young's modulus ( $E$ )	200.0 GPa
Poisson's ratio ( $\nu$ )	0.3
width of plate ( $H$ )	300 mm
length of plate ( $L$ )	300 mm
Thickness ( $t$ )	2 mm

**Figure 5.10. Non-perforated square plate model and boundary condition****Outcomes (results)**

The numerical results for the critical buckling load showed in the Table 5.9, (Figures 5.11, 5.12) presents the buckled shape of the plate without hole.



**Table 5.9. Comparison of critical buckling load for plate non-perforated.**

<b>Hole diameter</b> (mm)	<b>N<sub>cr</sub> (kN/m)</b>		<b>Difference</b>
	<b>ABAQUS</b>	<b>EBPLATE</b>	
d = 0	163.49	157.32	3%

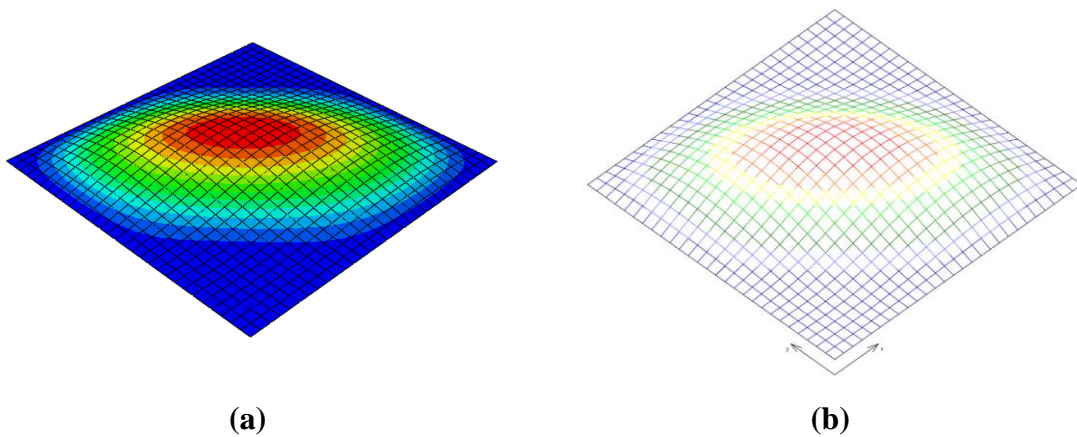


**Figure 5.10. Ultimate deformation configuration at the last stage of buckled shape. (a) Abaqus; (b) EBPLATE.**

### **Conclusion:**

Roughly speaking, the two software give practically the same values of the shear critical load with similar buckling deformed pattern.

### **5.2.3 Compression and Shear**

For more complicated loading pattern, that is combined compression added to shear acting on the peripheries of the plates has been explored.

For the sake of validation and verification of the computational modelling, the first model concerns the basic case of square plate under combined loading without hole. The general characteristics of the model, including geometry and material properties are the same as the previous cases summarises the essential of properties of the model to be compared between ABAQUS and EBPLATE software as a verification.

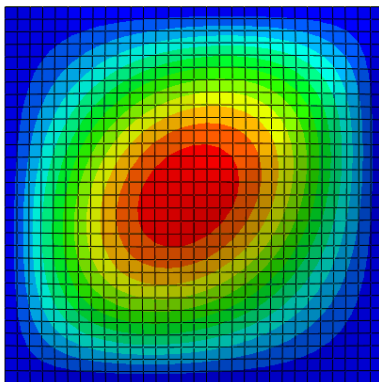
### Case of Square Plate without Hole

#### Outcomes (results)

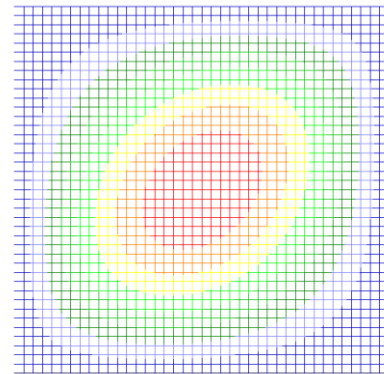
The numerical result for the critical buckling load showed in the table 5.10, (Figure 5.11) presents the buckled shape of the plate without hole in the both of software.

**Table 5.10. Comparison of critical buckling load for plate non-perforated.**

Hole diameter (mm)	Ncr (kN/m)		Difference
	ABAQUS	EBPLATE	
d = 0	56.61	58.30	2.8%



(a)



(b)

**Figure 5.11. Ultimate deformation configuration at the last stage of buckled shape. (a) Abaqus; (b) EBPLATE.**

#### Conclusion:

The same remarks can be made for this case, with a difference of less than 3% in predicting the critical loads and almost the same pattern of the deformed buckling shape.

### 5.3 General conclusion

As general conclusion of this investigation discussed in the above sections, the elastic buckling numerical analysis was used for different loading cases for different geometrical aspects of thin plates with and without cut-outs. The general conclusion may that the validation has been performed and the elastic buckling can be used in a more complicated and realistic situation which is the parametric inelastic buckling behaviour of thin plates. This will be presented in details in the next chapter of this thesis.

**CHAPTER 6**  
**PARAMETRIC ELASTIC AND INELASTIC**  
**BUCKLING ANALYSIS OF SQUARE PLATES**

This chapter deals with a numerical compressive parametric analysis carried out on unstiffened simply supported steel square plates to assess the elastic (eigen) and inelastic buckling capacity using Abaqus software. The parameters being investigated in this investigation are: plate thicknesses; type of loading, the size and form of the cut-out.

Initially, it was planned to carry out elastic and inelastic buckling investigation on square plate considering three types of loadings: compression, shear and combined. However, with the lack of time, it was decided to perform eigen elastic buckling with for the three cases but only the case of compression for both elastic and inelastic case as it gives the lowest values of  $N_{cr}$ .

## 6.1 Modelling of the studied cases

In this section, properties of the physical model are presented including the geometrical and the material. Figure 6.1, bellow, gives the general characteristics of the model of square plates being studied in this work.

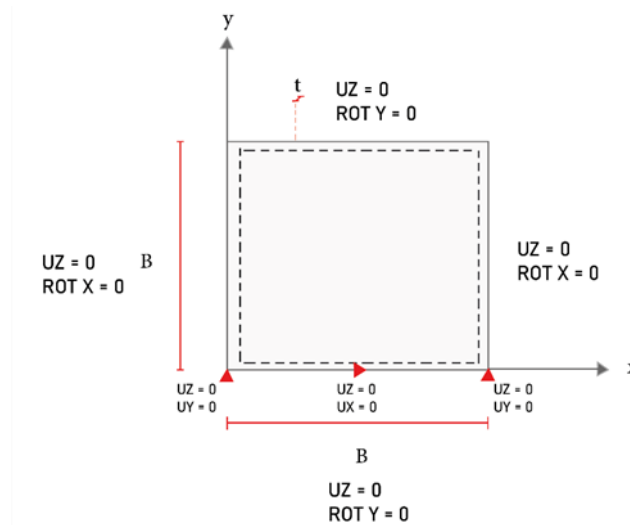


**Figure 6.1. Square plate model with boundary conditions**

### - Features of the computational models

In the following, the essential if the characteristics of the numerical 3D model including the geometrical, mechanical and boundary conditions will be described with some details. Furthermore, Figure 6.2 shows the different configurations of the models with and without cut-out. Also, the essential of dimensional parameters and material properties are Summarized in Table 6.1. Once again, Figure 6.1, shows the boundary conditions of the model. As it can be seen that freedom of the translational displacement in the plane of the plate and condition of non-occurrence of rigid body movement should be applied to the models. For this purpose, two joints at the bottom corners were fixed in the  $y$  direction and middle joint at the bottom edge was fixed in the  $x$  direction. Figures 6.3 to 6.6 show the general configuration of the considered models in terms of loadings. Figure 6.3 and 6.4 are relative to the elastic buck analysis, while Figure 6.5 is exclusively devoted to the inelastic buckling analysis.

**N.B.** It must be noted that the first parameter of this study is the thickness of plates. In fact, three different thicknesses have been considered that is: 10 mm; 20 mm and 40 mm. Also, as far as the cut-out is concerned, two kinds of holes have been studied with different sizes (proportions to the length of the square plate).

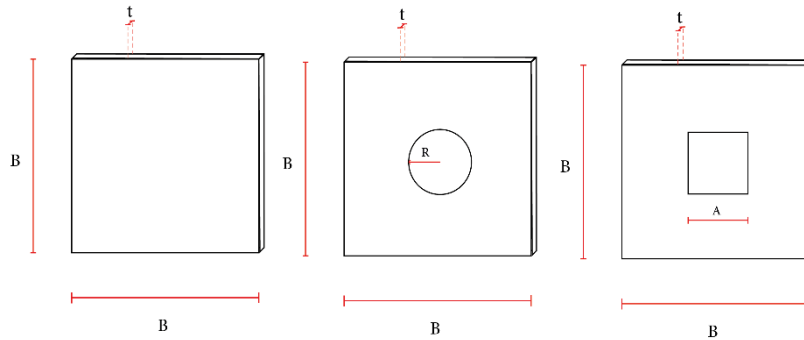


Figure 6.2 Dimensional parameters of the perforated plate on the side.

Table 6.1 Geometric dimensions and material properties of the perforated plate.

PARAMETERS	Plate length (B) in mm	Plate thickness (t) in mm	Radius of circular hole (R) in mm	Square hole length (A) in mm	Elastic modulus (E) in GPa	Poisson's ratio $\nu$	Load KN/m
VALUES	1000	- 10 - 20 - 40	- 50 - 200	- 100 - 400	210	0.3	355

The type of boundary condition used for the models is simple. Three different types of load are considered in the elastic and inelastic FE models: in-plane shear load and uniaxial compression load and combined compression and shear applied to the involved edges, see Figure 6.3. In the nonlinear buckling analyses, the prescribed displacement is applied incrementally for the particularly uniaxial compression loading. The above type of loadings are applied to intact and perforated square plates.

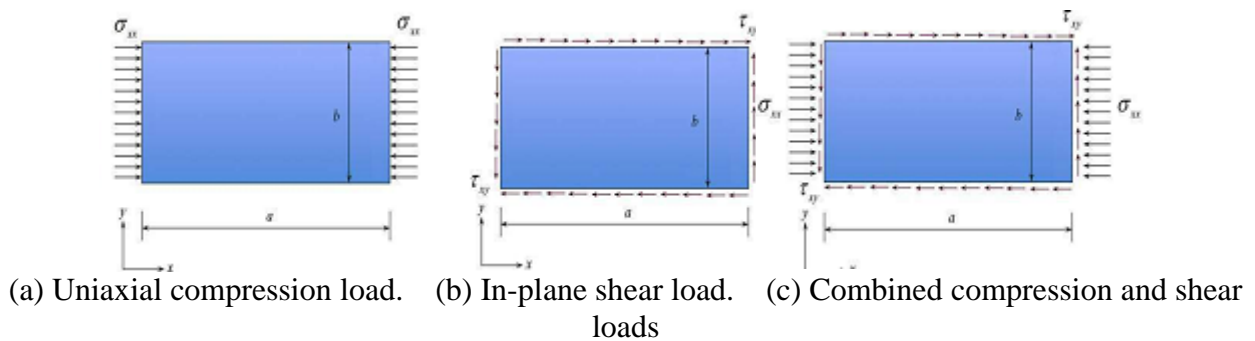


Figure 6.3 Types of loading used in the parametric elastic buckling analysis by FEA

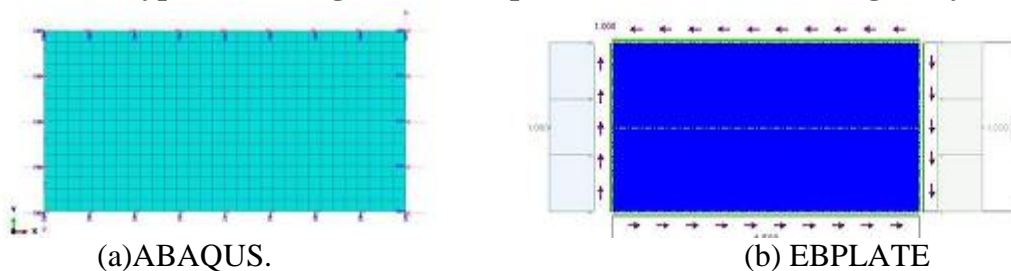
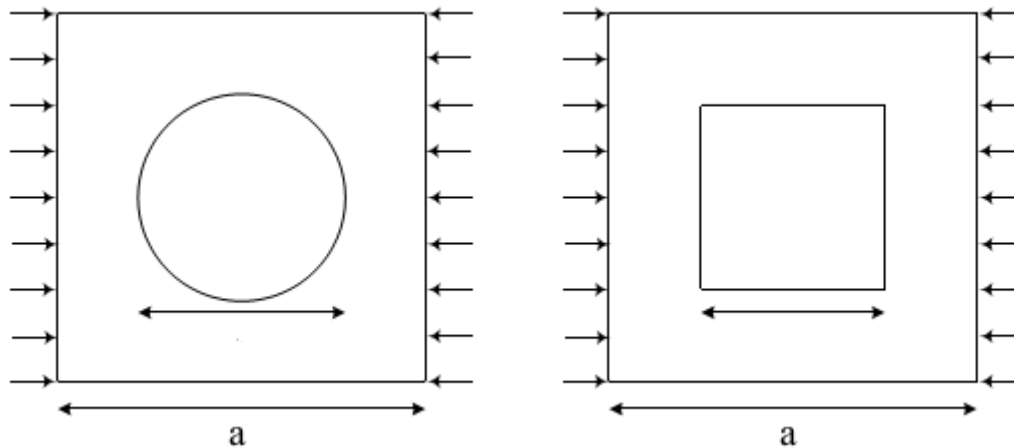


Figure 6.4 modelling the intact plates



**Figure 6.5 Plane view of square plate models with circle and square hole shapes used for inelastic buckling analysis by FEA by Abaqus.**

**N.B.** In Abaqus and EBPLATE software, the loading forces are input as uniformly distributed load N/mm.

### 6.2 Elastic buckling analysis results and discussion

As stated in previous chapters, the most basic form of buckling analysis in FEA is linear buckling. This is directly related to the classic Euler type of calculation. Elastic eigenvalue buckling analysis is an analysis that incorporates second order effects in structural stiffness matrix. Buckling loads and buckling deformations obtained from the analysis by theoretically making the determinant of the matrix equals to zero, are the eigenvalues and eigenvectors, respectively.

In this study, elastic buckling analysis is performed for two tasks. The result of the analysis is a series of eigenvalues and a set of mode shapes, or eigenvectors. The modes are completely independent in the linear analysis; so, mode 1 or 2 or 3, etc. could occur. It is important to assess the families of higher mode shapes and eigenvalues to see if any practical response implications occur. However often there may be only one dominant first mode, with the next set of modes completely infeasible and at very high critical loads.

For the sake of comparison and validation of the model built-up in Abaqus, EBPLATE free software was used.

- **Intact square plate**

Plates can be unstable because of the critical in-plane forces acting on the plates and these forces have effects also on flexural behaviour. And also, these plates acting with these forces may undergo buckling by becoming unstable. Tables 6.2 and 6.3 display the results obtained for an intact square plate with varying thicknesses. In term of eigenvalues obtained for the first buckling mode (fundamental) and the calculated critical loads given by the used software: Abaqus and EBPLATE.

**Table 6.2 Values of the first mode eigenvalue for intact square plate in terms of plate's thickness.**

First mode extracted eigenvalues							
Effect		Compression		Shear		Combined	
Software		ABQ	EBP	ABQ	EBP	ABQ	EBP
thickness	t= 10 mm	2.1269	2.139	5.3407	4.986	1.8694	1.847
	t= 20 mm	16.823	17.108	42.165	39.886	14.778	14.774
	t= 40 mm	131.15	121.668	325.19	319.084	114.92	118.18

**Table 6.3. Comparison of the calculated critical buckling load of an intact square in terms of plate's thickness.**

Critical buckling load Ncr KN/m							
Effect		Compression		Shear		Combined	
Logical		ABQ	EBP	ABQ	EBP	ABQ	EBP
thickness	t= 10 mm	755.04	759.34	1895.94	1770.03	663.637	655.68
	t= 20 mm	5972.16	6073.34	14968.57	14159.53	5246.19	5244.77
	t= 40 mm	46558.25	43192.14	115442.45	113274.82	40796.6	41953.9

Analyses were performed by using commercial finite element software package Abaqus and EBPLATE. The critical buckling loads of simply supported square intact plate subjected to in-plane uniaxial compressive, shear and combined compression and shear loads. Once assumed that the structure presents a linear elastic behaviour, a structural instability is foreseen, being the focus of the study the verification of the load that provokes the elastic buckling of the plate as shown in Table 6.2.

It can be seen from the Tables above and figure 6.6 that almost the same results given by the two used software. Figure 6.6 (Abaqus) shows out-of-plane (z direction) relative displacement of first buckling mode obtained from elastic eigenvalue buckling analysis for square intact plate with different thicknesses. As the thickness increase as the out-plane deformation decrease.

For the particular case of uniaxial compression, the critical load in KN/m increases with the increase of the thickness, which is logical, from 755.04, 5972.16, to 46558.25 for  $t = 10; 20$  and  $40$  mm respectively according to Abaqus. This tendency is quite similar according to EBPLATE with 759.34; 6073.34 and 43613.14 for  $t = 10; 20$  and  $40$  mm respectively according to EBPLATE.

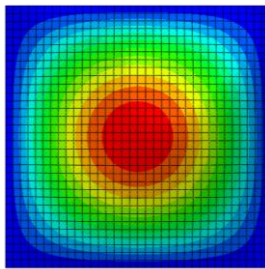
For shear loading, the following were found for the first mode of buckling: 1895.9; 14968.57 and 115442.45 for  $t = 10; 20$  and  $40$  mm respectively according to Abaqus. With EBLATE software, 1770.03; 14159.53 and 113274.82 were found and good agreement is noteworthy.

For the case of combined loadings, the same remarks can be made. Values obtained from software are: Abaqus gives 663.637; 5246.19; 40796.6 and EBP the values of 655.68; 5244.77; 41953.9 showing even better agreement than the two preceding load cases.

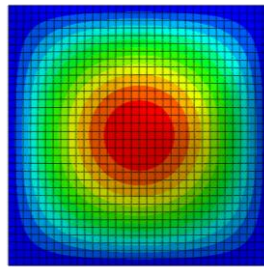
Bellow, are presented the deformed buckling shape relative to the first mode eigen values for the case of intact square plate:  $d = 0.$ , for three types of loading: compression, shear and combined.

Figure 6.6 displays the Abaqus out-come, while Figure 6.7 presents the results of EBPLATE. It can be seen from the following Figure 6.8 that the same pattern of deformation is obtained from EBPLATE as early discussed for Abaqus out comes.

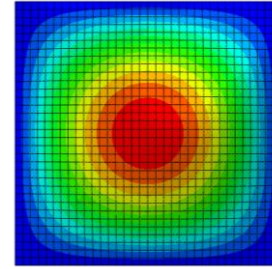
### Compression



t = 10 mm

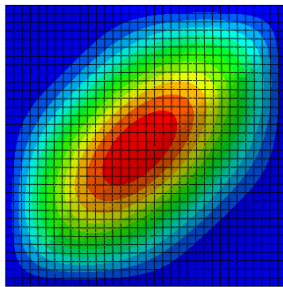


t = 20 mm

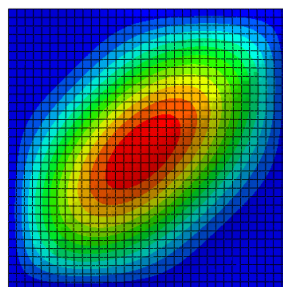


t = 40 mm

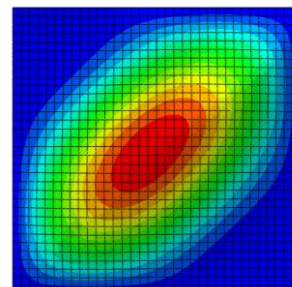
### Shear



t = 10 mm

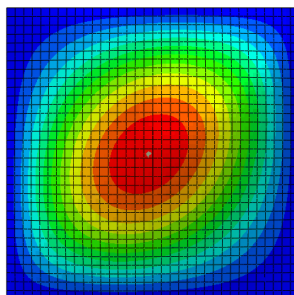


t = 20 mm

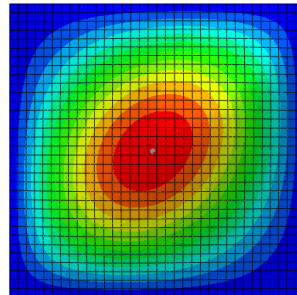


t = 40 mm

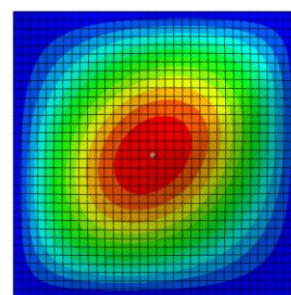
### Combined



t = 10 mm



t = 20 mm



t = 40 mm

**Figure 6.6. The first modal vibration mode shapes for an intact square plate by Abaqus**



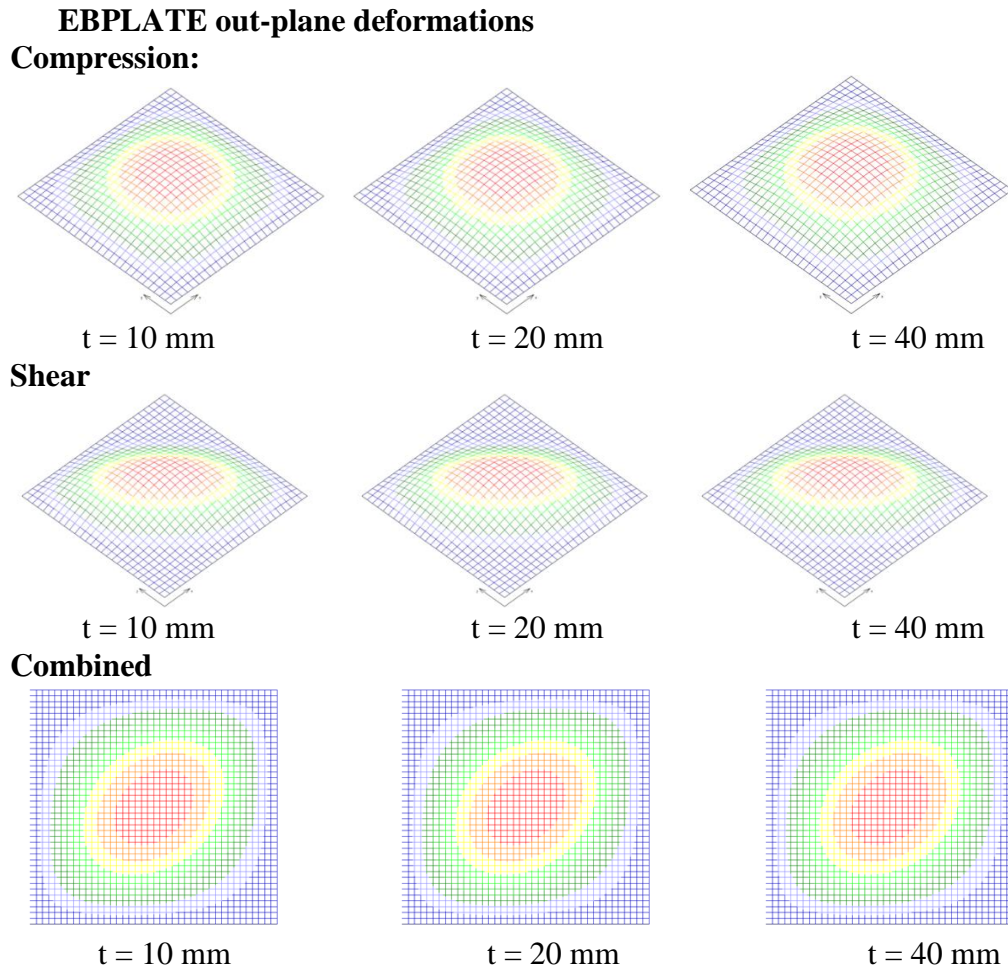


**Figure 6.7. The first modal vibration mode shapes for an intact square plate by EBPLATE**

- **Perforated square plate**

In the same manner as it was in the previous section, the buckling elastic results are given in terms of results of the first mode shape from Abaqus. The critical loads were calculated in accordance of the first eigen value and the out-plane displacement are also plotted. The cut-out made in the square plate are of two kinds: circular centered hole and square hole with different sizes.

As it can be seen from Table 6.3, the value of the critical load decreases with the increase of the size of the cut-out. This is true for both kind of hole shapes.

**Thickness  $t = 10$  mm**

**Table 6.5 Values of the first mode eigenvalue for perforated square plate in terms of plate's thickness.**

<b>First mode extracted eigenvalues</b>				
<b>Shape of hole</b>	<b>Circular (R)</b>		<b>Square (A)</b>	
<b>Hole diameter (d/b)</b>	<b>0.1</b>	<b>0.4</b>	<b>0.1</b>	<b>0.4</b>
<b>Compression</b>	2.0502	1.6115	2.0221	1.6046
<b>Shear</b>	5.0140	2.4888	4.8279	1.9858
<b>Combined</b>	1.7884	1.2059	1.7520	1.0846

**- Thickness  $t = 20$  mm**

**Table 6.6 Values of the first mode eigenvalue for perforated square plate in terms of plate's thickness.**

<b>First mode extracted eigenvalues</b>				
<b>Shape of hole</b>	<b>CIRCULAR (R)</b>		<b>SQURE (A)</b>	
<b>Hole diameter (d/b)</b>	<b>0.1</b>	<b>0.4</b>	<b>0.1</b>	<b>0.4</b>
<b>Compression</b>	16.224	12.707	15.982	12.570
<b>Shear</b>	39.720	19.659	38.189	15.666
<b>Combined</b>	14.154	9.5180	13.849	8.5308

- Thickness  $t = 40$  mm

**Table 6.7 Values of the first mode eigenvalue for perforated square plate in terms of plate's thickness.**

First mode extracted eigenvalues				
Shape of hole	Circular (R)		Square (A)	
Hole diameter (d/b)	0.1	0.4	0.1	0.4
<b>Compression</b>	126.59	98.441	124.49	96.228
<b>Shear</b>	306.91	150.78	294.51	119.85
<b>Combined</b>	110.18	73.494	107.61	65.363

Tables 6.5 to 6.8 show the eigen values for different cases of the first mode buckling shape, as it will be used to compute  $N_{cr}$ .

All eigen values are positive, which mean that the instability can occur before reaching the ultimate load capacity of the plate.

The effect of the diameter is very clear on the values of  $N_{cr}$ . As the diameter of the cut-out, regardless the form, decrease the critical load of the buckling capacity of the plate compared to the intact being discussed above.

$N_{cr}$  values decrease with increasing the cut-out, regardless the type of holes and the loading case, can be observed from relative Tables.

It can be also noted that  $N_{cr}$  in both shapes of holes are similar with a difference of less 5% for the favour of circular ones. This is true for all kind of loading and all plate thicknesses.

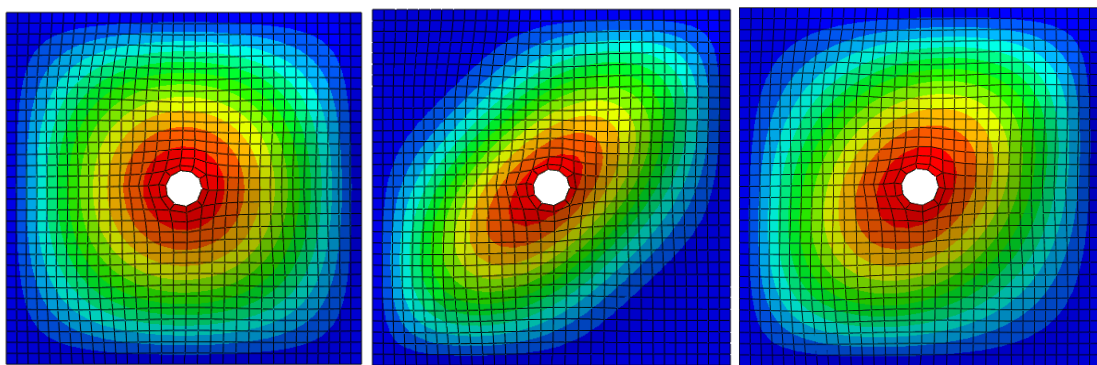
Same things can be said for the out-plane deformation as can be clearly demonstrated in relative figures.

The same patterns are obtained for the perforated plates as was the case for the intact ones, with obviously more severe values of deformation.

It must be also noted from results given in tables that the more severe load condition is that of compression with different sizes and shapes of the cut-out.

**Table 6.8 Critical buckling load for perforated square plates**

Critical buckling load (Ncr) KN/m				
Shape of hole	Circular (R)		Square (A)	
Hole diameter	50 mm	200 mm	100 mm	400 mm
<b>Compression</b>	727.82	572.08	717.84	569.63
<b>Shear</b>	1779.97	883.52	1713.90	704.95
<b>Combined</b>	634.88	428.09	621.96	385.03

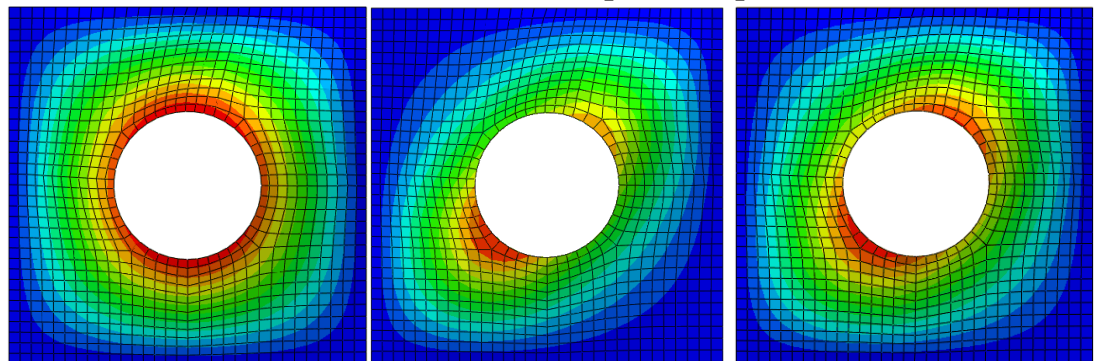


**Compression**

**Shear**

**Combined**

**Figure 6.8. Plate with hole R=50 mm Buckled shape in compression, shear and combined .**



**Compression.**

**Shear**

**Combined**

**Figure 6.9 Plate with circular hole R=200 mm Buckled shape in compression, shear and Combined.**

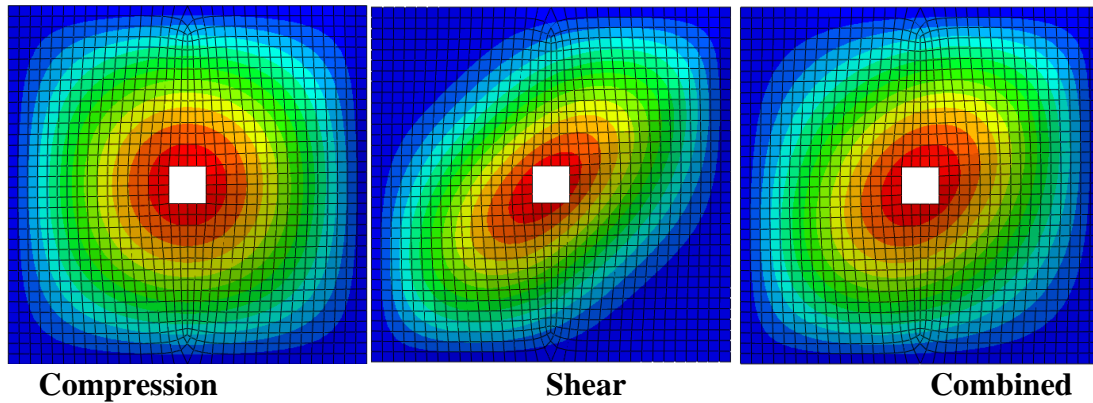


**Figure 6.10 Plate with Square hole  $A = 100$  mm Buckled shape in compression, shear and Combined.**

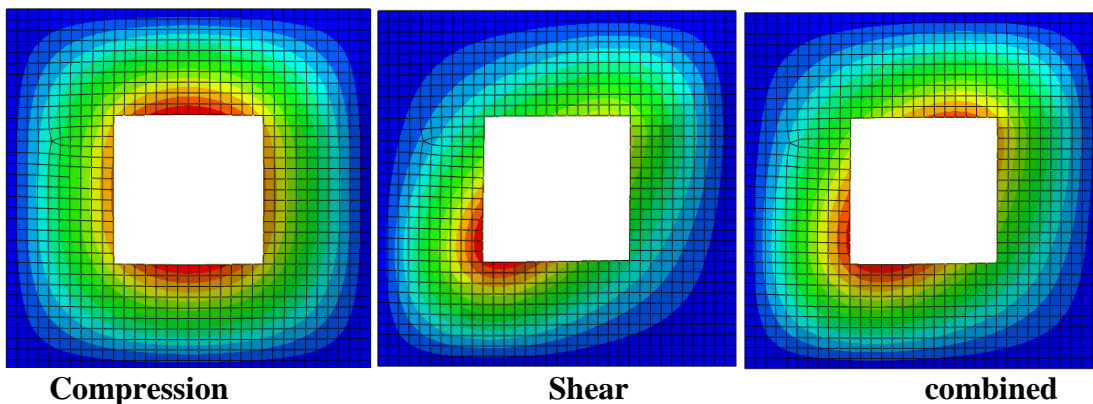


**Figure 6.11 Plate with Square hole  $A = 400$  mm Buckled shape in compression, shear and Combined.**

As a main conclusion from the elastic buckling analysis, for both kinds of plates with and without cut-out, the compression is found to be the severe loading condition as it gives the lowest values of the critical buckling load. Also, the critical buckling load decreases with the presence of cut-out, regardless the shape of the hole. The decrease of  $N_{cr}$  depends on the size of the hole, the bigger size, the least  $N_{cr}$ . This is true for all loadings conditions

## 6.3 Inelastic RIKS FEA

### 6.3.1 General consideration of the model

In order to investigate the hole shape and diameter effect on buckling of uniaxially loaded square plates, performed for non-perforated, square perforated, and circle perforated square plates. Holes on the plates are circular, and square shaped. Geometry and boundary conditions of the plate model with a circular hole is shown in Figure 6.2. The commercially available Abaqus software is utilised in this study.

The element type used is shell with 8 nodes per element. Each node has 6 degrees of freedom (three displacements in x, y, and z directions, and three rotations about x, y, and z-axes). To prevent rigid body motion and non-occurrence of rigid body movement, the in-plane boundary conditions are applied: i.e. hinge at bottom right corner and roller at right top corner of the plate. Out-of-plane displacements (z-direction displacements) of all four edges are restrained. Although all elements,

nodes, and loads are in  $x, y$  plane, in buckling analyses the out-of-plane displacements of all nodes other than the ones at the edges are not restrained.

The uniaxial axial compression was chosen as loading for the inelastic buckling FEA because, as demonstrated in the above section, regarding the elastic buckling analysis as it gives the least critical load compared to the remaining type of loads.

The inelastic buckling FEA analysis is performed on square plates, with and without holes through 3D models built-up in Abaqus using the RIKS method. An example of such analysis is detailed in Chapter 3.

For the RIKS analysis, minor modifications must be performed to the model. The NLGEOM flag must be turned on to account for non-linearities. Additionally, the unit compressive load must be replaced by the buckling load value predicted by the linear buckle analysis.

Load versus out-of-plane displacement curves were used to obtain the local buckling load with different support condition as shown in Figures 4 5. Bifurcation curve was seen in the local buckling of plates. This leads to gradual out-of-plane displacement even at lower axial compression loads. In Figure 4 and clamped support condition, the maximum and minimum out-of-plane displacement respectively was for plate with thickness of 3 and 10 mm. The highest and lowest values of out-of-displacement were 2 and 1.2 mm. In Figure 5 and simply support condition the

### 6.3.2 Characteristic of the model

Under the condition that the lighting area remains unchanged, two typical perforated plates are designed, as shown in Figure 6.12. The dimensional parameters and material properties are shown in Table 6.11

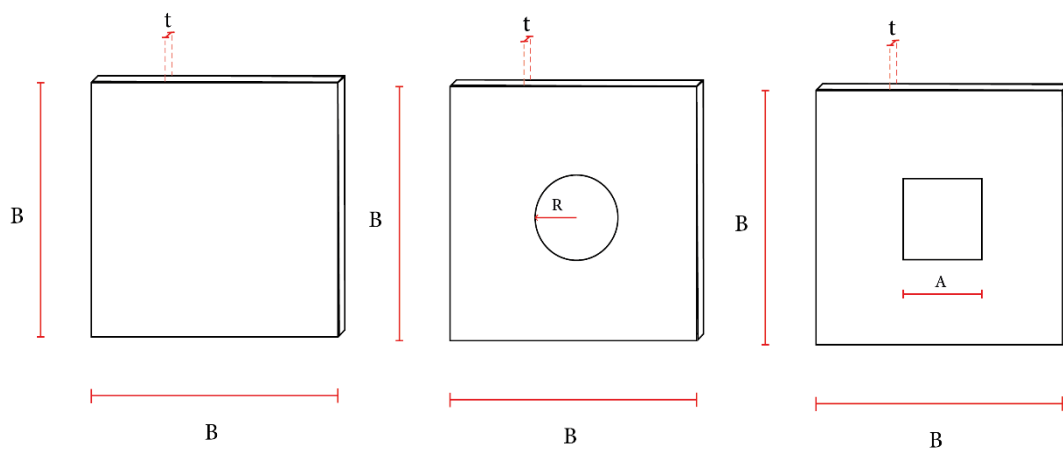


**Figure 6.12 Dimensional parameters of the perforated plate on the side.**

**Table 6.9. Geometric dimensions and material properties of the perforated plate.**

Parameters	Plate length (B)	Plate thickness (t)	Radius of circular hole (R)	Square hole length (A)	Elastic modulus (E)	Poisson's ratio (n)	Load (kN/m)
Values	1000 mm	- 10 mm - 20 mm - 40 mm	- 50 mm - 200 mm	- 100 mm - 400 mm	210 GPa	0.3	355 KN/m

## 6.4 Results and discussion

Buckling refers to the sudden collapse of a structural member, subjected to high axial compressive loading. This collapse takes the form of a sudden lateral deflection of the structural member. Therefore, the structure's load bearing ability is compromised under buckling. A structure's behaviour under loading is usually studied with the use of load-displacement plots. This applies also to studying the structural behaviour in the post-buckling region (past the bifurcation point).

The results of the present investigation will be presented and discussed in the terms of loading curve history: Buckling loads vs. out-plane displacement curves, the second part of the discussion is devoted to the stress and deformation pattern analyses by mean of available failure criteria implanted in ABAQUS: the Von Mises yield criterion which is by far the most common yield criteria in metals.

- **Load- out-plane deflections curves**

Load-deflections curves are chosen to be better retrace the loading history for studied different cases with and without cut-out. All load-deflection curves show two distinct parts: linear and nonlinear branches. The following Figures represent the skeleton curves of the FE-models of Load-out of plane deflection are depicted for models having the same features and to highlight the effect thicknesses effect  $t_s = 10, 20$  and  $40$  mm.

- **Case of intact square plate**

Figure 6.11 shows the elastic and inelastic buckling behaviour of intact square plates with varying thicknesses, that is  $t = 10, 20$  and  $40$  mm. As it can be seen from Figure 6.13, the plate with the higher thickness show a more rigid behaviour with very minor of buckling. This is to say that behaviour of square intact plate with  $t = 40$  mm likely to be is column-like buckling (Chapter 1 of this thesis). However, for the other extreme, that is  $t = 10$  mm, it can be seen from the figure bellow that is plate-like buckling can be unstable because of the critical in-plane forces acting on the plates and these forces have effects also on flexural behaviour. The intermediate case, that is  $t = 20$  mm a nonlinear behaviour with a decrease in stiffness after the critical load being reached.

This figure displays the behaviour of thick plate ( $t = 40$  mm), and a thin plate with an intermediate plate.

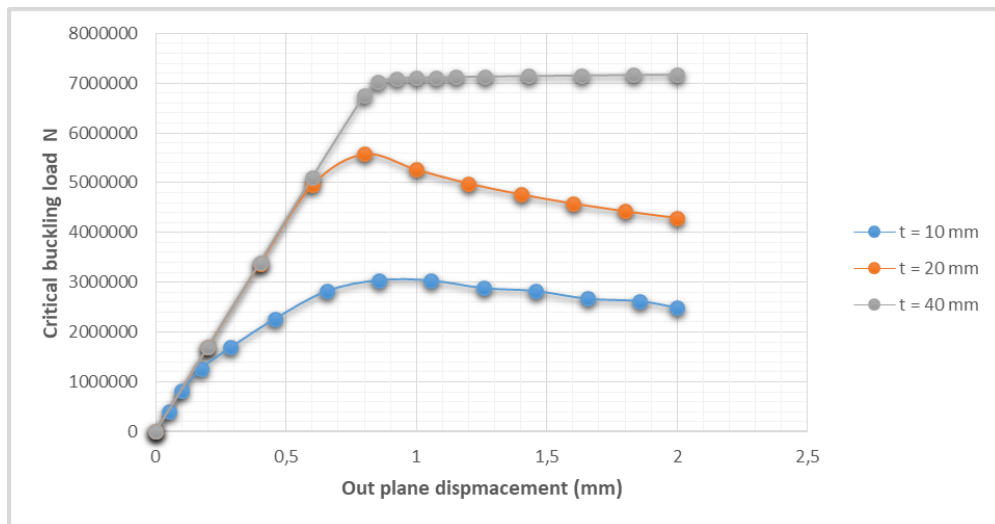


**Figure 6.13 Elastic and inelastic load- in plane deflection of intact plate square with different thicknesses**

- **Perforated square plates**
  - **Circular cut-out shape**

Figure 6.12 shows the load history vs. the in- plane displacement for a square plate having different diameters central circular hole for the particular case of thickness:  $t = 10$  mm. Three curves were drawn for the reference case (intact plate), and perforated plate with  $d = 100$  mm and  $300$  mm respectively.

As can be seen from Figure 6.12, the general behaviour is divided in two distinct parts that is pre-buckling phase before reaching  $N_{cr}$  and the post-buckling behaviour beyond  $N_{cr}$  characterised by a decrease of the stiffness. This plate is definitely a typical thin plate with a very flexure out-plane displacement. As expected, the values of  $N_{cr}$  of the perforated plates, depending on the diameter, are lesser that one intact plate.

It can be also noted that even in the pre-buckling area, some differences are visible for all cases.

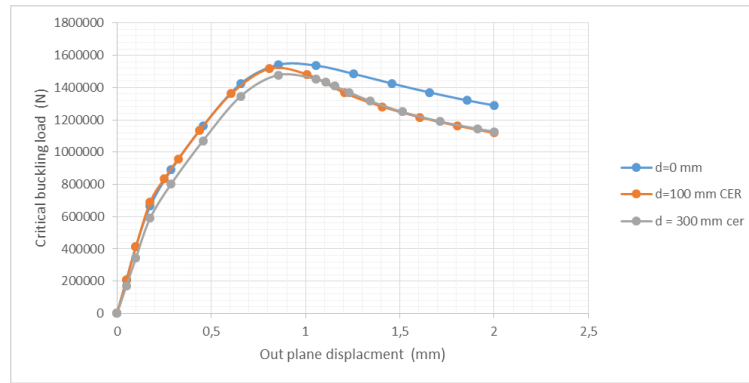
Figure 6.13 relative to plates with  $t = 20$  mm, displays almost the same curve configuration with more distinct behaviour of the pre-buckling stage.  $N_{cr}$  values for the three cases are comparable with little bit differences and higher than the values found in the previous case (Figure 6.12). However, the decrease in the stiffness is as stated in the previous case.

Figure 6.14 relative to plates with  $t = 40$  mm, displays almost quiet different pattern of curves with no significant decrease in stiffness, that is the thick plate case. A distinct pre-buckling behaviour is noticeable.  $N_{cr}$  values are really distinct a big gap is noticeable. It seems as if there are no post-buckling because the stiffness, beyond the bifurcation point remains almost constant.

The value of the critical load is almost three times as much for the case 2 comparing to the case one and almost five times as much for case 3 compared to the case 1. This indicates the effect of increasing the thickness from  $t = 10$  mm;  $20$  mm to  $40$  mm which tilts the behaviour from slender plates to thick plates.

The disparities of the inelastic results are probably due to the fact of taking the same imperfection sensitivity ( $B/1000$ ) for all cases.





**Figure 6.14 Elastic and inelastic load- in plane deflection of square perforated plate with  $t = 10$  mm**

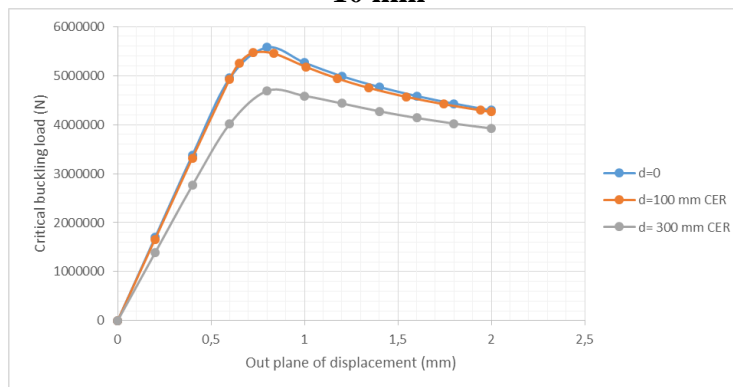


**Figure 6.15 Elastic and inelastic load- in plane deflection of square perforated plate with  $t = 20$  mm**

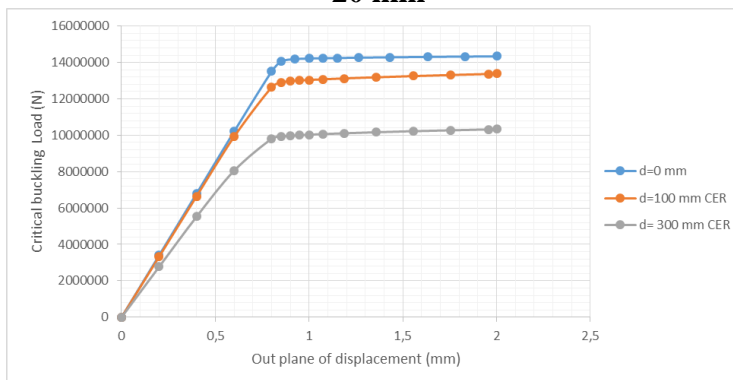


**Figure 6.16 Elastic and inelastic load- in plane deflection of square perforated plate with  $t = 40$  mm**

- **Square cut-out shape**

Basically, the same discussion made be held in the case of square cut-up shape with different sizes.

The same remarks made for the case of circular cut-out with slightly different values of critical loads.

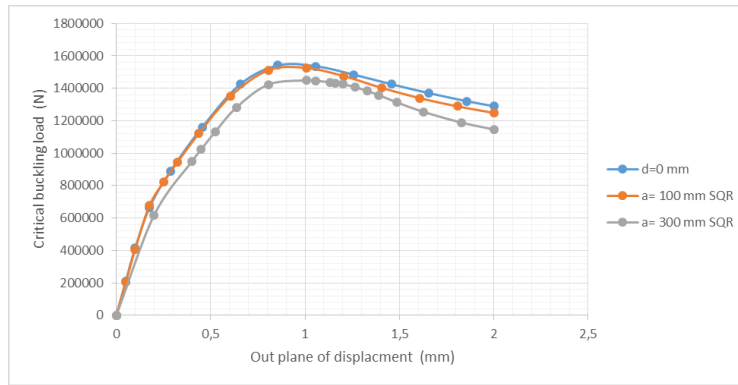


**Figure 6.17 Elastic and inelastic load- in plane deflection of square perforated plate with  $t = 10$  mm**

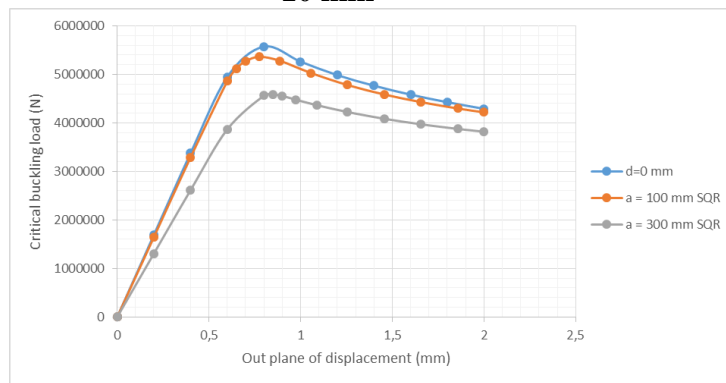


**Figure 6.18 Elastic and inelastic load- in plane deflection of square perforated plate with  $t = 20$  mm**

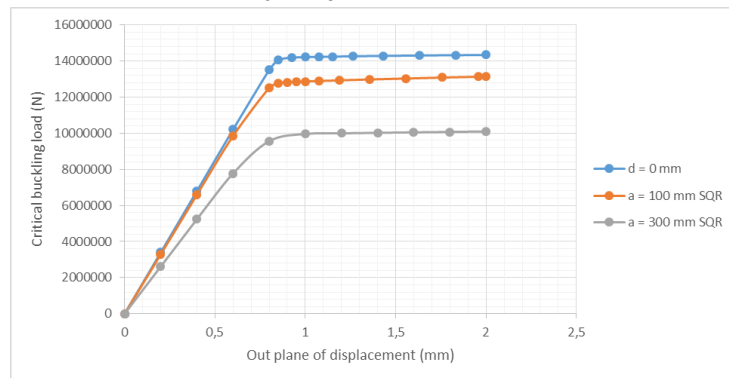


**Figure 6.19 Elastic and inelastic load- in plane deflection of square perforated plate with  $t = 40$  mm**

- Comparison results between circular and square cut-out**

The following figures depicted the differences between the uses of different shapes of cut-out. Figures 6.17 to 6.19 show the differences between the behavior of square plates with different shapes with  $d = 100$  mm. Figure 6.20 to 6.22 concern the size of cut-out = 300 mm.

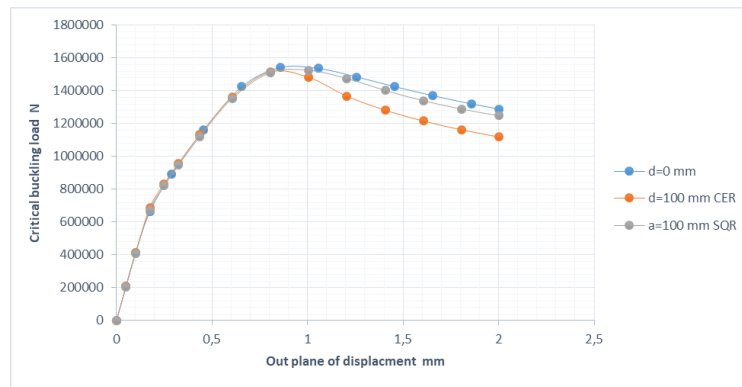


**Figure 6.20 Different hole shape same size 100 mm with thickness  $t = 10$  mm**

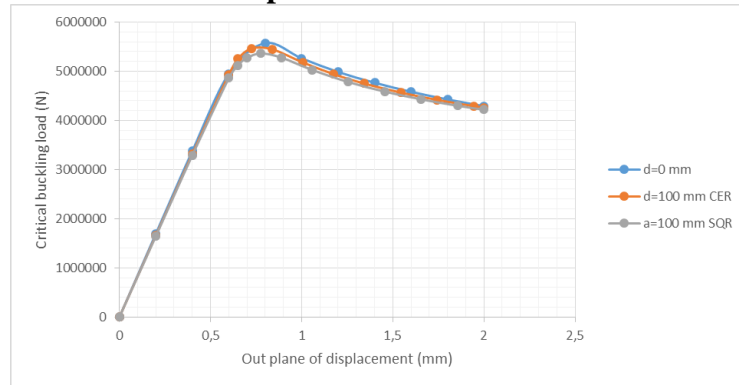


**Figure 6.21 Different hole shape same size 100 mm with thickness  $t = 20$  mm**

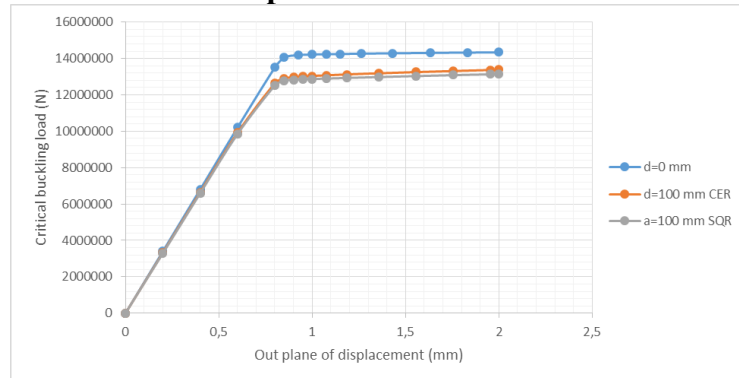


**Figure 6.22 Different hole shape same size 100 mm with thickness  $t = 40$  mm**

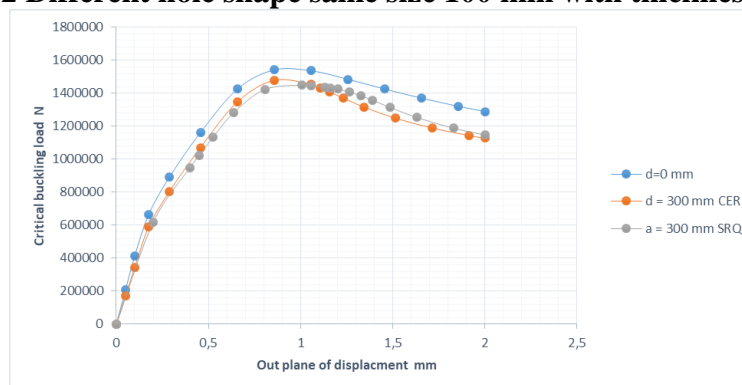


**Figure 6.23. Different hole shape same size 100 mm with thickness  $t = 10$  mm**

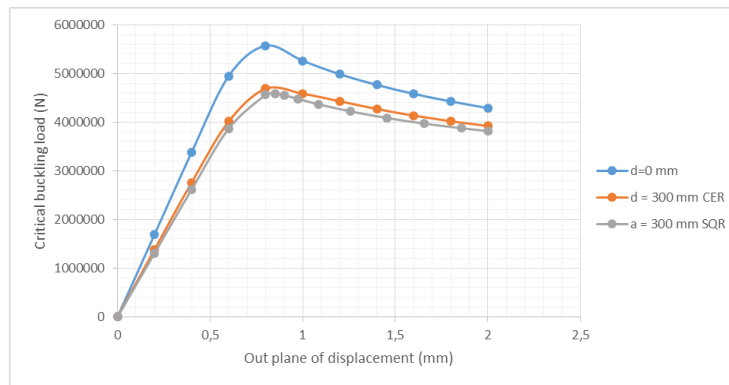


**Figure 6.24 Different hole shape same size 100 mm with thickness  $t = 20$  mm**

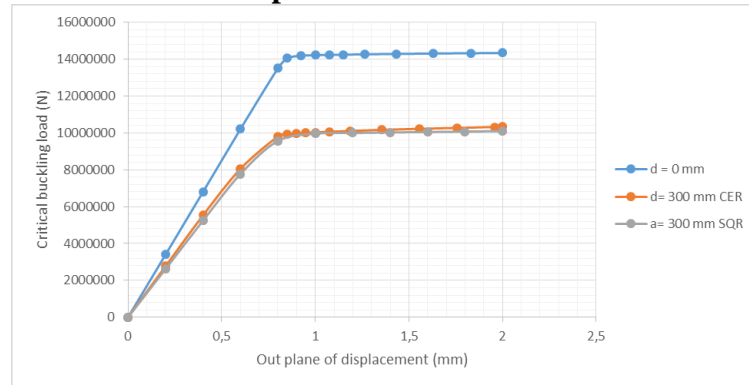


**Figure 6.25 Different hole shape same size 100 mm with thickness  $t = 40$  mm**

A general discussion for Figure 6.19 to 6.21 will be held. In fact, no major differences can be noticeable from results in terms of shape and the size of cut-out. The predictable values are almost the same regardless the shape of the holes.

- **All cases**

The following figures give the general tendency of all models being under considerations.

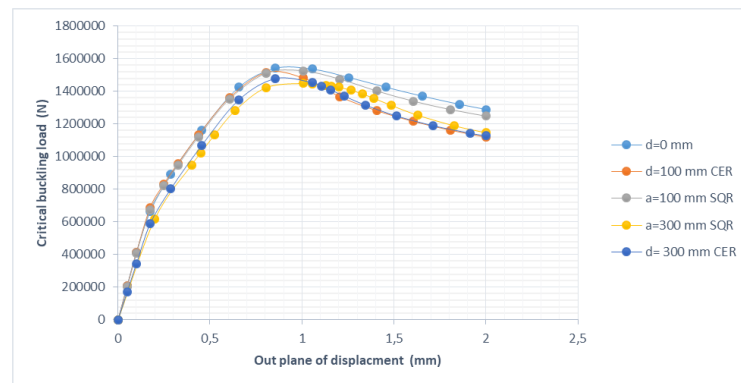


**Figure 6.26 Ratio between critical buckling load and the displacement for plates with the thickness  $t = 10$  mm**

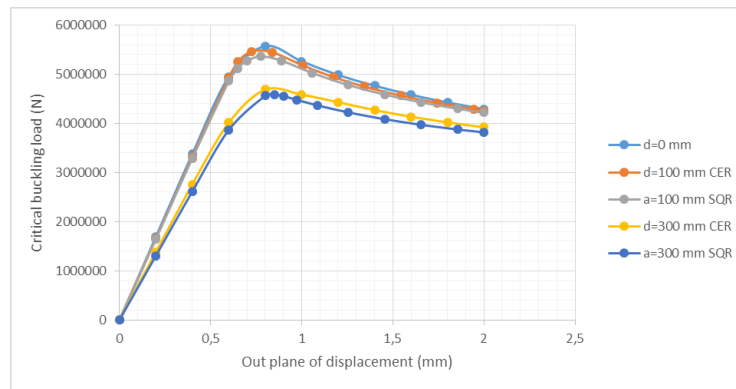


**Figure 6.27 Ratio between critical buckling load and the displacement for plates with the thickness  $t = 20\text{mm}$**

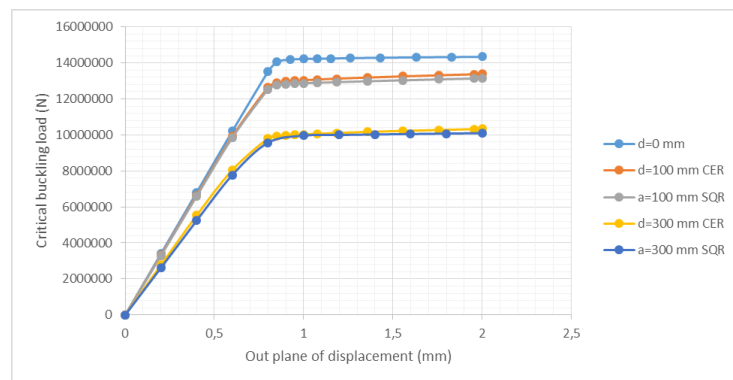


**Figure 6.28 Ratio between critical buckling load and the displacement for plates with the thickness  $t = 40\text{mm}$**

**Conclusions and remarks**

As demonstrated, the Riks algorithm is a powerful tool for assessing a structure’s behaviour in the post-buckling region. By introducing imperfections (either by mesh perturbation or by scaled mode shapes-as performed here-) we achieve a smoother transition to the post-buckling region. The cases shown above can be applied when investigating the behaviour of imperfection-sensitive structures. The results are showing the importance of the thickness of plate along with the imperfection sensitive and the effect of the shapes and sizes of the cut-out.

**Discussion of the patterns of Von Mises yielding criteria**

The following figures are extracted from the inelastic finite element by Abaqus. They are of two kinds: Stress and deformation contours at the ultimate deformation step of analysis obtained from inelastic analysis.

• Case of intact square plate

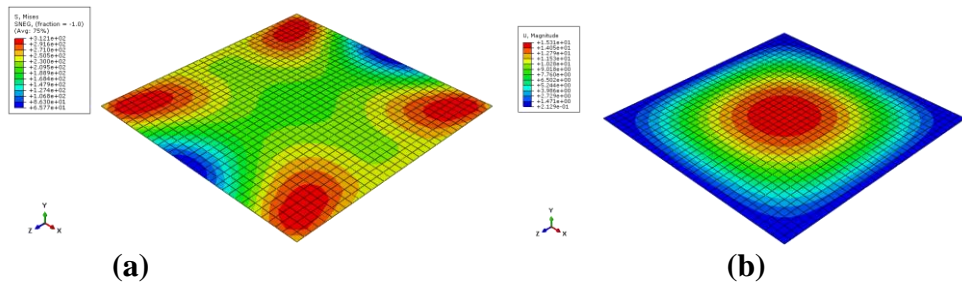


Figure 6.29 Contours of Von Mises stress and deformed shape  $t = 10$  mm

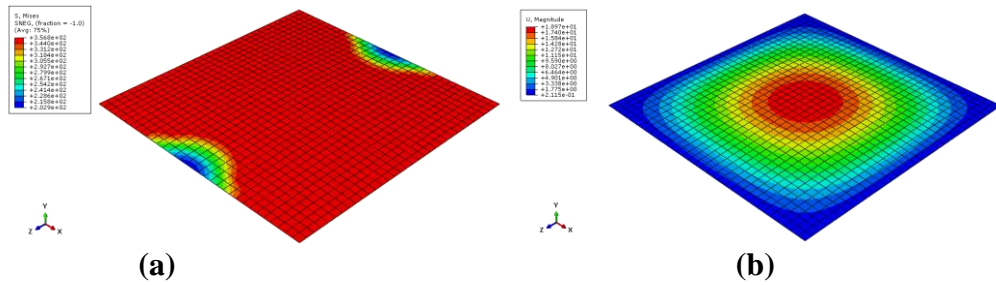


Figure 6.30 Contours of Von Mises stress distribution and deformed shape  $t = 20$  mm

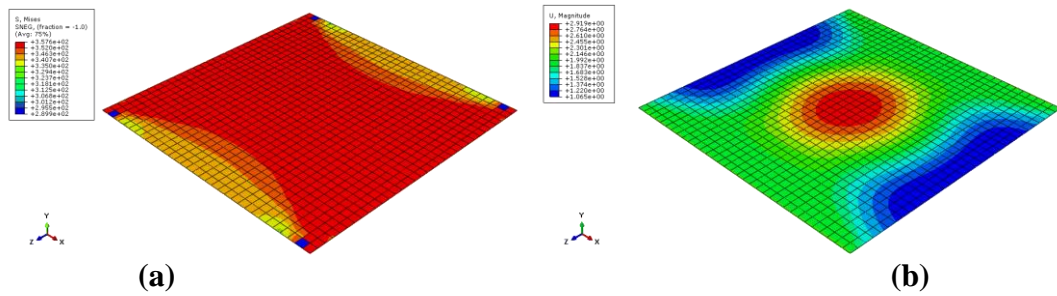


Figure 6.31 Contours of Von Mises stress distribution and deformed shape  $t = 40$  mm

• Case of circular hole  $d= 100$  mm

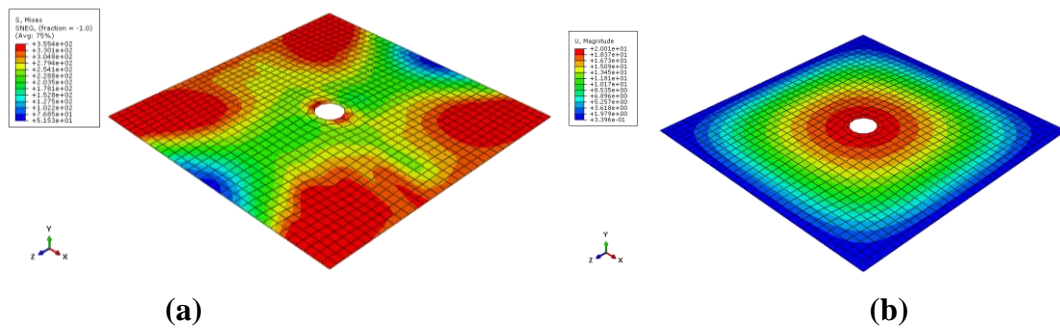


Figure 6.32 Contours of Von Mises stress distribution and deformed shape  $t = 10$  mm

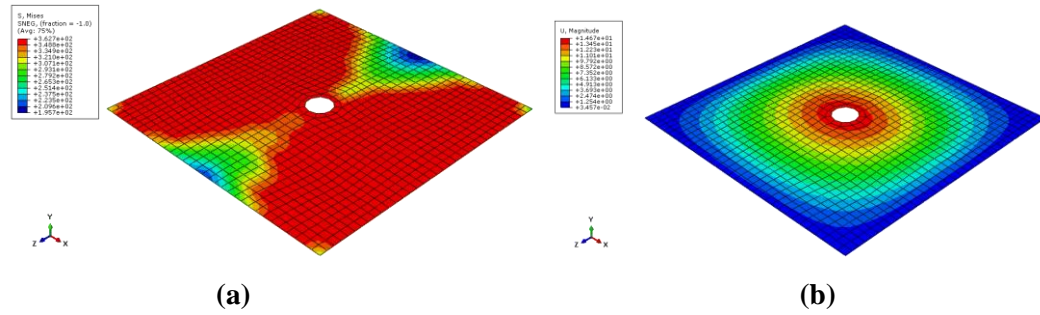


Figure 6.33 Contours of Von Mises stress distribution and deformed shape  $t = 20 \text{ mm}$

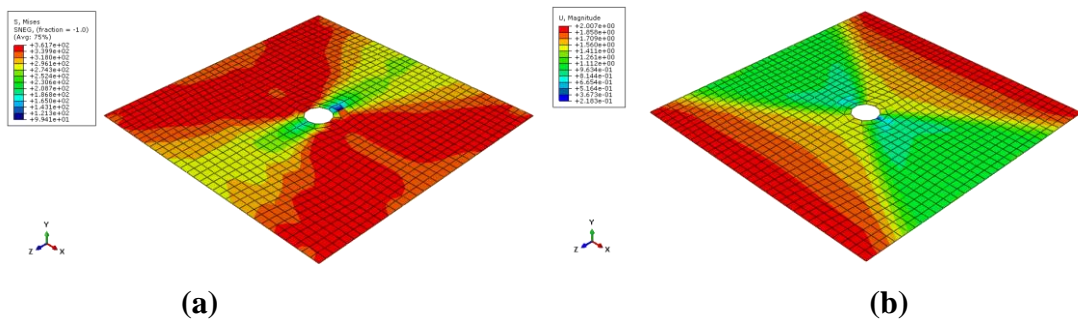


Figure 6.34 Contours of Von Mises stress distribution and deformed shape  $t = 40 \text{ mm}$

• Case of square hole  $d = 100 \text{ mm}$

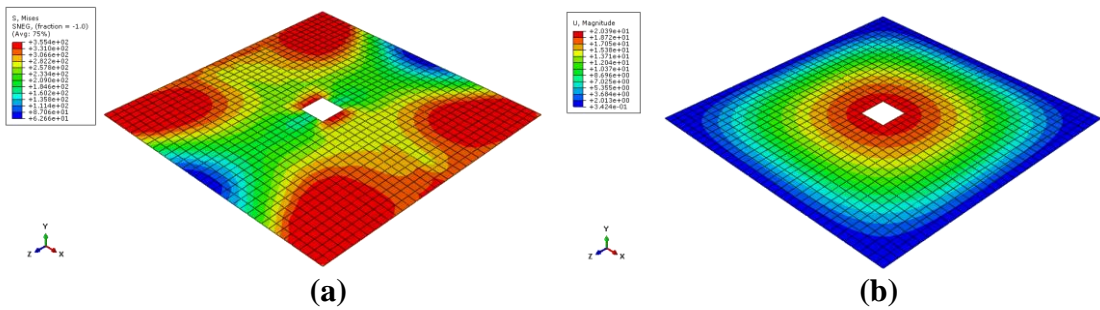


Figure 6.35 Contours of Von Mises stress distribution and deformed shape  $t = 10 \text{ mm}$

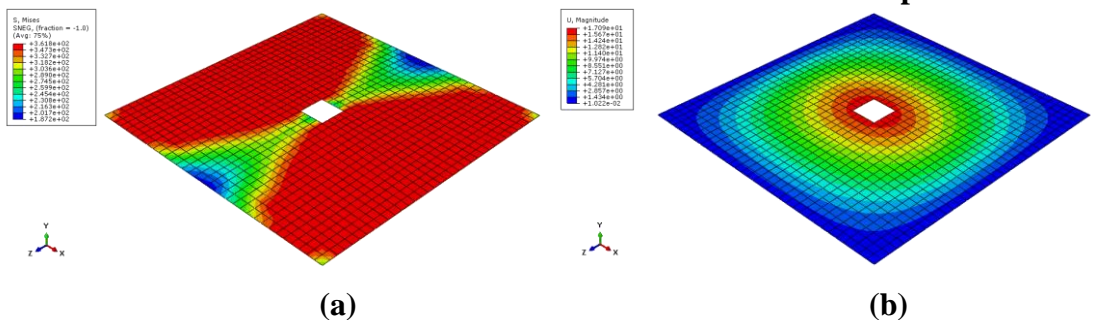


Figure 6.36 Contours of Von Mises stress distribution and deformed shape  $t = 20 \text{ mm}$

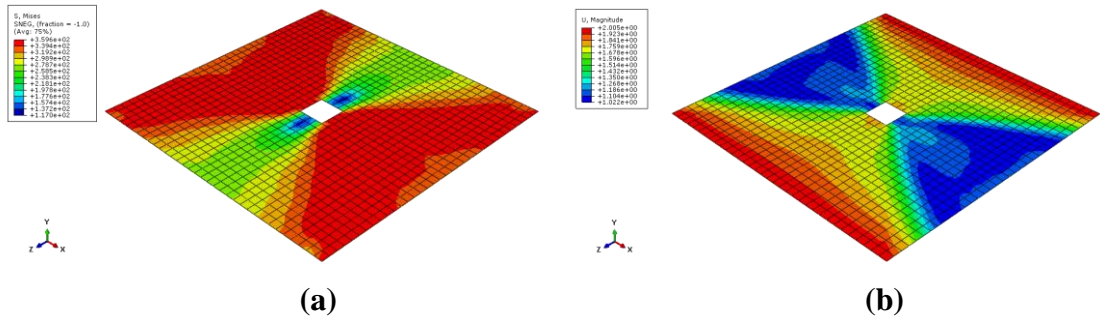


Figure 6.37 Contours of Von Mises stress distribution and deformed shape  $t = 40 \text{ mm}$

• Case of circular hole  $d= 300 \text{ mm}$

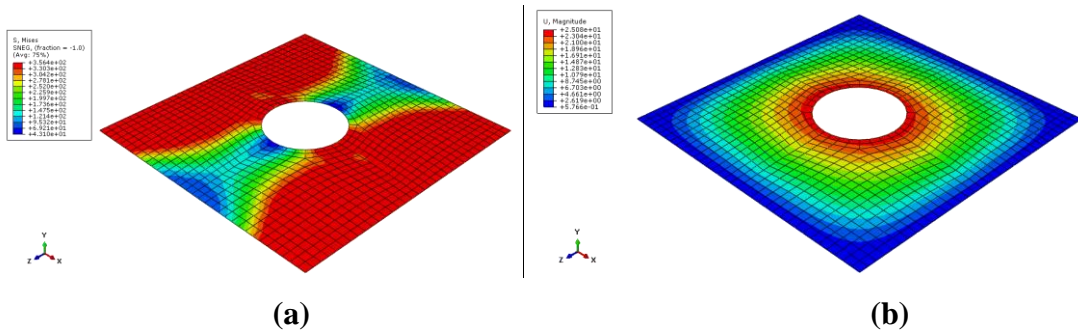


Figure 6.38 Contours of Von distribution Mises stress and deformed shape  $t = 10 \text{ mm}$

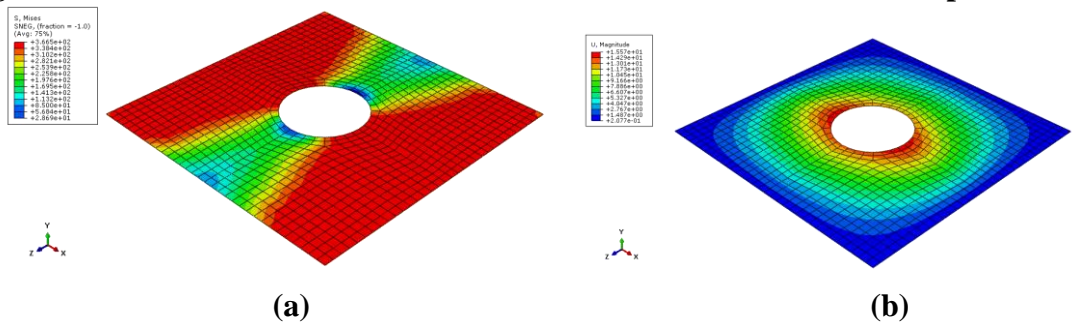


Figure 6.39 Contours of Von Mises stress distribution and deformed shape  $t = 20 \text{ mm}$

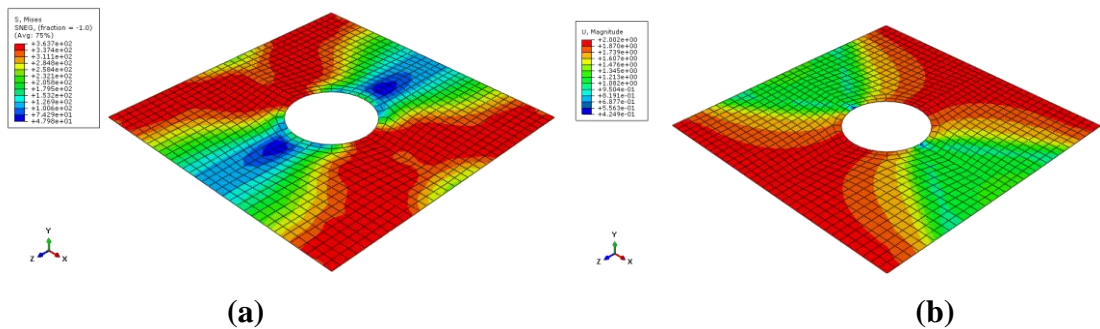


Figure 6.40 Contours of Von Mises stress distribution and deformed shape  $t = 40 \text{ mm}$



• Case of square hole  $d= 300$  mm

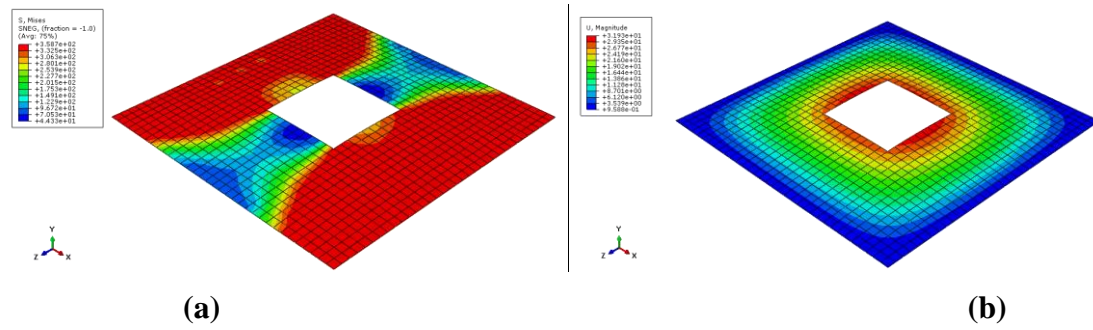


Figure 6.41 Contours of Von Mises stress distribution and deformed shape  $t = 10$  mm

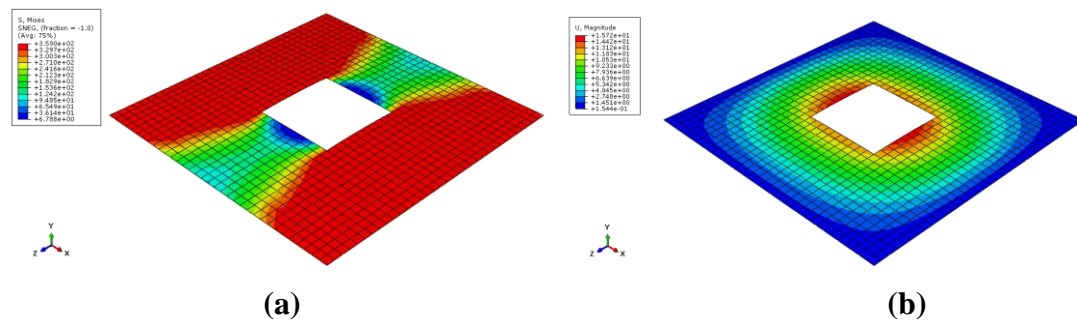


Figure 6.42 Contours of Von Mises stress distribution and deformed shape  $t = 20$  mm

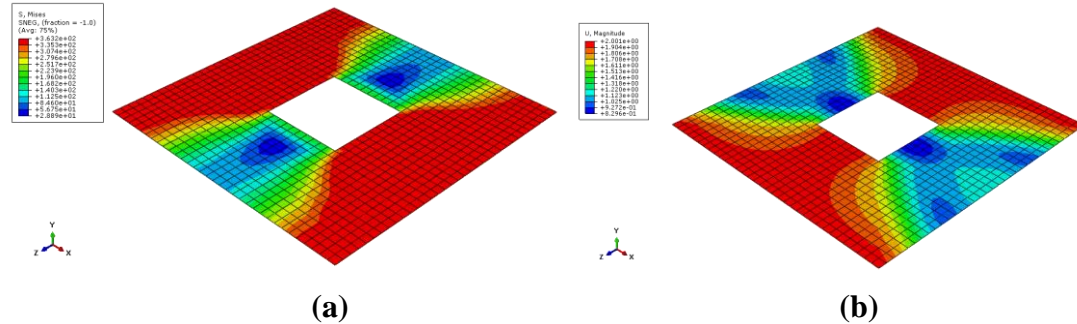


Figure 6.43 Contours of Von Mises stress distribution and deformed shape  $t = 40$  mm

### 6.5 General discussion

Generally speaking, thin-walled structures are slender structural elements rather sensitive for an influence of geometrical imperfections. The accuracy and stability of solutions is a difficult consideration in nonlinear analysis. As this study pertains to thin-walled steel structures, Von Mises yield criterion and isotropic strain hardening were used to define the yield surface and loading surface, while the associated flow rule was used to calculate the plastic strains.

Furthermore, nonlinear analysis was possible by a step realistic behaviour of the structure, which is programmed in ABAQUS/Standard. Incremental procedure based on RIKS algorithm is used to solve system of nonlinear equations is considered when non-linearity of the material, such as plasticity is present, or post-buckling behaviour is of interest this was possible by a step-by-step loading process, which simulates a more realistic behaviour of the structure, which is programmed in

ABAQUS/Standard. Incremental RIKS algorithm. The basic Riks algorithm is essentially Newton's method with load magnitude as an additional unknown to solve simultaneously for loads and displacements, thus, it can provide solutions even in cases of complex and unstable response

Another interesting result of inelastic buckling analysis is Von Mises stress distribution at any given compression load level. Von Mises stress distribution obtained from inelastic buckling analysis.

Clearly, yielding starts at certain parts of the perimeter of the opening and spreads towards the plate edge as the shear force is increased. Furthermore, at buckling compression force level, there is some area in the plate that is still in the elastic range.

The above figures indicate that the shape of the buckling behaviour for a given thickness all cases has maintained a similar pattern for Von Mises stress distribution contour or deformed shapes despite the configuration of the plate, that is with or without cut-out.

Providing thicker square plates leads to the enhancement of the square plate buckling strength. When the plate buckling strength exceeds the steel plate yield strength, the material plasticity leads to plastic deformation that redistributes the stresses, and paves the way towards extending the plastic stress region in a manner that enables the plate section to develop larger internal force resultant that balances the incremental applied loading. In this case, the development of plastic deformation region offered the desired ample warning prior to failure when steel Von Mises ( $\sigma_e$ ) stresses fell on the failure surface.

It can also noticeable, that imperfection sensitivity of the plate plays an important role for thicker square plates by resisting to the out-plane deformation as can be seen from relative figures despite the configuration of the square plate.

Same remarks can be made, as it was for the elastic buckling analysis, the value of the critical buckling load depends mainly on the thickness of the square plate and the buckling factor increases.

According to the results of this study, the shape of the cut-out does not signally affect the final results with a slightly advantage of the circular hole. Is no really matter cause the values of circular and square holes

It was observed during the extraction of results that Von Mises stress distribution stared, as demonstrated for the classical theory, from the corners moving to the centre of plate this mean that the effective stresses are in the corners so the plate is generally depend in the most on the edges and corners.

When the shape of hole is fixed and changed the size of the cut out the result was that in the thickness of 10 mm we didn't noticed a big difference in the curves of the cut-out size of 100 mm and the 300 mm but every time the thickness is increased, it can observed that the curves moves away from each the other, the plate with biggest hole diameter had a low critical buckling load than the small hole so in the end the hole size matter only when the big values of thickness.

## CONCLUSIONS AND SUGGESTIONS FOR FUTURE WORKS

### A- CONCLUSIONS

This thesis deals with a parametric study of the elastic and inelastic buckling of square plate with and without cut-out. A compressive series of implanted FEA model has been carried out covering several parameters: thickness of plates, shape and size of the centred cut-out. An accurate solution to a buckling problem requires more efforts than just following a numerical procedure, there are a number of factors to consider before a buckling solution can be accepted with confidence. In fact, a starting step should be a linear buckling analysis. Nonlinear buckling analysis capability can be performed restart the linear buckling analysis.

Plated structures are important in a variety of marine- and land-based applications, including ships, offshore platforms, box girder bridges, power/chemical plants, and box girder cranes. It is very likely in many cases to have holes in the plate elements for inspection, maintenance, and service purposes, and the size of these holes could be significant. The presence of these cut-out redistributes the membrane stresses in the plate and may cause significant reduction in its strength in addition to changing its buckling characteristics. In the pre-buckling regime, the structural response between loads and displacements is usually linear, and the structural component is stable. As the predominantly compressive stress reaches a critical value, buckling occurs.

It is vital to first develop a reliable and efficient FE model capable of producing realistic and accurate results particularly for elastic buckling, inelastic buckling and even post-buckling models. The validation of the linear FEA model has been successfully done with the data available in literature, which gives a more confidence in the models which will be used as initial condition for more complex buckling analysis of plate with and without cut-out.

The obtained results of elastic buckling analysis have shown that the most severe loading type for a plate is the compression. For that reason, it has been decided to exclusively, for the inelastic buckling behaviour, to carry out the parametric analysis on unstiffened plate with and without cut-out operated in the middle.

From the analysis undertaken in this thesis, some main conclusions may be drawn as follows:

- The thickness of the plate is of prime importance as it influences the elastic and inelastic buckling of square plate with and without cut-out as clearly shown and discussed in chapter 6.
- As a main conclusion from the elastic buckling analysis, for both kinds of plates with and without cut-out, the compression is found to be the severe loading condition as it gives the lowest values of the critical buckling load.

- While shear loading gives the highest value  $N_{cr}$ , loading shows an intermediate value despite the configurations combined
- Also, the critical buckling load decreases with the presence of cut-out, regardless the shape of the hole.
- The decrease of  $N_{cr}$  depends on the size of the hole, the bigger size, the least  $N_{cr}$ . This is true for all loading conditions.
- As far as deformation, the same general deformation patterns are obtained for the perforated plates as was the case for the intact ones, with obviously more severe values of deformation.
- The results of the present investigation are presented and discussed in the terms of loading curve history: Buckling loads vs. out-plane displacement curves, the second part of the discussion is devoted to the stress and deformation pattern analyses by mean of available failure criteria implanted in ABAQUS: the Von Mises yield criterion which is by far the most common yield criteria in metals.
- For the inelastic investigations, all load-deflection curves show two distinct parts: linear and nonlinear branches
- It was remarkable, that as the thickness of the plate increase with the same value of imperfection taken as 1 mm for all cases has given as if the plate with 40 mm of thickness does not suffer from any kind of buckling and then its conserves its strength capacity and the failure may be mechanic rather than geometric. It can be concluded that the imperfection sensitivity must be calculated considering both the width of the square plate and its thickness.
  - It can also state from results shown in Chapter 6, that imperfection sensitivity of the plate plays an important role for thicker square plates by resisting to the out-plane deformation as can be seen from relative figures despite the configuration of the square plate.
  - Providing thicker square plates leads to the enhancement of the square plate buckling strength.
  - According to the results of this study, the analysis of the Von Mises stress distribution obtained by Abaqus that the shape of the cut-out does not significantly affect the final results with a slightly advantage of the circular hole.
- It was observed during the extraction of results that Von Mises stress distribution started, as demonstrated for the classical theory, from the corners moving to the centre of plate this mean that the effective stresses are in the corners so the plate is generally depend in the most on the edges and corners.

Broadly speaking, it can be asserted that the initial objectives of this study, which were to focus on the investigation of the elastic and inelastic behaviour of steel plates were generally achieved. The author declares that, at the end of the work, has gained deeper understanding of the behaviour of plates, especially the inelastic one. Also, his ability of manipulation of 3D FEA for complex topics such as inelastic and Von Mises contours.

### **B- SUGGESTIONS FOR FURTHER WORKS**

To conclude this research topic, the following recommendations for future research works can be suggested:

1. Investigating the inelastic buckling of intact and perforated square plates under shear and combined loading compression associated with shear.
2. Assessment of the linear and nonlinear buckling of square with central opening under dynamic loadings.
3. Evaluation of the linear and nonlinear buckling of square with central opening under fire conditions.
4. Investigation of the instability phenomenon of intact and perforated square plate with different imperfection sensitivity.

## References

- |   |
|---|
| [1] Behavior Of Steel Plates Under Axial Compression And Their Effect On Column Strength Thesis · May 2002 Reads 392  |
| [2] Galambos, T. V. 1998. Guide to Stability Design Criteria for Metal Structures. 5th. edition. John Wiley & Sons Inc., New York.  |
| [3] Murray, N. W. 1986. Introduction to the Theory of Thin-Walled Structures. Oxford University Press, Oxford.  |
| [4] Walker, A. C. 1975. Design and Analysis of Cold-Formed Section. International Textbook Company Limited, London.   |
| [5] Finite Element Analysis And DESIGN OF META STRUCTURES EHAB ELLOBODY, RAN FENG, BEN YOUNG ISBN: 978-0-12-416561-8 2014   |
| [6] Mazen A. Musmar. (2022). Structural performance of steel Plates.p:8   |
| [7] Navier, C.L.M.N., Bulletin des Science de la Societe Philomarhique de Paris, 1823.  |
| [8] Kantorovich, L.V. and Krylov, V.I., Approximate Methods of Higher Analysis, John Wiley and Sons, New York, 1958.  |
| [9] Timoshenko, S.P. and Woinowski-Krieger, S., Theory of Plates and Shells, 2nd edn, McGraw-Hill, New York, 1959.  |
| [10] Guide 2009 Ch. 4 plates Schafer  |
| [11] Finite Element Analysis and DESIGN OF META STRUCTURES EHAB ELLOBODY, RAN FENG, BEN YOUNG ISBN: 978-0-12-416561-8 2014  |
| [12] Abaqus Analysis User's Manual Volume II 2012   |
| [13] Presentation Manuel of EBPlate 2006  |
| [14] Mauro De Vasconcellos Real And All/ Elastic And Elasto-Plastic Buckling Analysis Of Perforated Steel Plates /Vetor, Rio Grande,V. 23, N. 2, P. 61-70, 2013                     |
| [15] Fethullah USLU and all/ Buckling of Square and Circular Perforated Square Plates under Uniaxial Loading/jiciviltech, 4(2), 61-75, 2022   |
| [16] EL-SAWY, K. M.; NAZMY, A. S. Effect of aspect ratio on the elastic buckling of uniaxially loaded plates with eccentric holes. Thin-Walled Structures, v. 39, p. 993-998, 2001. |